



# LUND UNIVERSITY

## High-throughput screening of solid-phase extraction materials using mass spectrometry

Jagadeesan, Kishore

2017

*Document Version:*

Publisher's PDF, also known as Version of record

[Link to publication](#)

*Citation for published version (APA):*

Jagadeesan, K. (2017). *High-throughput screening of solid-phase extraction materials using mass spectrometry*. [Doctoral Thesis (compilation), Lund University]. Department of Biomedical Engineering, Lund university.

*Total number of authors:*

1

*Creative Commons License:*

CC BY

### General rights

Unless other specific re-use rights are stated the following general rights apply:

Copyright and moral rights for the publications made accessible in the public portal are retained by the authors and/or other copyright owners and it is a condition of accessing publications that users recognise and abide by the legal requirements associated with these rights.

- Users may download and print one copy of any publication from the public portal for the purpose of private study or research.
- You may not further distribute the material or use it for any profit-making activity or commercial gain
- You may freely distribute the URL identifying the publication in the public portal

Read more about Creative commons licenses: <https://creativecommons.org/licenses/>

### Take down policy

If you believe that this document breaches copyright please contact us providing details, and we will remove access to the work immediately and investigate your claim.

LUND UNIVERSITY

PO Box 117  
221 00 Lund  
+46 46-222 00 00

# High-throughput screening of solid-phase extraction materials using mass spectrometry

Kishore Kumar Jagadeesan



**LUND**  
UNIVERSITY

DOCTORAL DISSERTATION

by due permission of the Faculty of Engineering, Lund University, Sweden.

Organization LUND UNIVERSITY Department of Biomedical Engineering P O Box 118, SE 22 100, Lund, Sweden	Document name DOCTORAL DISSERTATION	
	Date of issue May 2017	
Author Kishore Kumar Jagadeesan	Sponsoring organization European Commission	
Title and subtitle High-throughput screening of solid-phase extraction materials using mass spectrometry		
<p>Abstract</p> <p>In biomarker analysis, sample preparation plays a crucial step in order to extract, isolate and concentrate the analytes of interest. Among the various sample preparation techniques, solid phase extraction (SPE) is one of the most common and popular, due to the high enrichment factor, good recovery, low consumption of organic solvents and the possibility to automate (off- or on-line) the whole process. Over the years, a wide variety of sorbents and affinity phases have been developed and used in SPE. Optimization of a SPE sample preparation step is essential for high-sensitivity detection, as well as analysis robustness and reproducibility. However, the process of optimizing the SPE sample preparation in the present commercially available formats can be quite time consuming and expensive, due to the large amounts of SPE phase required and limited options for use of different materials in commercially available configurations.</p> <p>In Paper I, we have applied our micro fabricated SPE sample preparation platform, the Integrated Selective Enrichment Target, (ISET) that interfaces directly with MALDI mass spectrometry for a rapid and parallel investigation of the SPE process using minute amounts of sample. In Paper II, we utilized the 384-well filter plate format for an automated, high-throughput SPE screening method. Compared with the ISET, the 384-well filter plate format provides advantages such as increased bed volume, and thus a larger binding capacity (needed to enable use of low-affinity materials), and can be used with analysis techniques other than matrix-assisted laser desorption/ionization (MALDI), for example, liquid chromatography–electrospray ionization mass spectrometry (LC ESI-MS). However, the developed high-throughput SPE MS optimization platforms generate huge datasets. To handle these huge datasets, MALDIViz, a comprehensive informatics tool for MALDI HTS data that facilitate visualization, statistical analysis, and high quality image and data export was developed in Paper III. In addition to the miniaturized platforms, a conventional cartridge based investigation of custom made SPE materials was undertaken for, SPE of phosphatidylethanol (PEth), a phospholipid biomarker for alcohol consumption (Paper IV). In Paper V, a newly prepared molecularly imprinted polymer in the form of microgel (MIP MG) stabilized Pickering emulsions (PEs) was investigated for the ability to catalyse the formation of disulphide bonds in peptides at an Oil/Water interface.</p>		
Key words: Sample preparation, Mass Spectrometry, Miniaturization, MIPs, Proteomics, Data analysis and visualization		
Classification system and/or index terms (if any)		
Supplementary bibliographical information ISRN: LUTEDX/TEEM - 1109 – SE Report: 3/17	Language: English	
ISSN and key title	ISBN 978-91-7422-518-1 (print) ISBN 978-91-7422-519-8 (digital)	
Recipient's notes	Number of pages: 135	
	Security classification	

I, the undersigned, being the copyright owner of the abstract of the above-mentioned dissertation, hereby grant to all reference sources permission to publish and disseminate the abstract of the above-mentioned dissertation.

Signature:  \_\_\_\_\_

Date: 24th April 2017

*To Appa, Amma and Sharanyha*

“தெய்வத்தான் ஆகா தெனீனும் முயற்சிதன்  
மெய்வருத்தக் கூலி தரும்” – திருக்குறள் (619)

*Even if fate or God doesn't aid, perseverance will pay  
the wages for one's efforts. – Thirukkural (619)*

- திருவள்ளுவர் , Thiruvalluvar (BC 4<sup>th</sup> Century)



## **Public defense**

May 23rd, 2017 at 09:15 in the Belfrage lecture hall, Klinikgatan 32, Lund.

## **Advisors**

Prof. Thomas Laurell

*Department of Biomedical Engineering, Lund University, Sweden*

Dr. Simon Ekström

*Department of Biomedical Engineering, Lund University, Sweden*

## **Faculty Opponent**

Prof. František Foret

*Department of Bioanalytical Instrumentation, Institute of Analytical Chemistry,  
Academy of Sciences of the Czech Republic, Czech Republic*

## **Board of Examination**

Dr. Lukas Orre,

*Department of Oncology-Pathology, Cancer Proteomics, Clinical Proteomics Mass Spectrometry,  
Karolinska Institutet, Sweden*

Dr. Johan Gobom

*Department of Psychiatry and Neurochemistry at Institute of Neuroscience and Physiology,  
Sahlgrenska Academy, University of Gothenburg, Gothenburg, Sweden*

Prof. Lei Ye

*Pure and Applied Biochemistry, Lund University, Lund, Sweden*

Deputy Member: Prof. Tautgirdas Ruzgas

*Department of Biomedical Science, Malmö University, Sweden*

## **Chairman**

Dr. Johan Nilsson,

*Department of Biomedical Engineering, Lund University, Sweden*

© Kishore Kumar Jagadeesan 2017

ISBN 978-91-7422-518-1 (printed version)

ISBN 978-91-7422-519-8 (electronic version)

ISRN: LUTEDX/TEEM - 1109 – SE

Report: 3/17

Printed in April 2017 by Tryckeriet E-huset, Lund, Sweden

# Table of Contents

List of Publications .....	7
Abbreviations.....	8
Introduction .....	9
Biomarker.....	10
Phosphoproteomics.....	11
ProGRP.....	11
PEth .....	11
Sample Preparation .....	12
Solid Phase Extraction (SPE) .....	12
Mechanism of the SPE Process .....	13
Different sorbent materials.....	14
The formats and procedures in SPE .....	19
ISET.....	20
ISET – MIP sample preparation .....	21
ISET MIP SPE protocol .....	21
384-well filter plate .....	23
384-well filter plate – MIP sample preparation .....	23
384-well filter plate MIP SPE protocol .....	24
Mass Spectrometry .....	25
Mass spectrometry for protein identification.....	25
Bottom-up proteomics.....	26
Top-down proteomics .....	26
Mass spectrometry Instrumentation.....	27
Ionization techniques.....	27
Mass analysers.....	30
Detectors .....	34
Operation modes for quantification .....	35
Data Visualization and Analysis .....	37
MALDIViz implementation .....	37
RStudio .....	38
R Packages.....	39

shiny.....	39
MALDIViz App .....	40
Summary of the Manuscripts.....	49
Paper I.....	49
Paper II .....	50
Paper III.....	51
Paper IV.....	52
Paper V .....	53
Popular Summary .....	54
Acknowledgements .....	56
References .....	58
Appendix: Paper I - V.....	65

# List of Publications

This thesis is based on the following papers, which will be referred to in the text by their Roman numerals. The papers are appended at the end of the thesis.

**I. Multiplexed MALDI-MS arrays for screening of MIP solid phase extraction materials**

Jagadeesan, K.K.; Wierzbicka, C.; Laurell, T.; Sellergren, B.; Shinde, S.; and Ekström, S. *Journal of Chromatography B* 2016 1021, 213-220.

The author was responsible for all the experimental work (except the preparation of the molecularly imprinted polymers). The author was also responsible for writing the major part of the paper.

**II. Filter Plate–Based Screening of MIP SPE Materials for Capture of the Biomarker Pro-Gastrin-Releasing Peptide**

Jagadeesan, K.K.\*; Rossetti, C\*.; Qader, A.A.; Reubsaet, L.; Sellergren, B.; Laurell, T. and Ekström, S. *SLAS Discovery* (Published 31st January 2017)

The author was responsible for all the experimental work (except the preparation of the molecularly imprinted polymers). The author was also responsible for writing the major part of the paper.

**III. MALDI-Viz - A comprehensive informatics tool for MALDI-MS data visualization and analysis**

Jagadeesan, K.K. and Ekström, S. (*Under Review*)

The author was responsible for all the experimental work. The author was also responsible for writing the major part of the paper.

**IV. Solid-phase extraction of the alcohol abuse biomarker phosphatidylethanol using newly synthesized polymeric sorbent materials containing quaternary heterocyclic groups**

Duarte, M.; Jagadeesan, K.K.; Billing, J.; Yilmaz, E.; Laurell, T. and Ekström, S. (*Under Review*)

The author's main contributions to the experimental work for this paper were in the initial optimization, development and evaluation of the SPE protocol. The author was also responsible for writing a substantial part of the paper.

**V. Catalytic Formation of Disulfide Bonds in Peptides by Molecularly Imprinted Microgels at Oil/Water Interfaces**

Shen, X.; Huang, C.; Shinde, S.; Jagadeesan, K.K.; Ekström, S.; Fritz, E. and Sellergren, B. *ACS Applied Materials & Interfaces* 2016 8 (44), 30484-30491

The author was responsible for the MALDI-MS method development and analysis.

\* Authors contributed equally. Printed with permission.

## Abbreviations

CID	collision induced dissociation	MOAC	metal oxide affinity chromatography
CHCA	$\alpha$ -cyano-4-hydroxycinnamic acid	MRM	multiple reaction monitoring
DHB	2,5-dihydroxybenzoic acid	MS	mass spectrometry
DVB	divinylbenzene	NTA	nitrilotriacetic acid
DNA	deoxyribonucleic acid	NIP	non-imprinted polymer
DC	direct current	PE	Pickering emulsions
ELISA	enzyme-linked immunosorbent assay	PEth	phosphatidylethanol
ESI	electrospray ionization	PMF	peptide mass fingerprinting
GRP	gastrin-releasing peptide	PTM	post-translation modification
HPLC	high performance liquid chromatography	PS-DVB	polystyrene-divinylbenzene
HTS	high-throughput screening	PVDF	polyvinylidene fluoride
ICR	ion cyclotron resonance	ProGRP	progastrin-releasing peptide
IDA	imidoacetic acid	3Q	triple quadrupoles
IMAC	immobilized metal ion affinity chromatography	RF	radio frequency
IQR	inter quartile range	SAN	styrene acrylonitrile
ISET	integrated selective enrichment target	SAX	strong anion exchange(r)
IS	internal standard	SCX	strong cation exchange(r)
IT	ion trap	SCLC	small cell lung cancer
LC	liquid chromatography	SDVB	styrene-divinylbenzene
LLE	liquid-liquid extraction	SIM	selected ion monitoring
LOC	Lab-on-chip	SPE	solid-phase extraction
LTQ	linear trap quadrupole	SRM	selected reaction monitoring
MAA	methacrylic acid	TOF	time-of-flight
MCP	micro channel plates	WAX	weak anion exchange(r)
MALDI	matrix assisted laser desorption ionization	WCX	weak cation exchange(r)
MIP	molecularly imprinted polymer		

# Introduction

The thesis is divided into two chapters. In the first part of the thesis, I introduce the biological and technology topics relevant to the bioanalytical applications, that I have studied during my research. The second part of the thesis contains my three published papers and two submitted manuscripts. The papers include rapid high-throughput investigation of solid phase extraction (SPE) protocols using a miniaturized platform developed at the department, the ISET platform, a sample preparation platform for MALDI-MS. This platform facilitates the usage of very small amounts of sorbents, samples and buffers (Paper I). Later, 384-well filter plates were chosen as a platform for the screening of SPE sorbents (Paper II), as this platform provides increased bed volume, and thus binding capacity (needed to enable use of low-affinity materials), also filter plates facilitates use with analysis techniques, for example, liquid chromatography–electrospray ionization mass spectrometry (LC ESI-MS). However, the key challenge with these multi-parametric experiments is how to best organize, simplify, visualize and analyse the data while retaining the relationships among the different samples/parameters. To address these challenges, a comprehensive informatics tool for MALDI was developed to facilitate the visualization, statistical analysis, and high quality image and data export (Paper III).

Apart from the miniature platforms, a conventional cartridge based investigation of in-house developed SPE materials was also undertaken in Paper IV. In Paper V, describes a newly prepared molecularly imprinted polymer micro gel (MIP MG); stabilized Pickering emulsions (PEs) for the ability to catalyse the formation of disulphide bonds in peptides at an Oil/Water interface.

# Biomarker

A “biomarker”, is clinically used to screen, diagnose or monitor the activity of diseases and predict the response of treatments. Biomarkers have “a characteristic that is objectively measured and evaluated as an indicator of normal biological processes, pathogenic processes, or pharmacologic responses to a therapeutic intervention” [1].

Historically, physical, physiological and molecular characteristics have long been used as “biomarkers”, this includes for example, pulse and blood pressure, however, the term is now typically synonymous with molecular biomarkers. Molecular biomarkers can be organized into categories based on their molecular class, which include protein, genomic (DNA and RNA), lipid, carbohydrate, and metabolites. These can be further classified into subcategories, that in turn contain specific molecular entities. Analysis methods can range from transcriptional profiling and DNA methylation studies which have shown strong potential for biomarker discovery in cancer [2], to metabolomic approaches as demonstrated for metabolic disease, drug and toxicity studies [3]. Proteins are likely to be the most affected entities during a pathological condition, and protein biomarkers have become one of the most valuable classes of biomarkers over the past years. As a consequence, proteomics holds special promise for biomarker discovery [4].

Protein biomarkers are sourced from various bio-samples, including blood, saliva, urine, faeces, cerebrospinal fluid, amniotic fluid, tissue/cells, etc. Among them, bio-fluids such as, blood serum and plasma are particularly attractive for clinical studies due to ease of accessibility, availability and the potential for development of large-scale, prognostic and diagnostic tests [5,6]. However, the extremely large dynamic range of protein concentrations of up to 12 orders of magnitude presents a number of challenges in biomarker determination from serum or plasma [6].

Within this thesis, I have studied and developed sample preparation methods for enrichment of phosphorylated compounds which are suggested as biomarkers for neurodegenerative diseases (Paper I), for alcohol over-consumptions (Paper IV); and pro-gastrin releasing peptide (ProGRP), a small cell lung cancer biomarker (Paper II).

## Phosphoproteomics

Phosphoproteins/phosphopeptides derived from phosphorylation, plays a major role in regulation of intracellular biological processes, such as signal transduction, degradation of proteins and cell survival, transcriptional and translational regulation, and metabolism [7,8]. Hence, changes in phosphorylation patterns can be an indicator of diseases such as cancer and neurodegeneration.

## ProGRP

Progastrin-releasing peptide (ProGRP) is a biomarker for small cell lung cancer (SCLC) [9]. It is a precursor of a neuropeptide hormone called gastrin-releasing peptide (GRP), a member of the bombesin family and is frequently produced by SCLC cells [10]. ProGRP is in particular used clinically to distinguish SCLC from other lung cancers by histology [11].

## PEth

In the cell membrane, a reaction between phosphatidylcholine and ethanol catalysed by phospholipase D leads to the formation of phosphatidylethanol (PEth), a non-endogenous phospholipid that can be used as a marker for alcohol abuse [12-14]. This group of phospholipids have a common polar head group, phosphoethanol and a long chain of carboxylic acid moieties attached at positions sn-1 and sn-2, which typically contains 14 to 22 carbon atoms with 0 to 6 double bonds as substituents [15,16]. Among these different species, PEth-16:0/18:1 and PEth-16:0/18:2 (Nomenclature: 'PEth-16:0/18:1'; 16,18 - number of carbons and 0,1 - number of double bonds) are the major species, and account for more than 60% of the total PEth in the blood [17]. The half-life of PEth in the blood is about 4 days and it can be found even after 14 days of alcohol abstinence. With this slow degradation rate, as well as higher sensitivity (94.5-100%) and specificity (100%) than other established markers [18,19], PEth has been suggested as an effective alcohol abuse marker, with a blood concentration reference value for alcohol overconsumption of 0.3  $\mu\text{M}$ .



# Sample Preparation

The biological samples are obtained from patients in the form of various body fluids such as blood, urine, cerebrospinal fluid, tissues, and biopsies or even tear fluid. These materials are very complex in terms of peptide and protein composition, and often have the analytes present in low concentration, and contains huge background of, salts, acids, bases and organic compounds [20]. These samples require a reduction of their complexity in order to improve detection of low-abundance protein and peptide biomarkers. Also, samples need to be made compatible with the analytical read-out, as most of the instruments are not directly compatible with the biological samples.

Sample preparation is a crucial step to extract, isolate and concentrate the analytes of interest. The employed methods are expected to be robust, reproducible, sensitive and selective, to ensure removal of salts, other impurities and depletion of high abundant interfering biomolecules [21].

Sample preparation methods varies from simple dilutions or protein precipitation techniques (PPT) [22] to complex multistep procedures involving liquid–liquid extraction (LLE) [23,24] or solid-phase extraction (SPE) or derivatization (chemical modification) of the analyte, affinity capture with antibody, etc.,

## Solid Phase Extraction (SPE)

Solid Phase Extraction (SPE) is one of the most common and popular sample preparation techniques, due to the high enrichment factor, good recovery, low consumption of organic solvents and the possibility to automate (off- or on-line) the whole process [25,26]. The high flexibility and throughput of SPE has facilitated application in many different fields such as; environmental, drug analysis, proteomics, and DNA analysis for purification, enrichment, desalting and fractionation [27,28].

## Mechanism of the SPE Process

The SPE process involves separation of analytes between a liquid and a solid (sorbent) phase. This technique enables concentration and purification of analytes from solution by sorption on a solid sorbent and purification by washing prior to elution.

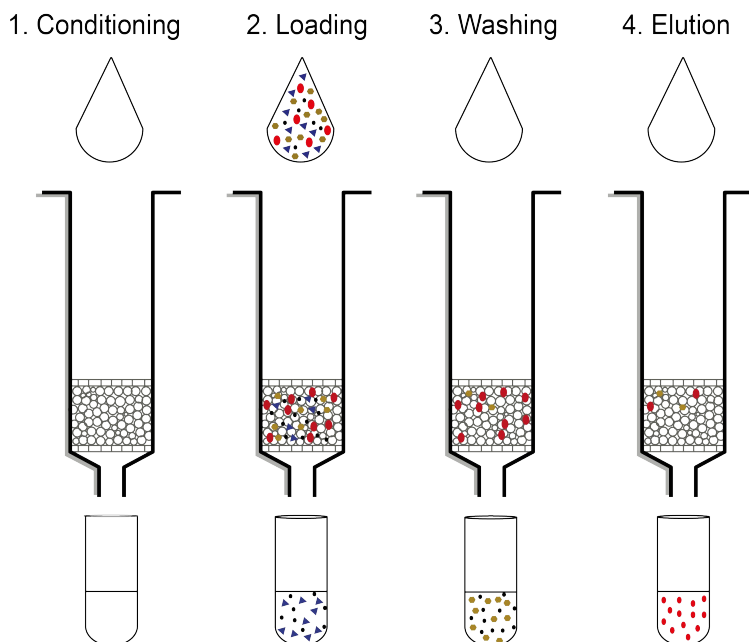


Figure 1. The four processing steps in the operation of SPE experiment.

The general SPE procedure involves four steps (Figure 1), the first step involves conditioning i.e., rinsing the sorbents with a suitable solvent, followed by equilibration using a solvent similar to the sample solvent. This step is crucial, as it enables the wetting of the sorbent, removes the air present in the column and fills the void volume with solvent. This step also serves to remove any impurities initially contained in the sorbent or the packaging. The nature of the conditioning solvent depends on the nature of the solid sorbent. When non-polar hydrophobic sorbents are used, rinsing with certain solvents, e.g., methanol or acetone, helps in wetting of the sorbent. As these sorbent materials, do not allow water to approach their surface easily. Care must also be taken to avoid drying of the sorbents between the conditioning and the sample treatment steps, to retain good recovery. If the sorbent dries for a prolonged time, it must be reconditioned.

The second step is the actual extraction step. Sample solution is introduced onto the SPE column, where the analytes encounter various attractive forces from the sorbent. These forces may be van der Waals forces (“non-polar interactions”), hydrogen bonding, dipole-dipole forces (“polar” interactions), or cation-anion interactions (“ionic” interactions). Each sorbent offers a unique mix of these properties which can be applied to a wide variety of extraction problems.

The third step involves an appropriate washing solvent, having a low elution strength, to wash away undesired components, that interfere or are not of interest and need to be removed from the sorbent.

The fourth and final SPE step involves the elution of analyte(s) of interest with a solvent that overcomes the retention interactions between sorbent and analytes of interest. Common solvents used for this step are methanol, acetone, ethyl acetate, or a buffer of different pH. In this step, the solvent volume and flow-rate should be adjusted so that quantitative recovery of the analytes is achieved with subsequent low dilution, for an efficient elution.

## **Different sorbent materials**

Over the years, a wide variety of sorbents, ranging from the traditional reversed-phase sorbents (C18, C8), normal phase (silica, alumina), and ion exchange, to mixed-mode (ion exchange + reversed phase) and functionalized resins based on styrene-divinylbenzene (SDVB) polymers have been developed and used in SPE. Also, affinity phases that separates analyte molecules based on their biological functions (antibodies, proteins, nucleic acids) or chemical structures (IMAC) have also been utilized as SPE sorbents (Table 1).

### *Silica particles*

The most common types of SPE sorbents are either silica-based or polymer based sorbents. The silica-based sorbents are mainly used in the case of nonpolar or medium polar analytes [26]. Silica particles chemically modified with appropriate functionalities for the intended application, e.g., polar functional groups like cyano, amine-, and diol- are added to the silica sorbent surface for normal phase SPE, while the octadecyl, octyl, cyclophenyl, or phenyl groups are added to the silica sorbent surface for reversed phase SPE [29].

However, the presence of residual silanol groups is common, this provide polar adsorption sites and makes the surface weakly acidic [27]. End-capping is often used to block these free silanol groups, commonly with methyl groups. However,

the end-capping process never completely eliminates all the silanols [30]. This remaining percentage has been found to vary among manufacturers of bonded silica. Particle chemistries can play an important role in the selectivity for many basic analytes [31]. Disadvantage with silica-based sorbents is that they are not very stable outside the pH range 2-8 [29]. Also, many silica-based materials contain “fines”, small (nm) particles that can leak during the sample preparation.

#### *Polymer-based sorbents*

Among organic polymer-based sorbents, the most widely used is porous polystyrene-divinylbenzene (PS-DVB) [32]. These sorbents display a hydrophobic structure and its interactions with analytes are mainly due to  $\pi$ - $\pi$  and van der Waals forces, involving the aromatic rings of the polymer. These sorbents have the advantages over silica-based sorbents that they are stable over a large pH range and often have higher surface areas. Also, these polymer sorbents impart a different selectivity than silica-based sorbents by nature of the aromatic rings and vinyl groups in its chemical structure. Thus, polymer sorbents can adsorb a wider range of analytes in general; some more polar analytes can be captured compared with traditional reversed phase bonded silica sorbents.

However, both PS-DVB and hydrocarbon modified silica sorbents have hydrophobic surfaces, which must be conditioned and activated to be compatible with aqueous samples [33]. Also, undesirable shrink-swell characteristics of PS-DVB copolymers have hampered their universal acceptance for SPE applications. To improve their compatibility with aqueous samples and increase the retention of polar compounds more hydrophilic polymer sorbents have also been developed [34]. These hydrophilic sorbents can be obtained by the introduction of hydrophilic precursor monomer or chemically modifying the PS-DVB polymer skeleton.

#### *Mixed-mode ion-exchange sorbents*

Initial ion-exchange sorbents were silica-based sorbents. These are prepared by chemical modification with ion-exchange groups. e.g., sulphonic acid for strong and carboxylic acids, for weak cation-exchange interactions, quaternary amines for strong anion-exchange interaction, and secondary and tertiary amines for weak anion-exchange interaction. However, these sorbents suffer the same problems as conventional silica-based sorbents mentioned previously.

Recently, the mixed-mode polymeric sorbents were developed, which combine a polymeric skeleton with ion-exchange groups, they can present two types of

interaction mechanisms: reversed-phase and ionic-exchange [35,36]. These sorbents are classified as cationic or anionic, and as strong or weak ion-exchange, depending on the ionic group attached to the resin. Each of these groups is designed to selectively extract analytes with certain chemical properties (i.e. strong/weak acidic or basic). However, the selectivity of the extraction process depends on choosing not only a suitable sorbent but also a suitable SPE protocol [37].

#### *Immobilized metal ion affinity chromatography (IMAC)*

Immobilized metal ion affinity chromatographic (IMAC) sorbents utilize the affinity of positively charged metal ions to isolate negatively charged analytes, e.g., phosphopeptides. In this approach, metal ions such as  $\text{Fe}^{3+}$ ,  $\text{Ga}^{3+}$  or  $\text{Ni}^{2+}$  are grafted onto the supporting substrate with a chelating ligands such as imidoacetic acid (IDA) and nitrilotriacetic acid (NTA), and acts as a stationary phase to which phosphopeptides in a mobile phase can bind [38]. Initially, this technique was used for the fractionation of proteins based on the affinity of histidine and cysteine residues to the IMAC resin [39]. Later, the binding of phosphoproteins and phosphoamino acids to metal ions, extended the IMAC utilization towards phosphopeptide enrichment [40]. However, the chelating ligands also bind to the carboxylic and amino groups, resulting in the enrichment of acidic peptides and peptides containing histidine [41,42]. Methyl-esterification of the carboxyl group prior to IMAC enrichment is one method used to reduce the non-specific binding. Although, the approach is limited due to sample losses and additional complexity caused by side reactions [43-45]. Higher enrichment factors for phosphopeptides have been obtained by using a loading buffer at pH 2–2.5, as most acidic amino acids will be protonated and cannot be bound to the positively charged metal ions, while most phosphate groups are still deprotonated, so they are able to bind to the positive metal ions [46].

#### *Metal oxide affinity chromatography (MOAC)*

As an alternative to IMAC, Metal oxide affinity chromatography (MOAC) exploits the affinity of metal oxide surfaces for phosphate groups and appears to have fewer limitations than IMAC [47]. Metal oxides, which have amphoteric properties based on unsatisfied valences show Lewis acid/base behaviour at different solution pH values [48], providing a reversible bidentate bridging binding between the amphoteric surface of the metal oxides and the phosphate groups [49-51]. The specificity of MOAC toward phosphopeptides using, for instance,  $\text{TiO}_2$  [41,52-54],  $\text{ZrO}_2$  [55,56],  $\text{Ga}_2\text{O}_3$  [57],  $\text{Nb}_2\text{O}_5$  [58],  $\text{ZnO}$  [59],  $\text{Al}_2\text{O}_3$  [60], and  $\text{SnO}_2$  [61] is higher than that of conventional IMAC sorbents. However, both

IMAC and MOAC approaches use metal cations to bind the negatively charged phosphopeptides, and protocols designed to achieve higher enrichment efficiencies have been constantly improved over the past decade.

**Table 1: Different SPE retention mechanisms, materials type and target analytes**

SPE Type	Retention Mechanism	Material	Target Analytes
<b>Reversed-phase</b>	<ul style="list-style-type: none"> <li>- Non-polar or hydrophobic interactions</li> <li>- Van der Waals or dispersion forces</li> </ul>	C3, C4, C8	Proteins
		C18	Peptides
<b>Normal phase</b>	<ul style="list-style-type: none"> <li>- Polar interactions</li> <li>- Hydrogen bonding, <math>\pi</math>-<math>\pi</math>, dipole-dipole and induced dipole-dipole</li> </ul>	ZIC-HILIC	Glycoproteins, glycopeptides
		Waters HILIC	Proteins, peptides
<b>Ion-exchange</b>	- Electrostatic attraction	WCX, SCX, WAX, SAX	Proteins
<b>Metal-chelating</b>	- Metal affinity, metal oxide affinity	Ti, Fe	Phosphopeptides
		Ga	Phosphopeptides
		Cu	(Phospho)peptides
<b>Affinity</b>	- Molecular recognition	Lectin	Glycans, glycopeptides
		Heparin	IgG
		RNA/DNA	Plasmids, DNA binding proteins
		Coenzymes	Coenzyme-dependent enzymes
		Antibodies	Proteins, peptides

### *Immunosorbents*

Molecular recognition processes are highly specific and can be applied in vitro for several purposes not only related to biochemical procedures, but also to other fields including specific or highly selective media for SPE. This type of sorbents includes immunosorbents, molecularly-imprinted materials, and aptamer-functionalized sorbents. Among the molecular recognition phases, immunosorbents based on immobilized antibodies generally display a high selectivity to target molecules [62,63]. Immunosorbents can extract and isolate the target analyte from complex matrices in a single step, thus avoiding the problems of co-extraction interferences [63]. The production of immunosorbents involves, the design of

antibodies capable of recognizing one or a group of analytes of interest. Once the antibodies are obtained, they are covalently bonded to a sorbent [64]. Although widely used, their application suffers from draw-backs such as antibody stability, availability, also time-consuming and expensive production [65].

### *Molecularly imprinted polymers*

An optional sorbent material for SPE are molecularly imprinted polymers (MIPs), which have attracted attention due to advantages, such as predetermined recognition ability, stability, relative easy and low cost manufacture, as well as applicability to a wide range of target molecules [66,67].

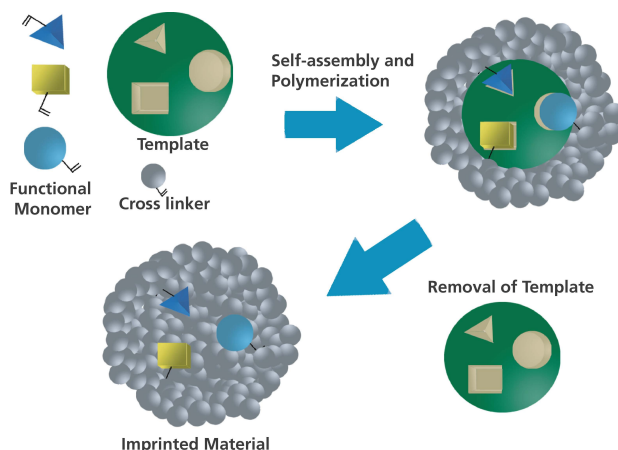


**Figure 2. Schematic representation of the different steps involved in the preparation of Molecularly Imprinted Polymers (MIP).**

The MIPs are made by synthesizing highly cross linked polymers in the presence of a template molecule facilitating the alignment of functional groups in a specific arrangement with polymer (Figure 2). Their recognition is due to the shape and different physicochemical properties, such as hydrogen bonding, ionic and hydrophobic interactions. Mostly, MIP-SPE is performed as an off-line method. A small amount of imprinted polymer (typically 15–500 mg) is packed in cartridges, and then through conditioning, loading, washing, and elution steps, the target compounds can be isolated. In the case of MIPs, the most successful applications have been for low molecular weight targets in non-aqueous systems [68,69], but recent developments in the MIP preparation process, including monoliths [70-72] and epitope targeting strategies [73-75], have expanded the technology to encompass biomolecule affinity applications such as proteins [75-77] and peptides [78-81].

## The formats and procedures in SPE

Optimization of the SPE sample preparation step is crucial for high-sensitivity detection, as well as analysis robustness and reproducibility. The SPE optimization process for a certain analyte usually starts with, screening for a suitable extraction phase or if the appropriate extraction phase is known, with the fine tuning of the sample preparation conditions i.e. the loading, washing and elution steps.

Current methods used for SPE screening and optimization are often based on any of the four widely available SPE formats [82] (Table 2); (1) SPE Disks, in which sorbent is immobilized; (2) Cartridges in which the sorbents are filled in a small, plastic or glass open-ended containers [83,84]; (3) 96-well microtiter plate or filter plate configurations, where a defined volume of sorbent is loaded into each well in the form of plaques or slurries in microtiter filter plate that mimics the standard 96-well microtiter plate [85] and (4) SPE pipette tips, in which sorbent is immobilized inside a pipette tip [72,86].

**Table 2. Comparison of formats and devices used in SPE**

	Cartridge	Disks	Pipette tips	Multiwell plates
Sorbent mass	g-mg	mg	mg- $\mu$ g	$\mu$ g
Solvent volume	mL	mL- $\mu$ L	$\mu$ L	$\mu$ L
Extraction time	+++++	++	+++	++
Flow rate	+++++	++++	+++	++
Parallelisation	8, 12 or 96	8,12 or 96	8, 12 or 96	96, 384
Operation	manual	manual	semi-automatic	semi-automatic or automatic
Cost	++++	+++++	+++	++



# ISET

The Integrated Selective Enrichment Target (ISET) is a sample preparation platform made of silicon, with 95 pyramidal array positions. In the original design each position could be filled with a SPE capture medium volume of max 0.6  $\mu\text{L}$ . The small bead volume required for filling the nanovials allows for convenient SPE optimization, as more than 500 samples (96 samples/ISET) can be subjected to SPE on the ISET platform using only 25 mg of stationary phase, i.e., less than the amount present in an ordinary 1 mL SPE cartridge. At the same time the parallelization provided by the ISET platform facilitates multiplexed testing of different SPE materials or sample preparation conditions with enough replicates to ensure the validity of the developed SPE protocol. For example, by using different solution protocols column-wise with respect to different SPE materials row-wise the ISET arrays enables easy, high-throughput and very economic multiplex optimization of the sample preparation protocol, Figure 3.

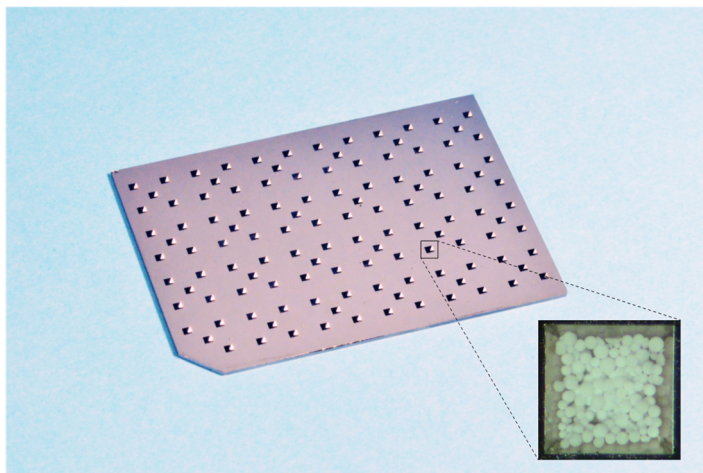


**Figure 3.** A photograph of an ISET chip produced in silicon. Every 4 positions have a central vial as a MALDI reference position for control samples.

The ISET chips were manufactured by anisotropic wet etching and deep reactive ion etching (DRIE) by GeSiM (Großberkmannsdorf, Germany) from 780  $\mu\text{m}$  thick 4" silicon wafers. During the sample preparation steps the ISET chip fits into a vacuum fixture made from an ordinary 384 microplate, Figure 4A, which facilitates use with commercial liquid handling robots and vacuum manifolds. Before insertion in the MALDI instrument the ISET was secured in a steel adaptor using tape (3M, 7955 MLP), Figure 4B, providing the same spot positioning as a normal MALDI target.

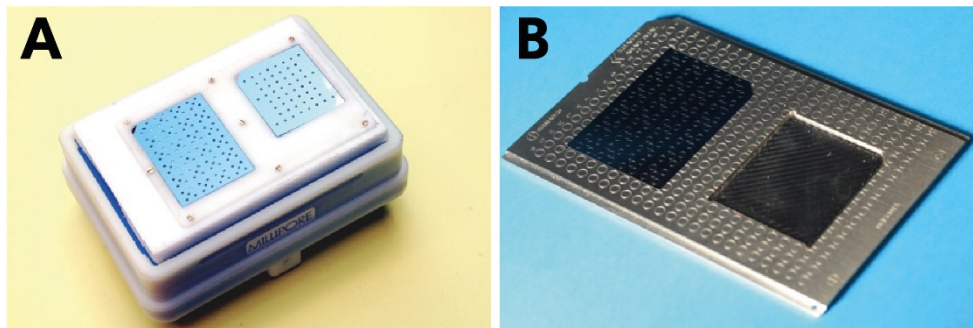


**Figure 4. (A) ISET chips (95 and 48 position) in a vacuum holder, (B) in-house adapted standard 384 MALDI plate with positions for a 95 and a 48 position ISET.**

## ISET – MIP sample preparation

All the SPE steps were performed using vacuum to enable liquid transport. Prior to loading the ISET nanovials the MIP particle concentration was adjusted in a test ISET so that a 2  $\mu\text{L}$  MIP slurry addition to a sample resulted in a final nanovial packing volume of 500-600 nL. During the final sample elution, the vacuum was lowered to allow surface tension to retain the analytes in a small spot around the outlet hole, this facilitated a confined crystallized MALDI spot on the underside of the ISET after matrix addition, Figure 5B. The ISET was subsequently turned upside down and used as a MALDI target plate. Figure 5A, depicts the general steps of the ISET sample preparation.

### ISET MIP SPE protocol

1. MIP material corresponding to a SPE volume of 500-600 nL was added to each sample in a microplate or standard Eppendorf tube and incubated for 90 min.

2. The captured analytes were transferred while bound to the MIP's to the ISET by aspiration of sample/MIP from the bottom of the container and then loaded into the ISET using a high vacuum (10-15 in Hg).
3. 5 x 2  $\mu$ L washing buffer was added to each well with a high vacuum (10-15 in Hg).
4. Turn off vacuum and remove the ISET chip from the vacuum fixture and rinse the entire underside of the chip with MQ water and ethanol. Dry the underside with a clean tissue.
5. For elution of the bound analytes, 2 x 1  $\mu$ L of elution solution was added with a low vacuum (1.5-2 in Hg).
6. Add 500 nL matrix solution: 2.5 mg Dihydroxybenzoic acid (DHB) (10 mg/mL DHB in 80% MeOH) in a low vacuum (1.5-2 in Hg).
7. The ISET was subsequently removed from the vacuum fixture turned over with matrix spots facing upwards, and placed in a MALDI adaptor plate for MS analysis.

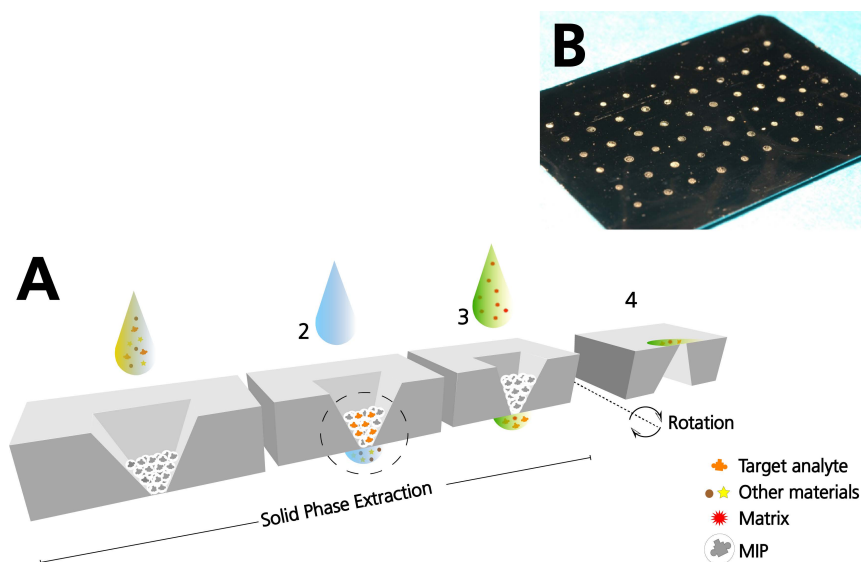


**Figure 5.** (A) The ISET sample preparation process. The analytes are applied to the SPE material (1) and washed to get rid of contaminants (2), and then the analytes are eluted with matrix (3) and crystallized on the backside of the ISET (4). (B) Back side of the ISET plate with well confined analyte crystal spots.

# 384-well filter plate

## 384-well filter plate – MIP sample preparation

Different MIP/NIP phases were tested in a 384-well platform (Figure 6). Many conditions were tested with more than 100 samples analysed to understand the nature of the unspecific background. Although the 384-well format has been extensively utilized for immunoassays and in vitro receptor binding studies, its use in SPE is relatively new. The 384-well filter plates used are either MultiScreen HTS 384-well filter plates from Millipore made of styrene acrylonitrile (SAN) with polyvinylidene fluoride (PVDF) membrane/polyester support or AcroPrep 384-well filter plates from Pall Life Sciences made of polypropylene (SAN) with glass fibre (borosilicate glass, 1.0  $\mu\text{m}$ ) membrane. Thermo Scientific (Waltham, MA) Nunc plates made of polystyrene were used as collection plates. Millipore MultiScreen® HTS Vacuum Manifold used to carry out the SPE. The whole SPE process is carried out in automation with Biomek® 3000 Workstation as in Figure 7.

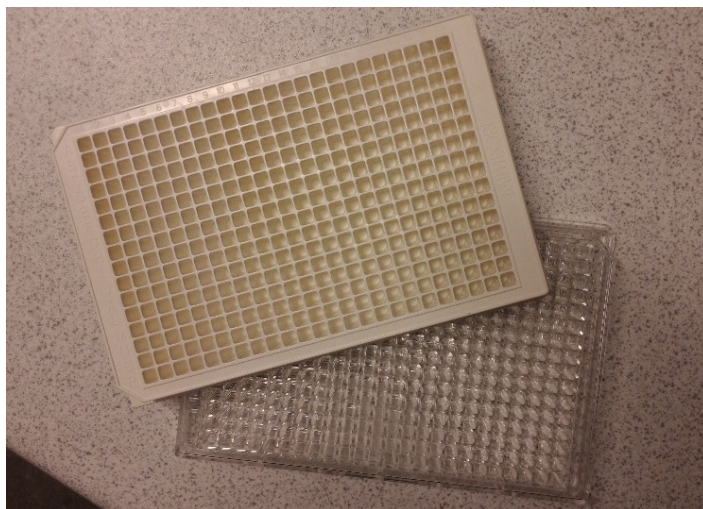
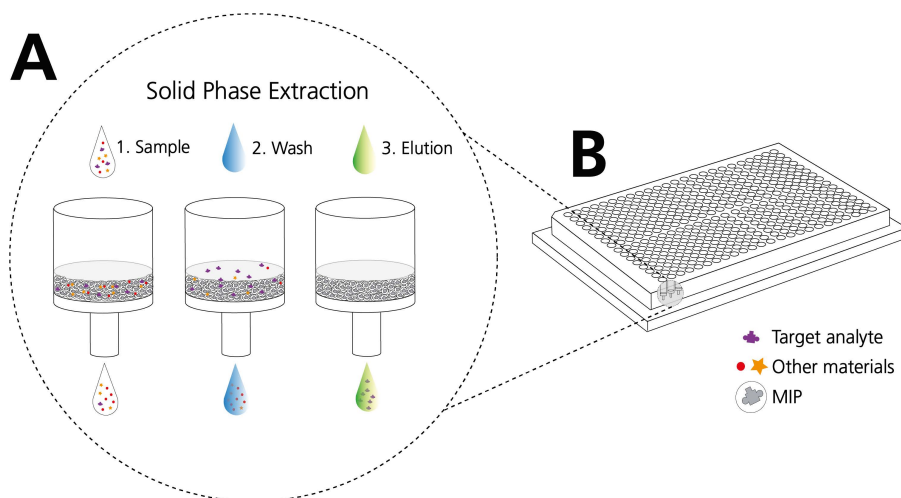


Figure 6. A photograph of a 384-well filter plate and a collection plate

### 384-well filter plate MIP SPE protocol

1. A fixed vacuum of 10–15 in Hg, was used for filling the wells with 20  $\mu\text{L}$  of MIP/NIP material.
2. Wash, 2 X 60  $\mu\text{L}$  of acetonitrile (ACN) was subsequently pulled through the wells.
3. Conditioning with 2 X 60  $\mu\text{L}$  of methanol (MeOH) followed by 2 X 60  $\mu\text{L}$  of 50 mM ABC buffer.
4. 20  $\mu\text{L}$  sample in loading buffer was added to each well.
5. 80  $\mu\text{L}$  of wash buffer was added to each well
6. For elution of the bound analytes 80  $\mu\text{L}$  of elution solution was added.
7. During the transfer of washing and elution buffers the vacuum was turned off and then turned on after the addition to facilitate a homogeneous wetting of the SPE bed.
8. MS analysis was performed on the collected fractions.



**Figure 7.** Schematic representation of the 384-well filter plates and the workflow of the SPE. (A) 384-well filter plate. (B) SPE sample preparation, where the sample is transferred to the microwell loaded with SPE material (1), followed by a wash step to remove undesired components (2), and the captured analytes are then displaced by the elution step (3).

# Mass Spectrometry

A mass spectrometer can determine the molecular weight of chemical compounds by ionizing, separating, and measuring ions per their mass-to-charge ratio ( $m/z$ ). The ions are generated in the ionization source by inducing either a positive or negative charge. Once the ions are formed in the gas phase they can be directed into a mass analyser, separated per mass and finally detected. The result of ionization, ion separation, and detection is a mass spectrum that can provide molecular weight or even structural information.

Development of the first mass spectrometer-like instrument dates to 1912, when the British Physicist Sir Joseph John Thompson constructed a "mass spectrograph" and managed to obtain mass spectra for  $O_2$ ,  $N_2$ ,  $CO$ ,  $CO_2$  and  $COCl_2$ . This instrument paved the way for the development of more advanced mass spectrometers. Ionization of the analytes is fundamental for the analysis and the first ionization techniques that were used required the analyte to be present in gas phase, limiting the analysis to small and volatile compounds. The possibility to use MS for the analysis of large and polar biomolecules such as proteins was not realized until several decades later.

In the 1980s, however, two new 'soft' ionization techniques, Matrix-assisted laser desorption ionization (MALDI) and electrospray ionization (ESI) were developed roughly at the same time by Michael Karas and Franz Hillenkamp [87] and John Fenn [88], this made it possible to study larger biomolecules such as peptides and proteins. Since then the MS technology has kept on developing at a high speed, and has now become an important tool for characterization and identification of proteins and peptides from biological samples can now be performed with an unprecedented speed and sensitivity.

## Mass spectrometry for protein identification

Protein identification via MS is carried out either in the form of whole-protein analysis ('top-down' proteomics) or analysis of enzymatically/chemically produced

peptides ('bottom-up' proteomics) [89]. Bottom-up or shotgun proteomics is the most common MS-based method for studying proteins.

### **Bottom-up proteomics**

Bottom-up proteomics studies are usually conducted by either a 'Sort-then-break' approach or by a 'break-then-sort' approach. In 'Sort-then-break' approach, a mixture of proteins is isolated using off-line protein fractionation and a proteolytic enzyme is used to cleave protein (digestion), followed by direct peptide analysis using 'peptide mass fingerprinting' (PMF) [90] or further peptide separation by LC interfaced to a tandem mass spectrometer. In the latter approach, commonly referred to as 'shotgun proteomics', protein digestion is performed prior to the separation using chromatography and other methods followed by tandem mass spectrometric analysis. A subsequent database search for the detected peptides is carried out to identify and confirm the protein present in the original sample.

For complex protein mixtures, PMF might not distinguish two peptides of equal mass and charge. For such cases, tandem MS or MS/MS setup is used to determine amino acid sequences of the peptides [91]. This kind of setup is also referred as "tandem in space", as the different mass analysers are connected in sequence to perform MS scan, fragmentation and MS/MS analysis. Alternatively, a "tandem in time" setup can be used, here a single trapping instrument to perform all the MS analysis steps (ion trap and orbitrap) [92]. More information about these setups will be provided in the mass analyser section.

However, not all peptides resulting from the digestion of a protein can be observed or correctly identified with MS analysis, especially those with diverse or unexpected modifications. Also, due to differences in ionization efficiency not all peptides will be detectable in the mass spectrometer and therefore complete sequence coverage will very rarely be obtained.

### **Top-down proteomics**

In this approach, intact protein ions are fragmented in the mass spectrometer to generate detectable fragment ions. Theoretically, this approach places the entire sequence of the protein under examination, and consequently the top-down approach should enable a more complete characterization of protein isoforms and any post-translation modifications (PTMs) than the bottom-up approach [93]. In addition, the exclusion of the protein digestion step is beneficial from a time and cost perspective. Although the top-down approach is powerful in protein modification analysis, due to the increased complexity of the fragment ions, it is

primarily performed with direct infusion of a single protein or simple protein mixture [94].

## Mass spectrometry Instrumentation

In MS, proteins are analysed based on their mass and charge. The instrumentation consists of three parts: an ionization source, a mass analyser and a detector (Figure 8).

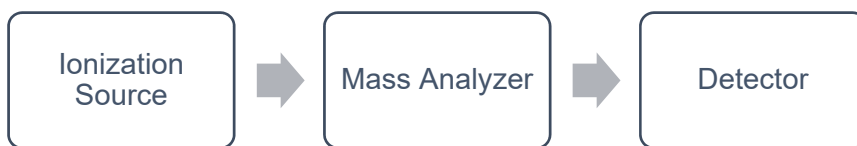


Figure 8. Mass spectrometry instrumentation

### Ionization techniques

Ionization is the first step of the process, where the analytes from the liquid or solid phase are converted into gas-phase ionized species. The choice of the ionization source can significantly impact MS analysis. It was shown that by varying the ionization, different set of serum metabolites could be identified [95]. And also, quantitative data were altered in terms of lower limit of quantification and the linear range [96]. Usually the ionization technique is selected based on the structure of the analyte of interest as well as the desired application.

For analysis of biomolecules such as proteins and peptides using MS, an efficient and non-destructive ionization method is required. Electrospray ionization (ESI) and matrix assisted laser desorption ionization (MALDI) are commonly used soft ionization techniques that can ionize analytes with little or no fragmentation. For instance, in Paper I, II, III and V we have used MALDI and ESI in Paper II and IV, hence these modes are briefly described further.

#### *MALDI*

The MALDI technique was introduced principally by Karas and Tanaka in 1987, which were awarded part of the 2002 Nobel Prize in Chemistry. MALDI has since become a widespread and powerful technique for generating intact gas-phase ions



from a wide variety of large thermally labile compounds including proteins, oligonucleotides, synthetic polymers and large inorganic compounds.

The MALDI technique is a two-step process. In the first step, the sample is pre-mixed with a UV-light absorbing matrix solution, usually weak organic acids. The matrix-analyte solution mixture is then dried to remove any liquid solvent. The result is a co-crystal of matrix-analyte where the analyte molecules become incorporated into the matrix crystals so that they are completely isolated from one another. The second step, which occurs under vacuum conditions inside the ion source, involves irradiation of the matrix-analyte mixture with intense UV laser (337 nm) pulses. The exact mechanism of the process is still not fully understood [97]. However, as shown in Figure 9, one theory is that irradiation by the laser induces rapid heating of the co-crystals through the accumulation of a large amount of energy resulting in the vaporization of the matrix. The analyte molecules within the co-crystal vaporize as well but without having to directly absorb energy.

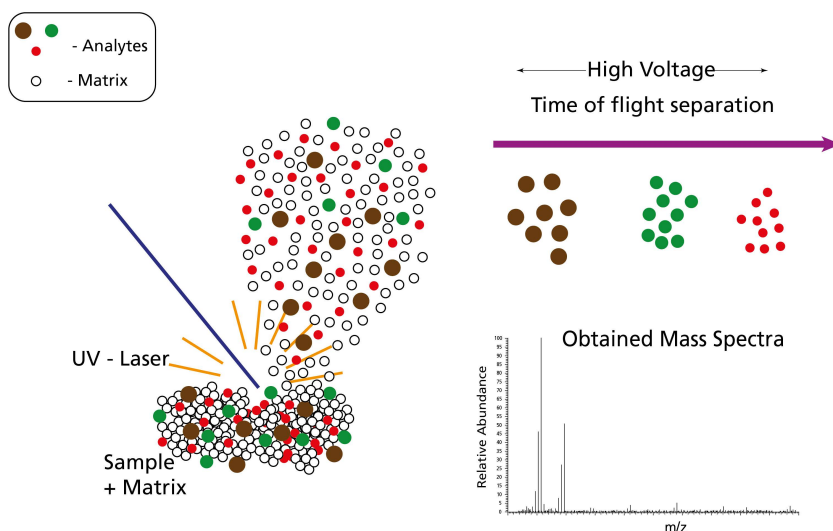


Figure 9. Schematic representation of the different steps involved in MALDI.

The matrix which consists of an organic solid or liquid species, performs two important functions: (1) it absorbs photon energy from the laser beam and transfers it into excitation energy, and (2) it serves as a solvent for the analyte, so that the intermolecular forces are reduced and aggregation of the analyte molecules is kept to a minimum. The matrix is usually a solution of organic molecules. Typically examples of MALDI matrices are  $\alpha$ -cyano-4 hydroxycinnamic acid (CHCA), 3,5-

dimethoxy-4-hydroxycinnamic acid (sinapinic acid), 3-amino-4 hydroxybenzoic acid and 2,5-dihydroxy-benzoic acid (DHB).

MALDI is widely used in proteomic research as it is characterized by easy sample preparation and has relatively large tolerance to contamination by salts, detergents and buffers [98]. However, this technique has some limitations, such as low shot-to-shot reproducibility, and strong dependence on the sample preparation protocol [99].

## ESI

In mid-1980s, Fenn demonstrated the use of Electrospray ionization (ESI) as an interface for mass spectrometry [88], revealing the power of the technique and winning the Nobel prize for Chemistry in 2002. ESI is most widely linked to LC-separations in modern mass spectrometry, as it is a versatile mode to produce gas phase analyte ions from continuous flowing solutions and is almost ideal for biological analytes.

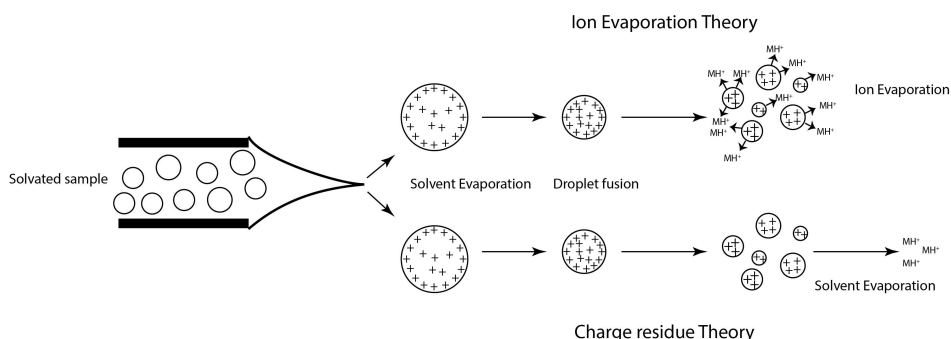


**Figure 10.** The formation of ions during electrospray ionization. The sample solution is passed through a charged capillary, resulting in the creation of charged droplets that evaporate with the aid of a stream of nitrogen. Coulomb explosion will break the highly-charged droplets into smaller ones and eventually ions are desorbed from the surface according to the ion evaporation theory or solvent is completely evaporated as speculated based on the charge residue theory. This scheme represents ions as positively charged; the same mechanism applies in the case of negative ion mode.

In ESI-MS, sample containing the analyte in a preferably polar solvent, is pumped at low flow rates into the ionization source under atmospheric pressure through a hypodermic needle. As the sample is being constantly sprayed, a high electrical potential is applied at the needle (3–6 kV), resulting in the formation of small, micro meter-sized monodisperse highly charged droplets (i.e., nebulization). The

dispersed droplets evaporate in the presence of a sheath gas, like nitrogen, and the resulting ions are drawn into a mass spectrometry inlet by the vacuum and the electric field.

Under these conditions, two different mechanisms have been proposed for the ion generation in ESI. In the first ion evaporation mechanism, the droplets break down and, while shifting inside the source, their size is continuously being reduced. Eventually, the repulsive forces, also termed the coulombic forces, among the ions on the surface of the shrinking droplets become very high. These forces will ultimately exceed the surface tension of the solvent, resulting in ions that desorb into the gas phase [100].

An alternative mechanism is the charge residue model [101]. This is supposed to be dominant in the case of ions with very high  $m/z$ , such as proteins [102]. This mechanism involves continuous evaporation of the solvent accompanied by droplet fragmentation so that a single ion (probably multiply charged) is formed at the end of this process (i.e., solvent is completely evaporated). Figure 10 illustrates the different proposed mechanisms of ion formation during the ESI process.

ESI is suitable for a wide range of compounds with high to moderate polarity as well as varying molecular weight. For large molecules with several ionisable sites such as proteins, ESI produces multiply charged ions that allow for their analysis in mass analysers with limited  $m/z$  range, such as quadrupoles. However, ion suppression is a major drawback when using ESI, because the presence of a high concentration of non-volatile compounds or analytes may change the efficiency of droplet formation or evaporation, which in turn inhibits ion release into the gas phase. In high concentration samples, the competition between compounds for limited charges or space on the droplet surface can also decrease the efficiency of ion formation.

## Mass analysers

The mass analyser is, literally and figuratively, central to the technology. Mass analysers are an integral part of each instrument because they can store ions and separate them based on the mass-to-charge ratios. Ion trap (IT), Orbitrap, and ion cyclotron resonance (ICR) mass analysers separate ions based on their  $m/z$  resonance frequency, quadrupoles (Q) use  $m/z$  stability, and time-of-flight (TOF) analysers use flight time of a fixed distance after accelerating species of different mass and charge across a potential. Each mass analyser has unique properties, such as mass range, analysis speed, resolution, sensitivity, ion transmission, and dynamic range; and each has its advantages and limitations. Several different analysers can

be combined in sequence forming so called hybrid instruments to increase the versatility and allow multiple experiments to be performed.

There are two broad categories of mass analysers: the scanning and ion-beam mass spectrometers [103], such as TOF and Q; and the trapping mass spectrometers, such as IT, Orbitrap, and FT-ICR. The scanning mass analysers like TOF are usually interfaced with MALDI to perform pulsed analysis, whereas the ion-beam and trapping instruments are frequently coupled to a continuous ESI source. The analysers used in the studies underlying this thesis are discussed below.

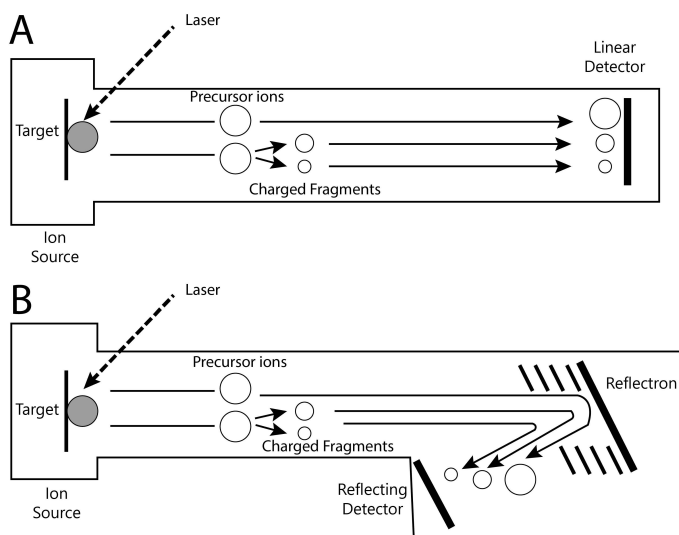


**Figure 11. Schematic diagrams of linear (A) and reflectron (B) MALDI-TOF mass spectrometers. The flight paths of precursor and fragment ions in each instrument are shown.**

### *TOF*

In TOF analysers the  $m/z$  ratio is determined by measuring the time it takes for an ion to fly a field-free flight in a tube between the source and the detector, as depicted in Figure 11. At the start of the flight tube all the ions have been accelerated by the same potential difference thus having gained the same kinetic energy. However, their velocities (and hence arrival times at the detector) will differ due to differences in their masses; an ion with a high mass will have a lower velocity than another ion with the same charge but lower mass. Thus, the time of flight of each ion depends on its  $m/z$  ratio. The major drawback of a linear TOF instrument is that it has insufficient mass resolution for many applications, due to small

variations in the initial kinetic energies of ions of the same  $m/z$ , leading to differences in the flight times.

To overcome this problem, “reflectance” using a reflection, as in Figure 11B, are commonly employed and were applied in the MALDI-TOF instrument used in Paper I. A reflectron is a series of rings or grids located after the flight tube used to focus ions of the same  $m/z$  but different kinetic energies. The reflectron creates a reversing field in which the ions enter to different depths depending upon their kinetic energies and are then reflected back to the flight tube. Ions of the same  $m/z$  but higher kinetic energies spend more time in the reflectron, whereas those with lower kinetic energy return to the flight tube more quickly, thus their spread is reduced and the resolution improved.

In comparison to triple quadrupoles (3Q) instruments, discussed below, TOF instruments provide higher sensitivity in full-scan mode since they generally have a higher transmission of ions than a scanning analyser. They also have a higher resolving power than 3Q instruments, which facilitates discrimination of analytes with close  $m/z$  ratios. MALDI is usually coupled to TOF analysers that measure the mass of intact peptides or proteins, and those masses are matched to the theoretical peptide masses generated from a sequence database. Identification of proteins obtained in this way is known as peptide mass fingerprinting (PMF), or peptide mapping.

### *Triple Quadrupole*

Triple quadrupoles (3Q) are the most universal instruments for quantitative LC/MS analyses and were employed in Paper IV. A 3Q consists of three sequential quadrupoles (Q1 Q2 Q3) (Figure 12). Q1 and Q3 can be used as scanning or selecting analysers while Q2 is operated in the RF-only mode, as a wide-band filter for the ions or a collision cell when filled with a neutral collision gas such as nitrogen or argon. The transfer of kinetic energy from the stream of collision gas causes fragmentation of ions. This process is called collision-induced dissociation (CID). CID is the most often applied ion fragmentation method, but ion fragmentation can also be induced by techniques called electron capture induced dissociation or surface induced dissociation. In Q1 and Q3 the ions can be separated by their  $m/z$  values.

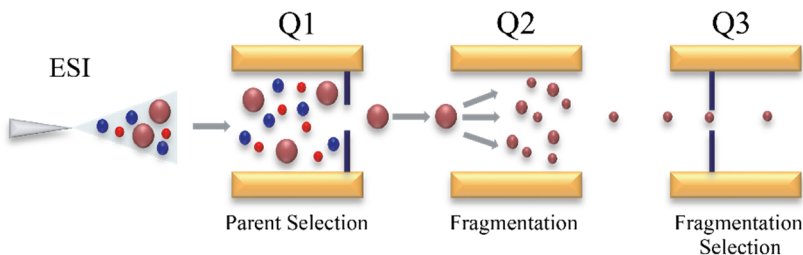


**Figure 12. Schematic representation of the different steps in triple quadrupoles**

A quadrupole consists of four cylindrical rods to which a fixed direct current (DC) and an alternating radio frequency (RF) are applied, creating a quadrupole field that only allows ions within a certain  $m/z$  range to pass through. The ions outside that  $m/z$  region hit the rods and discharge. The resolving power of quadrupoles is usually the same throughout their functional mass range, which is often up to  $m/z$  4000 Da. Several MS/MS modes, such as precursor ion, product ion or neutral loss scanning, and selected ion (SIM) or selected reaction monitoring (SRM), are available, depending on the Q1 and Q3 settings applied.

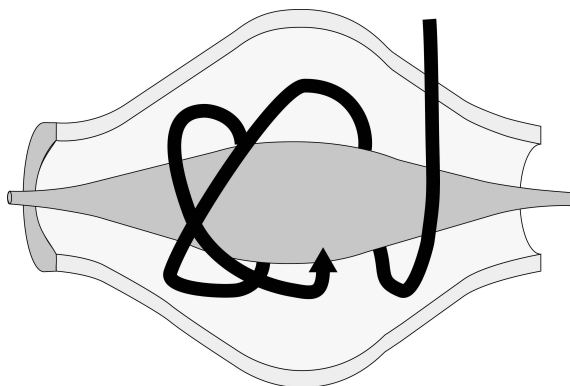


**Figure 13. Cross section of the Orbitrap analyser. Ion trajectories in an Orbitrap indicated by the black arrow.**

#### *LTQ - Orbitrap*

The orbitrap was introduced in 1999 [104] and is a high resolution electrostatic ion trap mass analyser. The Orbitrap mass analyser consists of three electrodes as shown in Figure 13, where the outer electrodes have the shape of cups facing each other and electrically isolated by a hair-thin gap secured by a central ring made of a dielectric. A spindle-like central electrode holds the trap together and aligns it via

dielectric end-spacers. Ions are injected into the volume between the central and outer electrodes. When a voltage is applied between the outer and the central electrode, incoming ions are trapped and they orbit around a central electrode, much like a planet in the solar system and oscillate harmonically along its axis (the z-direction) with a frequency characteristic for their  $m/z$  values, inducing an image current in the outer electrodes that is Fourier transformed into the time domain producing mass spectra [105,106].

When coupled to an LTQ ion trap, the hybrid instrument has the advantage of running in a parallel fashion: The Orbitrap acquires MS full scans while the LTQ carries out fragmentation reactions [107]. Compared to the quadrupole mass analyser, the LTQ - Orbitrap has a much higher resolving power (resolution) and mass range as well as better mass accuracy, while having a lower dynamic range. In addition, they can operate in two different detection modes. In the first mode, the Orbitrap mass analyser acquires the full MS spectra and the LTQ the MS/MS fragment ion spectra, also called the FT-IT mode. In the alternative mode, both the MS and MS/MS scans are analysed in the Orbitrap detector. This mode is referred to FT-FT. Several generations of Orbitrap mass spectrometers are currently available encompassing the Classic, XL, Discovery, Velos, Velos Pro and Elite. Fusion and Lumos are the latest.

## Detectors

The last component of the MS instrument is the ion detector, which records the ions separated per their mass to charge ratios. The detector registers the number of ions at each  $m/z$  value, by detecting their impact on the detector surface. The resulting measurement called mass spectrum consists of a plot of the mass-to-charge ratio ( $m/z$ ) versus its corresponding intensity value. In TOF instruments, the detector measures the differences in the flight times of the ions, thus a detector with faster responses is required. Micro channel plates (MCPs), consisting of two-dimensional parallel arrays of miniaturized electron multipliers, are the most commonly used detectors in TOF instruments. For the 3Q instruments, electron multiplier detectors and photomultiplier tube detectors are the most common kinds of detector. In a photomultiplier tube the ions exiting the mass analyser are converted to electrons, which travel through an electron multiplier and each electron induces the emission of several secondary electrons.

## Operation modes for quantification

In MS, the recorded ion current of the analyte molecule is used for quantification. While quantification can be performed in the SIM mode, there is a high risk of interfering molecules in a complex biological sample being co-isolated, since two completely different molecules can have identical  $m/z$ . In MS/MS, the precursor ion is isolated, fragmented and quantification is performed by monitoring specific fragments to increase selectivity [108]. An internal standard (IS) can be added to a sample to correct for variations in sample preparation and fluctuation in MS signal associated with analyte ionization and matrix effects. When coupled to LC, quantification is performed by integrating the area under the chromatographic peak acquired.

### *Selected reaction monitoring*

Selected reaction monitoring (SRM), sometimes referred to as multiple reaction monitoring (MRM), is a targeted MS/MS method that has been used for over three decades in small molecule analysis, and has also emerged as an alternative to immunoassays for protein and peptide quantification [109]. This type of targeted MS analysis is performed using a triple quadrupole mass spectrometer. The first quadrupole is set to transmit an ion (precursor ion) according to its  $m/z$ . The ion is then fragmented in the second quadrupole, filled with an inert gas (*e.g.*, argon or nitrogen), by collision induced dissociation (CID) as it collides with the gas molecules. The third quadrupole is set to transmit one or more specific product ions generated in the second quadrupole to the detector (Figure 12). The combination of a precursor ion and a specific product ion is referred to as a transition. SRM greatly increases selectivity compared to SIM, since interfering ions with identical  $m/z$  co-isolated in the first quadrupole will most likely not give rise to product ions with identical  $m/z$  to that of the analyte of interest [110].

### *Internal standard (IS)*

An IS, corresponding to the analyte to be measured, is used to control variability in the sample preparation and analytical procedure, depending on at which stage the standard is introduced. For absolute quantification of peptides, recombinant or synthesized peptides with incorporated stable isotopes such as  $^{15}\text{N}$  or  $^{13}\text{C}$  are most commonly used [111]. These standards, often called “heavy” standards due to their mass increase, are easily differentiated from the endogenous peptide in the mass spectrometer. Being chemically equivalent to the endogenous peptides, as their amino acid sequence is identical to the target peptide, they will have identical yield



through all sample preparation steps, co-elute with the target peptide during LC as well as having identical ionization efficiency and fragmentation behaviour in the mass spectrometer. Quantification is performed by extrapolating the concentration using the MS signal ratio of the endogenous peptide to the IS from a calibration curve constructed with known concentrations of the analyte.

**Table 3. Performance comparisons of the mass spectrometry instruments**

Instrument	Resolution	Mass accuracy ppm	Sensitivity	Range	Scan rate	Ion Source
TOF, TOF-TOF	20000	10–20	Femto mole	1e4	Fast	MALDI
LIT (LTQ)	2000	100	Femto mole	1e4	Fast	ESI, MALDI
TQ (TSQ)	2000	100	Attomole	1e6	Moderate	ESI
LTQ-Orbitrap	100,000	2	Femto mole	1e4	Moderate	ESI, MALDI
LTQ-FTICR, Q-FTICR	500,000	<2	Femto mole	1e4	Slow, Slow	ESI, MALDI
Q-TOF, IT-TOF	10,000	2–5	Attomole	1e6	Moderate, fast	ESI, MALDI
Q-LIT	2,000	100	Attomole	1e6	Moderate, fast	ESI

# Data Visualization and Analysis

A key challenge with any multi-parametric high-throughput screening (HTS) dataset is how to best organize, simplify, visualize and analyse the data while retaining the relationships among the different samples/parameters [112]. Furthermore, a generic data import and export functionality is also required for future assignment and consistent interpretation of deduced results.

There are no devoted software tools for analysis of MALDI HTS data, but more general tools such as R [113], SPSS and Matlab [114] packages can be used. Several open source libraries and frameworks such as OpenMS, Proteowizard, MsInspect, Bioconductor have been developed to facilitate MS data analysis [115-118]. While many open-source software tools are intended to be used by users with a software profile, requiring programming skills, there has been a lot of progress in user-friendliness. DanteR [119] and InfernoRDN [120] are examples of user-friendly graphical interfaces to the R framework that facilitates normalization, statistical analysis based on ANOVA and various multivariate analysis to be carried out.

Despite the existence of such a great variety of software tools that can enable analysis of MS generated proteomic datasets there is still a lack of specific tools that cover the need for MALDI data visualization and analysis. Most of the tools are intended to be used by a user with a software profile, requiring programming skills. The fast generation of MALDI data necessitates data to be visualized and analysed by different statistical techniques compared to LC-MS data. The MALDIViz software tool presented in Paper III provides several visualisation tools dedicated for MALDI HTS data.

## MALDIViz implementation

MALDIViz App is a Shiny-based Web application, accessible independently of the user operating system and without the need to install the program locally. The app can be used to do quality checks, visualization and analysis of MALDI MS data. It has been implemented entirely in the R language (R version 3.2.3).

## RStudio

R is a language and data analysis software that is valued for its rich plugin ecosystem, providing powerful packages for statistics and visualization [121]. RStudio is a free and open-source Integrated Development Environments (IDE) for R. RStudio offers many useful features a console, syntax-highlighting editor that supports direct code execution, as well as tools for plotting, history, debugging and workspace management [122]. RStudio can be run as a desktop application for Mac, Windows, or Linux, but it is also available as a server install. When a user opens RStudio, whether in the desktop version of the application or through a server, the initial screen will look much like what is seen in Figure 14A. The RStudio screen has four panes, which are shown in their default arrangement in Figure 14A.

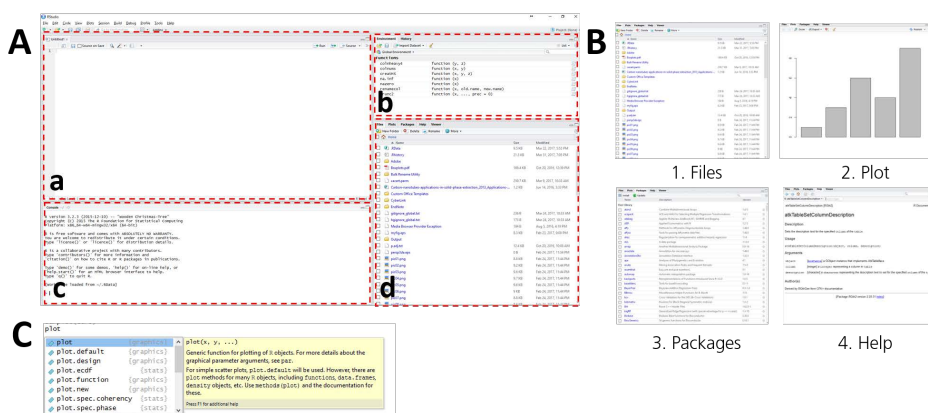


Figure 14. Panes in RStudio

The first pane allows users to view files and data. This is a useful feature because it allows users to view a spreadsheet-like representation of their data, which they can scroll through. This is also the pane where documentation can be written by users, such as .R files or RMarkdown documents. The second pane allows users to view a list of all the objects loaded into the work environment. For example, all datasets loaded will appear here, along with any other objects that have been created (special text or spatial formats, vectors, etc.). The third pane is the console, and provides the command line for users to enter R code. The console pane is where most work takes place – the other panes provide support for the user, but no code interpretation. The console looks like the standard R GUI, but it also provides support for users. For example, if a user begins to type a function and then hits the ‘tab’ key on their keyboard, RStudio will do code completion and provide a hovering hint from the documentation of the function, as in Figure 14C. The

fourth pane provides integrated views of files, plots, packages and help, as in Figure 14B. When a user runs code in the console creating a plot, the Plots tab will be automatically selected.

## R Packages

Packages are groups of R functions, data, and compiled code in a clear format. The directory where packages are stored is called the library. R comes with a standard set of packages. Others are available for download and installation. Once installed, they must be loaded into the session to be used.

Table 4: The following R-packages are used in the MALDIViz

R- packages	Usage	Ref
ggplot2, plotly	plotting	[123,124]
reshape2, dplyr, data.table	basic data manipulation	[125,126]
shiny, shinydashboard	to build interactive web applications	[127] [128]
d3heatmap, pheatmap	heatmap	[129]
pcamethods	PCA plot	[130]
rgl	3D plotting	[131]
MALDIquant	MALDI data pre-processing	[113]

### shiny

shiny is an R package that enables developers to create web applications using R code. In this way, R packages and scripts used to analyse and visualize data can be transformed into a more accessible web interface. It allows application users to choose input parameters using web controls like sliders, dropdowns, and text fields, and also encompass outputs in the form of plots, tables, and summaries. Using the Shiny framework, a web application can be developed and rendered in web browsers without having to write any HTML, CSS or JavaScript code.

#### *Code Structure*

Shiny apps consist of two components:

1. A user-interface script, called ui.R
2. A server script, called server.R

The ui.R defines the user interface and layout of the application, while the server.R is responsible for the application logic and for performing computations, producing plots, etc. The server.R consists mainly of reactive expressions that are coupled to each other, to input elements representing user interactions, and to output elements, such as plots or data tables.

## MALDIViz App

Before starting to explain the main structure of the app, it is necessary to comment a package that has also been crucial for the design of the app MALDIViz: the shinydashboard package. This package provides a theme on top of shiny, allowing users to easily create visually attractive dashboards. Shinydashboard helps create interface items such as the side menu, and facilitates the user's navigation through the different tabs.

Users can browse through the visualization and analysis steps by going to each of the tabs in the left side panel. All tabs work in a similar fashion: e.g. changing the settings in the left panel will automatically renew the image or table on the right. When moving from one tab to another, settings are saved automatically.

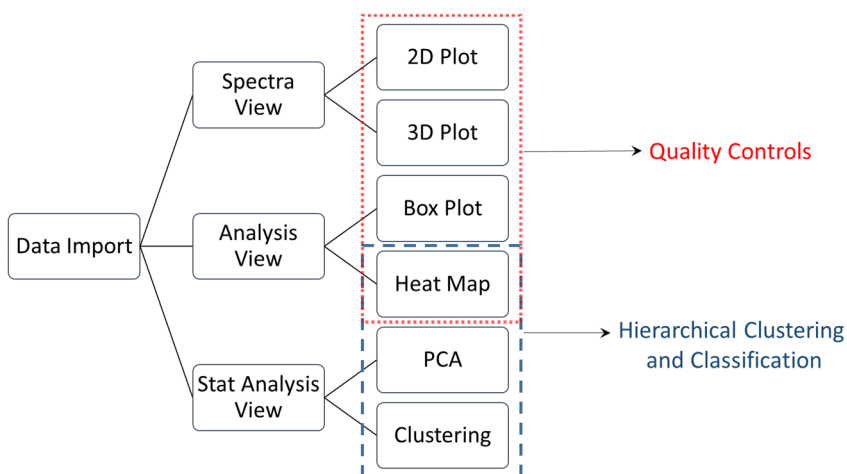


**Figure 15.** The main workflows and operations that MALDIViz can perform

The menu has been divided in four basic groups, each containing the operations the program can perform: “Data Import”, “Spectra View”, “Analysis View” and “Stat Analysis View” (Figure 15). Options in each group are explained below.

### *Data Import*

- Load sample/user data: Users can directly load the data from an Excel (.csv) file, or similar file. It is possible, as well, to load one of the predefined data sets.
- Input data for analysis can be any data table (crosstab) containing columns of mass and intensities, with additional columns corresponding to informational

metadata from each experiment, such as, type of separation phase, buffer condition, replicate details, or clinical outcomes.

- In the present version of MALDIViz, up to four columns representing different metadata can be added by the user. An example showing a typical dataset loaded, from the web app, is displayed in Figure 16.

Dataset

Show 25 entries

Numeric Data

V1	mz	intensity
1	850.1798	2480.5
2	850.2289	4470.1
3	850.2506	4582.8

Meta data + Annotations for heatmap1

Annotations for heatmap2

material	condition	p_replicate	a_replicate
SPE1	Con1	1	1
SPE1	Con1	1	1
SPE1	Con1	1	1

Search:

Figure 16. A screenshot of a dataset loaded in the MALDIViz app.

### Spectra View

- This window mode provides both 2D and 3D plots which are useful for finding features and patterns across the experiment in one quick step instead of looking at the individual spectra.

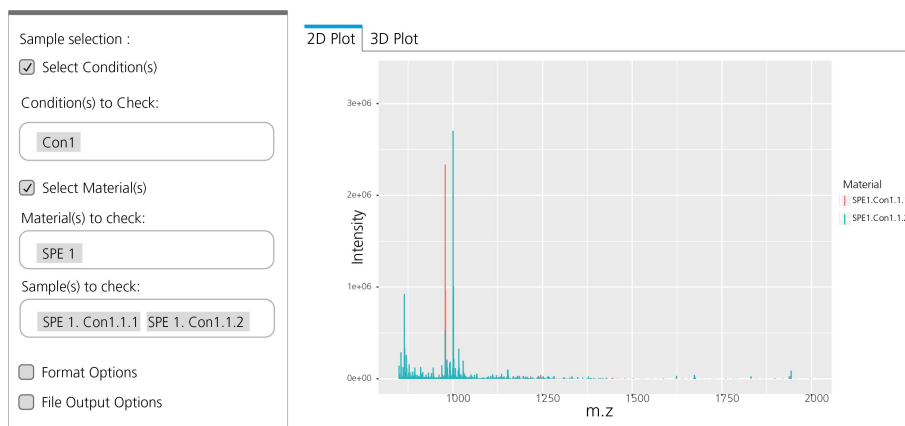


Figure 17. 2D Spectra view Screenshot The sidebar panel features and a representative 2D spectra are displayed

- Spectra View has a set of options that users must select from to generate the desired 2D and 3D plot, as in Figure 17. These options are divided into two groups, Main Options, and Appearance Options, depending on their importance.

- Main Options
  - Condition (s)
  - Material (s)
- Appearance Options
  - Format Options
    - mz filter
    - colour of the plots
  - File Output options
    - Plot width
    - Plot height

### *Analysis View*

- This window allows for comparison of the experimental data using grouping based on metadata. Significant differences between groups can be visualized using boxplots and heatmap functions.
- Each analysis plot has a set of options that users must select to get the desired Boxplot and heatmap. These options are like the spectra view divided into: Main Options, and Appearance Options.
  - Main Options
    - Peptide list
    - Condition (s)
    - Cluster Options (Heatmap 1)
  - Appearance Options
    - Format Options
      - Colour
      - Rotate (Heatmap 1)
      - Annotations (Heatmap 1)
    - File Output options
      - Plot width
      - Plot height
- Peptide list (mz values)
  - A user supplied list of masses, this option can be used to identify trends of masses of interest among various conditions.
  - Users can also directly load a peptide list from an Excel (.csv) file. The function can be tested by loading one of the predefined peptides list for the sample dataset.

- Boxplots provides a clear visual interpretation of the differences between groups and a measure of the within-group variation, Figure 18. The grouping can be accomplished based on user supplied values in the metadata. Boxplots are quite complex plots that summarize the distribution of a given data set [132]. They consist of three different parts:
  - A box, covering 50% of the data. The limits of the box are the first and third quartiles.
  - A line is drawn at the median value.
  - Whiskers that extend from the limit of the box to indicate how far the data goes on each side of the box. Whiskers, however, must never be longer than 1.5 times the Inter Quartile Range (IQR).
  - Points further than 1.5 times the IQR are considered outliers and drawn individually as black dots above and below the boxes.

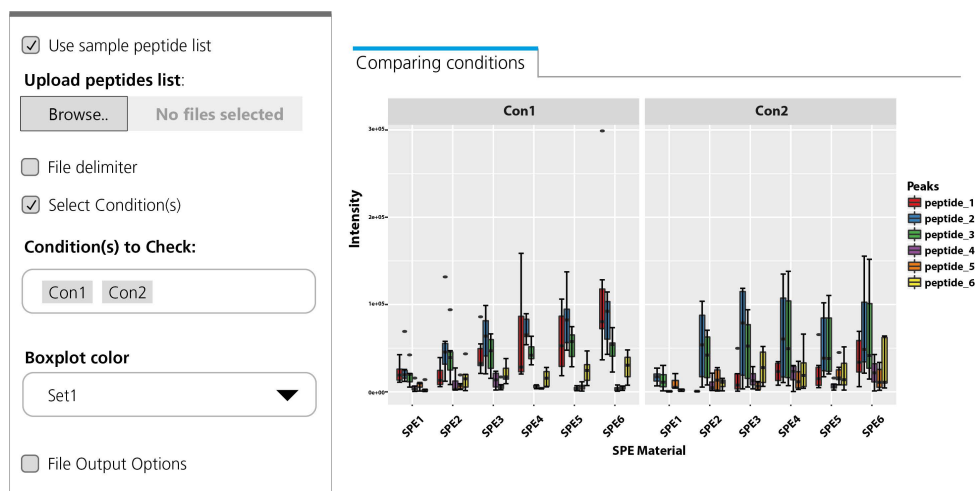


**Figure 18. Box Plot Screenshot.** The sidebar panel features and a representative box plot are displayed

- Heatmap 1
  - Heatmap 1 plots a heatmap only for any user defined m/z values, Figure 19. Here, the vertical axis represents the samples, and the horizontal axis represents the different masses and the colours corresponding intensities [133].



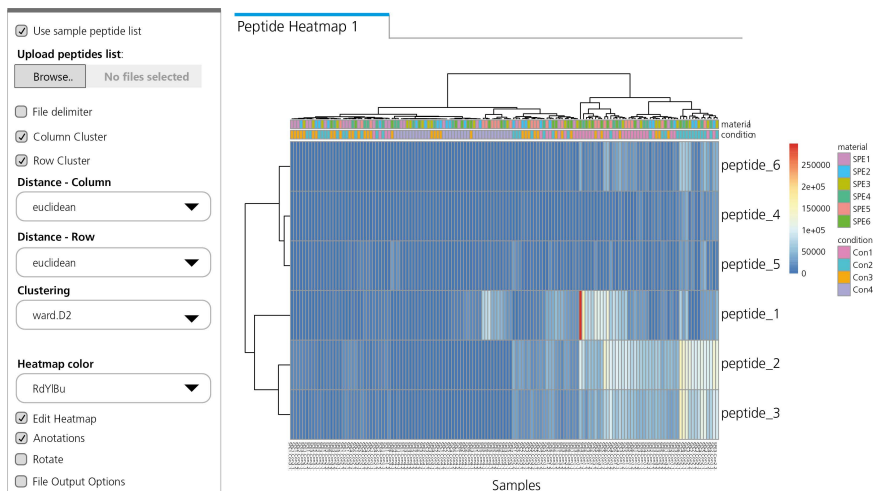


**Figure 19. Heatmap1 Screenshot. The sidebar panel features and a representative heatmap are displayed.**

- Annotations can also be added on top of the heatmap, to get an overview which annotated groups are separated better than others.
- Optionally, rows and/or columns can be clustered based on user defined distance and linkage methods.

### *Stat Analysis View*

- Heatmap 2
  - Like Heatmap 1, Heatmap 2 is plotted with hierarchical clustering and annotation options to columns and/or rows based on the user inputs. However, Heatmap 2 plots the heatmap using the all m/z values in the dataset.
- Cluster analysis
  - The Cluster Analysis window shows the dendrogram resulting from hierarchical clustering of the data, Figure 20.
  - The cluster analysis window has a set of options where users can select the desired inter-individual distance (distance matrix) and inter-group distance (linkage) for the cluster analysis [134].
  - A dendrogram is a tree-graph whose terminal vertices (“leaves”) correspond to the objects classified.

- The dendrogram is usually drawn upside down: the leaves are in the bottom and the root is on the top. The y-axis indicates the “distance” between individual observations and groups of observations.

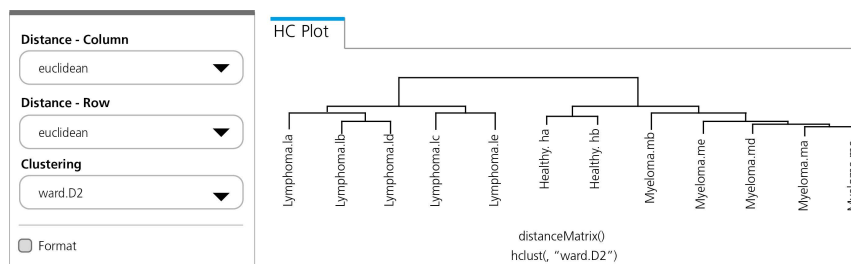


**Figure 20. Cluster analysis Screenshot. The available sidebar panel features and a representative dendrogram are displayed.**

- Cluster analysis methods partition objects into groups so that the objects in one group are similar to each other, and as dissimilar as possible compared to the objects in other groups. For cluster analysis, MALDIViz use the agglomerative hierarchical clustering (HC) method, as in Figure 21.

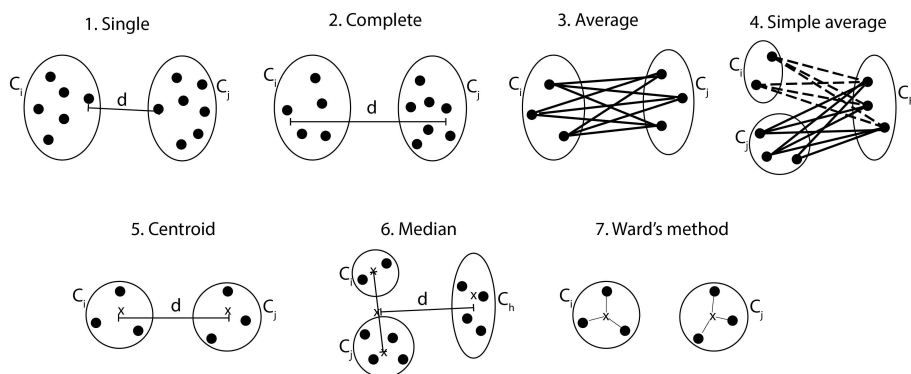


**Figure 21. Geometric illustration of six distance-optimizing agglomerative clustering methods**

- Before the HC process can begin, an inter-individual distance matrix or (dis)similarity matrix needs to be calculated. There are many ways to calculate distances or (dis)similarities between pairs of individuals (Table 5).

**Table 5. Standard distance methods.**

Method	Used with	Definition
Euclidean	Similarity or distance	Shortest straight line connecting two pair of objects in a group
Maximum	Similarity or distance	Longest distance between pair of objects in two groups or clusters.
Pearson	Similarity	Calculates the cosine between two vectors

- After the inter-individual distance matrix calculation, a method to compute the distance between the individual groups is used, so that the two most similar groups or clusters that are close to each other can be merged (Figure 21). Such a method is referred to as linkage [135]. There are several possibilities to calculate the distance between groups or clusters, such as single, complete, average and Ward's method (Table 6)

**Table 6. Standard agglomerative hierarchical clustering methods.**

Method	Used with	Definition
Single	Similarity or distance	Shortest distance between pair of objects in two groups or clusters.
Complete	Similarity or distance	Longest distance between pair of objects in two groups or clusters.
Average	Similarity or distance	Average distance between pair of objects in two groups or clusters
Centroid	Distance	Squared Euclidean distance between mean vectors
Median	Distance	Squared Euclidean distance between weighed centroids
Ward's method	Distance	Increase in sum of squares within clusters, after fusion, summed over all variables

- Principal component analysis (PCA)
  - The PCA window provides user selectable options for generating a 3D PCA plot, Figure 22. Options to change the appearance of the PCA plot are also available for the user.
  - Principal component analysis (PCA) is an unsupervised feature selection technique used for data compression, information extraction and preliminary visualisation of observations or samples [136].

- The main function of a PCA is to reduce the number of variables of the multivariate data to a few dimensions that capture the main source of variability in the data. Each dimension or principal component (PC) represents a linear combination of the original variables.

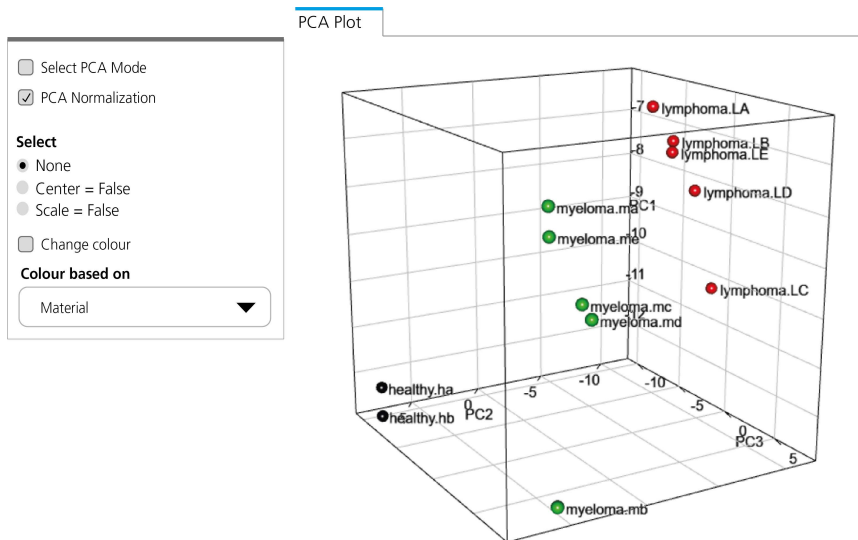


Figure 22. PCA plot screenshot. The sidebar panel features and a representative 3D PCA plot are displayed.

- The first principal component accounts for most of the variability of the data. The next principal component accounts for the variability not accounted for by the first component and so on. Typically, the first few principal components are identified and then the data set is projected onto these components for dimension reduction.
- The weights of the individual variables in the principal components are termed loadings. They are useful for identifying the important variables in individual PCs, and contain information on how the variables relate to each other.
- Scores are the coordinates of the original data in the new space and contain information on how samples relate to each other with groups of samples indicating similar behaviour.

### *Interactivity of the plots*

Interactive mode is available for all plots (2D plot, 3D plot, PCA plot and heatmap) which allows to click, zoom and hover over specific areas of the plot.

### *File download*

The plots and data generated by the MALDIViz application can be saved to the local file system as .eps, .pdf and .csv files by clicking on the “Download” button located above each plot.

# Summary of the Manuscripts

## Paper I

*Title: Multiplexed MALDI-MS arrays for screening of MIP solid phase extraction materials*

In Paper I, the in-house developed Integrated Selective Enrichment Target (ISET), was interfaced with MALDI mass spectrometry to provide an efficient, economic and generic optimization process for SPE sample preparation. This method facilitates rapid investigation of solid phase extraction protocols using very small amounts of sorbent, which can save both time and money (Figure 23). The SPE is performed in a rapid and parallel fashion, with a processing time off only 2 hrs per ISET with 96 samples. Each of the 96 wells on the ISET can hold 600 nL of SPE sorbent. The ability to work with small amounts of sorbent and samples in the ISET platform provides a big advantage when developing affinity sorbents, such as molecularly imprinted polymers (MIPs). It was demonstrated that an amount of 25 mg phosphoserine imprinted MIP (pS-MIP) sorbent can allow for analysis of more than 500 ISET nanovials using a multitude of different conditions. In the presented case, the multiplexed experiments allowed for early discovery of unspecific interactions and subsequent minimization of these, resulting in a protocol that provided improved enrichment of phosphopeptides.

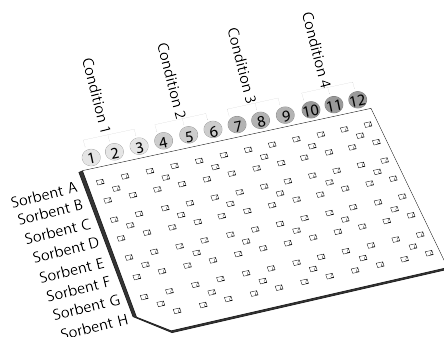


**Figure 23.** Integrated selective enrichment target (ISET) with labelling illustrating how an experimental set-up for SPE optimization can be facilitated. In the drawing 8 different sorbents (A–H row wise) can be tested in triplicate under four different conditions.

## Paper II

### *Title: Filter Plate–Based Screening of MIP SPE Materials for Capture of the Biomarker Pro-Gastrin-Releasing Peptide*

In Paper II, a  $\mu$ -SPE method for screening of MIP-SPE materials using a commercial 384-well filter plate was developed (Figure 24). The method allows for rapid and automated screening using 10–30  $\mu$ L of packed SPE sorbent per well and sample volumes in the range of 10–70  $\mu$ L. This enables screening of many different SPE sorbents while simultaneously identifying optimal SPE conditions. In addition, the 384-well format also facilitates detection with a multitude of analytical platforms. Performance of the  $\mu$ -MIP-SPE method was investigated using a series of MIPs designed to capture pro-gastrin-releasing peptide (ProGRP). Fractions coming from sample load, cartridge wash, and elution were collected and analysed using mass spectrometry (MS). The top-performing MIPs were identified, together with proper SPE conditions.

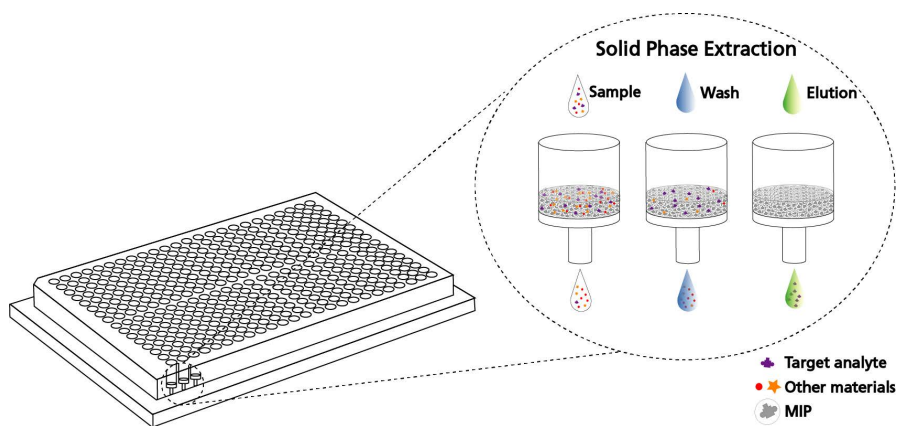


Figure 24. Schematic representation of the 384-well filter plates and the workflow of the solid phase extraction step in the micro well. (A) Shows the 384-well filter plate and (B) shows the SPE sample preparation where the sample is transferred to the micro well loaded with SPE material (1) followed by a wash step to remove undesired components (2), and the captured analytes were then displaced by the elution step (3).

## Paper III

*Title: MALDI-Viz - A comprehensive informatics tool for MALDI-MS data visualization and analysis*

In Paper III, a comprehensive informatics tool for MALDI was developed to facilitate visualization, statistical analysis, and high quality image and data export. This tool is a R-Shiny based Web application, accessible independently of the operating system and without the need to install software locally. It allows easy visualization of data, comparison of multiple experiments, and permits export to high quality images. The app can be used to do quality checks, visualizations and analysis of mass spectrometry data, coming from proteomics experiments (Figure 25).

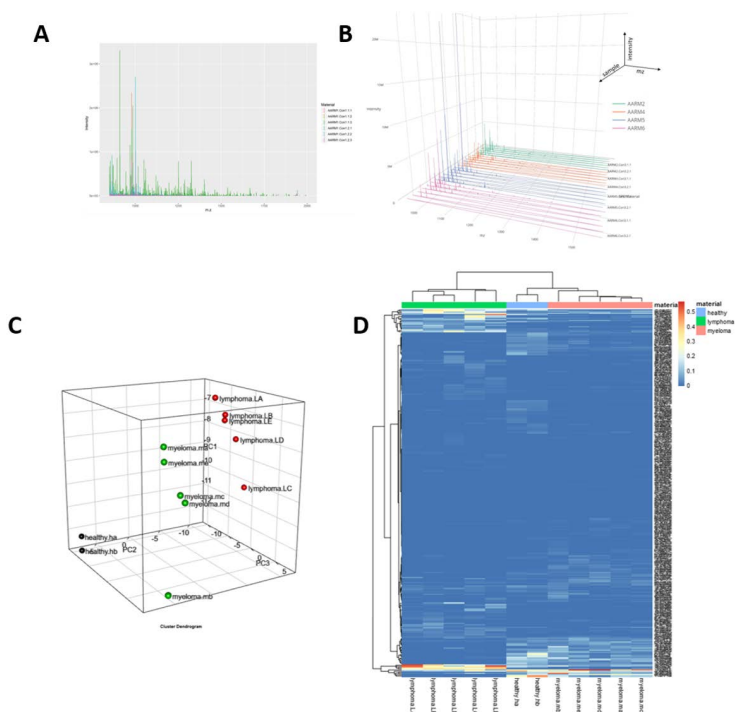


Figure 25. A. 2D and B. 3D Spectra views. C. Principal component analysis view of the Cancer dataset presenting three different clusters, one for each type of sample. D. Detail of the heatmap visualization. The upper annotations automatically colour samples from the same condition. While the upper dendrogram and the side dendrogram groups the more similar m/z values.



## Paper IV

*Title: Solid-phase extraction of the alcohol abuse biomarker phosphatidylethanol using newly synthesized polymeric sorbent materials containing quaternary heterocyclic groups*

Paper IV, a series of screening procedures using different SPE materials were carried out for phosphatidylethanol (PEth) extraction. PEth is an interesting biomarker finding increased use for detecting long term alcohol abuse with high specificity and sensitivity. After the initial screening of SPE materials, and identification of the core mechanism of retention, new polymers were synthesized. It was concluded that a good SPE material for PEth should include strong anion exchange capabilities and that a very hydrophobic backbone will be detrimental for the recovery of PEth. Additionally, quaternary heterocyclic groups seem to perform better than quaternary alkyl amino groups. The best material described in this paper contains strong anion exchange functionalities in the form of quaternary imidazole groups with a cross-linker of intermediary hydrophobicity (TRIM). It is also shown in Paper IV that even though conventional mixed-mode ion-exchangers might be inadequate for more complex matrices, fine tuning of the solid-phase characteristics can make SPE viable option for sample preparation.

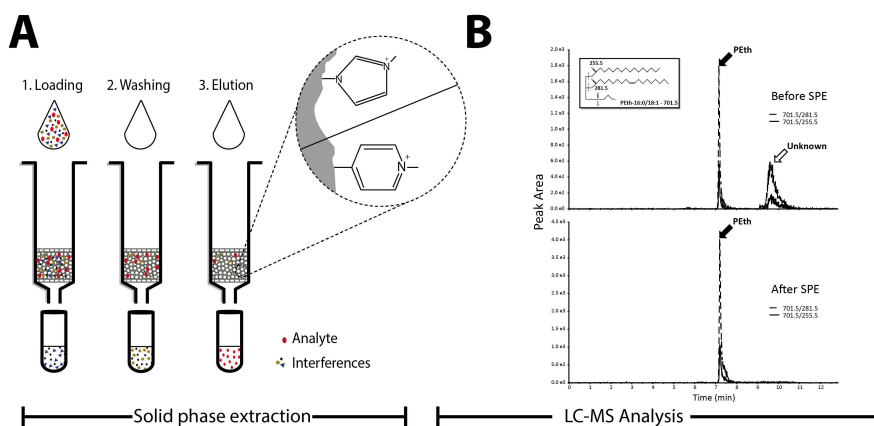


**Figure 26.** A. SPE scheme for phosphatidylethanol (PEth) extraction and B. ESI-MS/MS chromatograms of elution fraction collected after SPE with the material V, containing the sample load of 5  $\mu$ M PEth 16:0/18:1 ( $m/z$  701.5/255.5 and  $m/z$  701.5/281.5) spiked in human plasma.

## Paper V

### *Title: V. Catalytic Formation of Disulfide Bonds in Peptides by Molecularly Imprinted Microgels at Oil/Water Interfaces*

Paper V, describes the preparation and investigation of molecularly imprinted polymer microgel (MIP MG) stabilized Pickering emulsions (PEs) for their ability to catalyse the formation of disulphide bonds in peptides at the Oil/Water interface. The MIP MGs were synthesized via precipitation polymerization and a programmed initiator strategy. A template rebinding experiment showed that the MIP MGs bound over two times more template (24 mg/g) compared to the uptake displayed by a non-imprinted reference polymer (NIP) MG (10 mg/g) at saturation. Using the MIP MGs as stabilizers, catalytic oxidation systems were prepared by emulsifying the oil phase and water phase in the presence of different oxidizing agents. During the cyclization, the isolation of the thiol precursors and the oxidizing reagents non-selectively decreased the formation of the by-products, while the imprinted cavities on the MIP MGs selectively promoted the intramolecular cyclization of peptides. When  $I_2$  was used as the oxidizing agent, the MIP-PE- $I_2$  system showed a product yield of 50%, corresponding to a nearly 2-fold increase compared to that of the non-imprinted polymer NIP-PE- $I_2$  system (26%). We believe the interfacial catalysis system presented in this work may offer significant benefits in synthetic peptide chemistry by raising productivity while suppressing the formation of by-products.

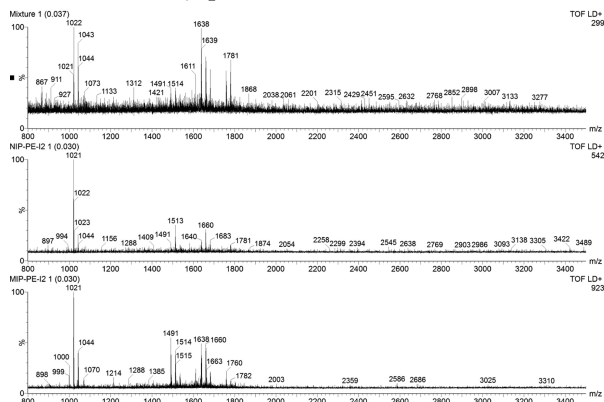


**Figure 27.** MALDI analysis of the cyclic somatostatin (SST, mass 1638) and the by-products after a 30-min reaction. The oil phase was a mixture of 300  $\mu$ L of ethyl acetate and 100  $\mu$ L of toluene. The oxidizing reagent was 100  $\mu$ L of 2.5 mmol  $L^{-1}$   $I_2$  in methanol solution. m/z 1639: SST +  $H^+$ . m/z 1491: SST lost Cys residue. m/z 1660: SST +  $Na^+$ . m/z 3277: SST dimer +  $H^+$ .

# Popular Summary

The term "biomarker" can be used to describe a physical, physiological and molecular characteristic, used to evaluate or as an indicator of normal biological or pathogenic processes. Biomarkers can also be used for monitoring pharmacologic responses to a therapeutic intervention. Protein are likely to be the most affected entities during a pathological condition, and protein biomarkers have become one of the most valuable classes of biomarkers over the past 100 years. Therefore, proteomics holds special promise for biomarker discovery.

Protein biomarkers are sourced from various bio-compartments, among them, bio-fluids such as, blood serum and plasma are particularly attractive for clinical studies due to easy accessibility at relative low-cost. However, the extremely large dynamic range of protein concentrations, presents several challenges in biomarker determination from serum or plasma.

In biomarker analysis, sample preparation plays a crucial step to extract, isolate and concentrate the analytes of interest. Among the various sample preparation techniques, Solid Phase Extraction (SPE) is one of the most common and popular, due to the high enrichment factor, good recovery, low consumption of organic solvents and the possibility to automate (off- or on-line) the whole process. The SPE process involves separation of analytes between a liquid and a solid (sorbent) phase. SPE technique enables the concentration and purification needed for detailed biomarker studies.

Over the years, a wide variety of sorbents, ranging from the traditional reversed-phase sorbents (C18, C8), normal phase (silica, alumina), and ion exchange, to mixed-mode (ion exchange + reversed phase) and functionalized resins based on styrene-divinylbenzene (SDVB) polymers has been developed and used in SPE. Affinity phases that separates analyte molecules based on molecular recognition (antibodies, proteins, sugars, nucleic acids) or chemical structures (salts/IMAC) have also been utilized as SPE sorbents.

Optimization of a SPE sample preparation step is crucial for high-sensitivity detection, as well as analysis robustness and reproducibility. The SPE optimization

process for a certain analyte usually starts with, screening for a suitable extraction phase or if the appropriate extraction phase is known, with the fine tuning of the sample preparation conditions i.e. the loading, washing and elution steps. However, the process of screening SPE sample preparation in the present commercially available formats can be quite time consuming and expensive, due to the large amounts of SPE phase required and limited options for use of different materials in commercially available configurations. As a solution, we have applied our micro fabricated SPE sample preparation platform, the Integrated Selective Enrichment Target, (ISET) that interfaces directly with MALDI mass spectrometry for a rapid and parallel investigation of the SPE process using minute amounts of sample (Paper I). We also utilized the 384-well filter plate format for an automated, high-throughput SPE screening method. This platform was used for screening of molecularly imprinted sorbents, to identify promising candidates (Paper II). Compared with the ISET, the 384-well filter plate format provides advantages such as increased bed volume, and thus a larger binding capacity (needed to enable use of low-affinity materials), and can be used with analysis techniques other than matrix-assisted laser desorption/ionization (MALDI), for example, liquid chromatography–electrospray ionization mass spectrometry (LC ESI-MS).

The high-throughput SPE method optimization experiments with MS leads to the production of a huge dataset. As a solution to this, MALDIViz, a comprehensive informatics tool for MALDI that facilitate visualization, statistical analysis, and high quality image and data export was developed (Paper III). MALDIViz is a R-Shiny based Web application, accessible independently of operating system and without the need to install any program locally. It allows easy visualization of data, comparison of multiple experiments, and can be used to do quality checks, visualization and analysis of data from MALDI screening experiments.

Apart from the miniature platforms, conventional cartridge based investigation of SPE protocols was used for materials with ion-exchange capabilities, to extract phosphatidylethanol (PEth), a phospholipid biomarker for alcohol consumption from blood (Paper IV). A newly prepared molecularly imprinted polymer microgel (MIP MG) stabilized Pickering emulsions (PEs) for their ability to catalyse the formation of disulphide bonds in peptides at the Oil/Water interface was investigated in Paper V.

# Acknowledgements

It is my great pleasure to thank all those people who made this thesis possible.

First and foremost, I am heartily thankful to my supervisor, Thomas, for providing me an opportunity to pursue this PhD education. Thank you for believing in me, always encouraging, inspiring and guiding me throughout this PhD process.

Many thanks to Simon, my assistant supervisor, who was most helpful and supportive throughout entire time, from the first day I arrived at Sweden. Indeed, you guided me throughout this PhD process, advised and helped me in difficult times with the project and practical things. For always being nearby for the discussions, and for your never-ending enthusiasm.

I would also like to thank all my current and former colleagues at Elmät/BMC-D13 departments for practical help and for great memories, and for creating such nice atmosphere at work. Some specific thanks go out to: Johan, for helping me out in various practical and administration things. Ulrika, Eva, Desiree, and Malgo, for helping me out with administration. Belinda and Hong for your help with the ISET and MALDI experiments. Björn for your help with microscopy and practical things. Sameer for discussions on various things inside and outside of the lab. Melinda and Yutaka for your help with BMC mass spectrometers. Mariana, for the good work environment at the office.

I am thankful to collaborators in PEPMIP project who hosted me for secondments. Cecilia, and Léon for their help with mass spectrometry during my stay at the University of Oslo, Oslo. Mariana and Ece for their help with affinity materials during my stay at MIP Technologies AB, Lund. Sudhir and Börje for their help to understand MIPs at Malmö University, Malmö. Celina, Silje, Loreta, Mark, Roberto Chuixiu and Xiantao, for their help to recognise different perspective on the project during their secondments in Lund. I am immensely grateful to all people involved in PEPMIP project for making a great atmosphere and collaboration.

Thanks for co-authors of articles and manuscripts: Celina, Cecilia, Sudhir, Börje, Abed, Léon, Xiantao, Chuixiu, Mariana, Johan B and Ece.

The financial support of the European Commission through the Marie Curie ITN project PEPMIP and Lund University is gratefully acknowledged.

I would like to thank all my friends outside of the lab that made my journey enjoyable. Some specific thanks go out to: Kesav and Ram for the dinner discussions, and helping me in difficult times. Barani, Annapoorani, Ganesh, Saravanan and Loganathan for their long-distance support and invaluable conversations.

Most of all, I would like to thank my family, who encouraged me so much in life and helped me to become the person I am today. Even though you were far away from me all these years, I always felt your love, guidance and endless support. Subash, my brother for the support and animation videos provided during my studies. Appa and Amma for being very supportive and believing in my dreams.

Sharanyha for being with me every day and for your support, care and smile.

# References

- (1) Strimbu, K.; Tavel, J. A. *Current opinion in HIV and AIDS* **2010**, *5*, 463-466.
- (2) Ramaswamy, S.; Perou, C. M. *The Lancet* **2003**, *361*, 1576-1577.
- (3) Fernie, A. R.; Trethewey, R. N.; Krotzky, A. J.; Willmitzer, L. *Nat Rev Mol Cell Biol* **2004**, *5*, 763-769.
- (4) Rifai, N.; Gillette, M. A.; Carr, S. A. *Nat Biotech* **2006**, *24*, 971-983.
- (5) Good, D. M.; Thongboonkerd, V.; Novak, J.; Bascands, J.-L.; Schanstra, J. P.; Coon, J. J.; Dominiczak, A.; Mischak, H. *Journal of Proteome Research* **2007**, *6*, 4549-4555.
- (6) Anderson, N. L.; Anderson, N. G. *Molecular & Cellular Proteomics* **2002**, *1*, 845-867.
- (7) Hunter, T. *Cell* **2000**, *100*, 113-127.
- (8) Mann, M.; Jensen, O. N. *Nat Biotech* **2003**, *21*, 255-261.
- (9) MOLINA, R.; AUGÉ, J. M.; FILELLA, X.; VIÑOLAS, N.; ALICARTE, J.; DOMINGO, J. M.; BALLESTA, A. M. *Anticancer Research* **2005**, *25*, 1773-1778.
- (10) Miyake, Y.; Kodama, T.; Yamaguchi, K. *Cancer Research* **1994**, *54*, 2136.
- (11) Molina, R.; Holdenrieder, S.; Augé, J. M.; Schalhorn, A.; Hatz, R.; Stieber, P. *Cancer biomarkers : section A of Disease markers* **2010**, *6*, 163-178.
- (12) Hansson, P.; Caron, M.; Johnson, G.; Gustavsson, L.; Alling, C. *Alcoholism: Clinical and Experimental Research* **1997**, *21*, 108-110.
- (13) Torrente, M. P.; Freeman, W. M.; Vrana, K. E. *Expert review of proteomics* **2012**, *9*, 425-436.
- (14) Varga, A.; Hansson, P.; Lundqvist, C.; Alling, C. *Alcoholism: Clinical and Experimental Research* **1998**, *22*, 1832-1837.
- (15) Helander, A.; Zheng, Y. *Clinical chemistry* **2009**, *55*, 1395-1405.
- (16) Gnann, H.; Engelmann, C.; Skopp, G.; Winkler, M.; Auwärter, V.; Dresen, S.; Ferreiros, N.; Wurst, F. M.; Weinmann, W. *Analytical and bioanalytical chemistry* **2010**, *396*, 2415-2423.
- (17) Isaksson, A.; Walther, L.; Hansson, T.; Andersson, A.; Alling, C. *Drug testing and analysis* **2011**, *3*, 195-200.
- (18) Aradottir, S.; Asanovska, G.; Gjerds, S.; Hansson, P.; Alling, C. *Alcohol and alcoholism (Oxford, Oxfordshire)* **2006**, *41*, 431-437.

- (19) Viel, G.; Boscolo-Berto, R.; Cecchetto, G.; Fais, P.; Nalesso, A.; Ferrara, S. D. *International journal of molecular sciences* **2012**, *13*, 14788-14812.
- (20) Hortin, G. L.; Sviridov, D. *Journal of Proteomics* **2010**, *73*, 629-636.
- (21) Kataoka, H. *TrAC Trends in Analytical Chemistry* **2003**, *22*, 232-244.
- (22) Biddlecombe, R. A.; Pleasance, S. *Journal of Chromatography B: Biomedical Sciences and Applications* **1999**, *734*, 257-265.
- (23) Peng, S. X.; Branch, T. M.; King, S. L. *Analytical Chemistry* **2001**, *73*, 708-714.
- (24) Pedersen-Bjergaard, S.; Rasmussen, K. E.; Grønhaug Halvorsen, T. *Journal of Chromatography A* **2000**, *902*, 91-105.
- (25) Camel, V. *Spectrochimica Acta Part B: Atomic Spectroscopy* **2003**, *58*, 1177-1233.
- (26) Hennion, M.-C. *Journal of Chromatography A* **1999**, *856*, 3-54.
- (27) Poole, C. F. *TrAC Trends in Analytical Chemistry* **2003**, *22*, 362-373.
- (28) Augusto, F.; Hantao, L. W.; Mogollón, N. G. S.; Braga, S. C. G. N. *TrAC Trends in Analytical Chemistry* **2013**, *43*, 14-23.
- (29) Thurman, E. M.; Mills, M. S. *Solid-phase extraction : principles and practice*; New York : Wiley, cop. 1998, 1998.
- (30) Cox, G. B. *Journal of Chromatography A* **1993**, *656*, 353-367.
- (31) Rogers, S. D.; Dorsey, J. G. *Journal of Chromatography A* **2000**, *892*, 57-65.
- (32) Fontanals, N.; Marcé, R. M.; Borrull, F. *Journal of Chromatography A* **2007**, *1152*, 14-31.
- (33) Sun, J. J.; Fritz, J. S. *Journal of Chromatography A* **1992**, *590*, 197-202.
- (34) Fontanals, N.; Galià, M.; Cormack, P. A. G.; Marcé, R. M.; Sherrington, D. C.; Borrull, F. *Journal of Chromatography A* **2005**, *1075*, 51-56.
- (35) Fontanals, N.; Trammell, B. C.; Galià, M.; Marcé, R. M.; Iraneta, P. C.; Borrull, F.; Neue, U. D. *Journal of Separation Science* **2006**, *29*, 1622-1629.
- (36) Fontanals, N.; Marcé, R. M.; Borrull, F.; Cormack, P. A. G. *TrAC Trends in Analytical Chemistry* **2010**, *29*, 765-779.
- (37) Wilson, I. D. *Bioanalytical separations*; Elsevier, 2003; Vol. 4.
- (38) Porath, J. *Protein Expression and Purification* **1992**, *3*, 263-281.
- (39) Porath, J.; Carlsson, J. A. N.; Olsson, I.; Belfrage, G. *Nature* **1975**, *258*, 598-599.
- (40) Andersson, L.; Porath, J. *Analytical Biochemistry* **1986**, *154*, 250-254.
- (41) Negroni, L.; Claverol, S.; Rosenbaum, J.; Chevet, E.; Bonneau, M.; Schmitter, J.-M. *Journal of Chromatography B* **2012**, *891-892*, 109-112.



- (42) Dunn, J. D.; Watson, J. T.; Bruening, M. L. *Analytical Chemistry* **2006**, *78*, 1574-1580.
- (43) Yang, C.; Zhong, X.; Li, L. *ELECTROPHORESIS* **2014**, *35*, 3418-3429.
- (44) Ficarro, S. B.; McClelland, M. L.; Stukenberg, P. T.; Burke, D. J.; Ross, M. M.; Shabanowitz, J.; Hunt, D. F.; White, F. M. *Nature biotechnology* **2002**, *20*, 301-305.
- (45) Ficarro, S. B.; Salomon, A. R.; Brill, L. M.; Mason, D. E.; Stettler-Gill, M.; Brock, A.; Peters, E. C. *Rapid Communications in Mass Spectrometry* **2005**, *19*, 57-71.
- (46) Iwase, Y.; Honma, S.; Matsuzaki, M.; Miyakawa, Y.; Kanno, T.; Ishii, K.; Furuichi, N.; Furukawa, K.; Horigome, T. *Journal of Biochemistry* **2010**, *147*, 689-696.
- (47) Leitner, A. *TrAC Trends in Analytical Chemistry* **2010**, *29*, 177-185.
- (48) Grün, M.; Kurganov, A. A.; Schacht, S.; Schüth, F.; Unger, K. K. *Journal of Chromatography A* **1996**, *740*, 1-9.
- (49) Tani, K.; Ozawa, M. *Journal of Liquid Chromatography & Related Technologies* **1999**, *22*, 843-856.
- (50) Pinkse, M. W. H.; Uitto, P. M.; Hilhorst, M. J.; Ooms, B.; Heck, A. J. R. *Analytical Chemistry* **2004**, *76*, 3935-3943.
- (51) Wolschin, F.; Wienkoop, S.; Weckwerth, W. *PROTEOMICS* **2005**, *5*, 4389-4397.
- (52) Larsen, M. R.; Thingholm, T. E.; Jensen, O. N.; Roepstorff, P.; Jørgensen, T. J. D. *Molecular & Cellular Proteomics* **2005**, *4*, 873-886.
- (53) Mazanek, M.; Mituloviae, G.; Herzog, F.; Stingl, C.; Hutchins, J. R. A.; Peters, J.-M.; Mechtler, K. *Nat. Protocols* **2007**, *2*, 1059-1069.
- (54) Vilasi, A.; Fiume, I.; Pace, P.; Rossi, M.; Pocsfalvi, G. *Journal of Mass Spectrometry* **2013**, *48*, 1188-1198.
- (55) Sugiyama, N.; Masuda, T.; Shinoda, K.; Nakamura, A.; Tomita, M.; Ishihama, Y. *Molecular & Cellular Proteomics* **2007**, *6*, 1103-1109.
- (56) Kweon, H. K.; Håkansson, K. *Analytical Chemistry* **2006**, *78*, 1743-1749.
- (57) Li, Y.; Lin, H.; Deng, C.; Yang, P.; Zhang, X. *PROTEOMICS* **2008**, *8*, 238-249.
- (58) Ficarro, S. B.; Parikh, J. R.; Blank, N. C.; Marto, J. A. *Analytical Chemistry* **2008**, *80*, 4606-4613.
- (59) Chen, W.-Y.; Chen, Y.-C. *Analytical and bioanalytical chemistry* **2010**, *398*, 2049-2057.

- (60) Li, Y.; Liu, Y.; Tang, J.; Lin, H.; Yao, N.; Shen, X.; Deng, C.; Yang, P.; Zhang, X. *Journal of Chromatography A* **2007**, *1172*, 57-71.
- (61) Sturm, M.; Leitner, A.; Smått, J.-H.; Lindén, M.; Lindner, W. *Advanced Functional Materials* **2008**, *18*, 2381-2389.
- (62) Martí n-Esteban, A.; Fernández, P.; Cámara, C. *Fresenius J Anal Chem* **1997**, *357*, 927-933.
- (63) Pichon, V.; Bouzige, M.; Miège, C.; Hennion, M.-C. *TrAC Trends in Analytical Chemistry* **1999**, *18*, 219-235.
- (64) Płotka-Wasyłka, J.; Szczepańska, N.; de la Guardia, M.; Namieśnik, J. *TrAC Trends in Analytical Chemistry* **2016**, *77*, 23-43.
- (65) Martín-Esteban, A. *Fresenius J Anal Chem* **2001**, *370*, 795-802.
- (66) Alexander, C.; Andersson, H. S.; Andersson, L. I.; Ansell, R. J.; Kirsch, N.; Nicholls, I. A.; O'Mahony, J.; Whitcombe, M. J. *Journal of Molecular Recognition* **2006**, *19*, 106-180.
- (67) Whitcombe, M. J.; Kirsch, N.; Nicholls, I. A. *Journal of Molecular Recognition* **2014**, *27*, 297-401.
- (68) Flavin, K.; Resmini, M. *Analytical and bioanalytical chemistry* **2009**, *393*, 437-444.
- (69) Lee, W.-C.; Cheng, C.-H.; Pan, H.-H.; Chung, T.-H.; Hwang, C.-C. *Analytical and bioanalytical chemistry* **2008**, *390*, 1101-1109.
- (70) Tan, J.; Jiang, Z.-T.; Li, R.; Yan, X.-P. *TrAC Trends in Analytical Chemistry* **2012**, *39*, 207-217.
- (71) Zhang, W.; Chen, Z. *Talanta* **2013**, *103*, 103-109.
- (72) Du, T.; Cheng, J.; Wu, M.; Wang, X.; Zhou, H.; Cheng, M. *Analytical Methods* **2014**, *6*, 6375-6380.
- (73) Rachkov, A.; Minoura, N. *Journal of Chromatography A* **2000**, *889*, 111-118.
- (74) Rachkov, A.; Hu, M.; Bulgarevich, E.; Matsumoto, T.; Minoura, N. *Analytica Chimica Acta* **2004**, *504*, 191-197.
- (75) Yang, K.; Liu, J.; Li, S.; Li, Q.; Wu, Q.; Zhou, Y.; Zhao, Q.; Deng, N.; Liang, Z.; Zhang, L.; Zhang, Y. *Chemical Communications* **2014**, *50*, 9521-9524.
- (76) Kryscio, D. R.; Peppas, N. A. *Acta Biomaterialia* **2012**, *8*, 461-473.
- (77) Yang, K.; Zhang, L.; Liang, Z.; Zhang, Y. *Analytical and bioanalytical chemistry* **2012**, *403*, 2173-2183.
- (78) Shinde, S.; Bunschoten, A.; Kruijtzter, J. A.; Liskamp, R. M.; Sellergren, B. *Angewandte Chemie International Edition* **2012**, *51*, 8326-8329.

- (79) Xu, L.; Hu, Y.; Shen, F.; Li, Q.; Ren, X. *Journal of Chromatography A* **2013**, *1293*, 85-91.
- (80) Helling, S.; Shinde, S.; Brosseron, F.; Schnabel, A.; Müller, T.; Meyer, H. E.; Marcus, K.; Sellergren, B. r. *Analytical Chemistry* **2011**, *83*, 1862-1865.
- (81) Li, D.-Y.; Qin, Y.-P.; Li, H.-Y.; He, X.-W.; Li, W.-Y.; Zhang, Y.-K. *Biosensors and Bioelectronics* **2015**, *66*, 224-230.
- (82) Żwir-Ferenc, A.; Biziuk, M. *Polish J Environ Stud* **2006**, *15*, 677-690.
- (83) Kecili, R.; Billing, J.; Nivhede, D.; Sellergren, B.; Rees, A.; Yilmaz, E. *Journal of Chromatography A* **2014**, *1339*, 65-72.
- (84) Ji, W.; Ma, X.; Xie, H.; Chen, L.; Wang, X.; Zhao, H.; Huang, L. *Journal of Chromatography A* **2014**, *1368*, 44-51.
- (85) Chassaing, C.; Stokes, J.; Venn, R. F.; Lanza, F.; Sellergren, B.; Holmberg, A.; Berggren, C. *Journal of Chromatography B* **2004**, *804*, 71-81.
- (86) Yan, H.; Yang, C.; Sun, Y.; Row, K. H. *Journal of Chromatography A* **2014**, *1361*, 53-59.
- (87) Karas, M.; Hillenkamp, F. *Analytical Chemistry* **1988**, *60*, 2299-2301.
- (88) Fenn, J. B.; Mann, M.; Meng, C. K.; Wong, S. F.; Whitehouse, C. M. *Science* **1989**, *246*, 64.
- (89) Chait, B. T. *Science* **2006**, *314*, 65.
- (90) Henzel, W. J.; Watanabe, C.; Stults, J. T. *Journal of the American Society for Mass Spectrometry* **2003**, *14*, 931-942.
- (91) Steen, H.; Mann, M. *Nat Rev Mol Cell Biol* **2004**, *5*, 699-711.
- (92) Aebersold, R.; Mann, M. *Nature* **2003**, *422*, 198-207.
- (93) Siuti, N.; Kelleher, N. L. *Nature methods* **2007**, *4*, 817-821.
- (94) Han, X.; Jin, M.; Breuker, K.; McLafferty, F. W. *Science* **2006**, *314*, 109.
- (95) Nordstrom, A.; Want, E.; Northen, T.; Lehtio, J.; Siuzdak, G. *Analytical Chemistry* **2008**, *80*, 421-429.
- (96) Buse, J.; Purves, R. W.; Verrall, R. E.; Badea, I.; Zhang, H.; Mulligan, C. C.; Peru, K. M.; Bailey, J.; Headley, J. V.; El-Aneel, A. *Journal of Mass Spectrometry* **2014**, *49*, 1171-1180.
- (97) Karas, M.; Krüger, R. *Chemical Reviews* **2003**, *103*, 427-440.
- (98) Rappsilber, J.; Moniatte, M.; Nielsen, M. L.; Podtelejnikov, A. V.; Mann, M. *International Journal of Mass Spectrometry* **2003**, *226*, 223-237.

- (99) Yates, J. R.; Ruse, C. I.; Nakorchevsky, A. *Annual review of biomedical engineering* **2009**, *11*, 49-79.
- (100) Iribarne, J. V.; Thomson, B. A. *The Journal of Chemical Physics* **1976**, *64*, 2287-2294.
- (101) Dole, M.; Hines, R. L.; Mack, L. L.; Mobley, R. C.; Ferguson, L. D.; Alice, M. B. *Macromolecules* **1968**, *1*, 96-97.
- (102) Awad, H.; Khamis, M. M.; El-Aneed, A. *Applied Spectroscopy Reviews* **2015**, *50*, 158-175.
- (103) Domon, B.; Aebersold, R. *Science* **2006**, *312*, 212.
- (104) Makarov, A. *Analytical Chemistry* **2000**, *72*, 1156-1162.
- (105) Zubarev, R. A.; Makarov, A. *Analytical Chemistry* **2013**, *85*, 5288-5296.
- (106) Perry, R. H.; Cooks, R. G.; Noll, R. J. *Mass Spectrometry Reviews* **2008**, *27*, 661-699.
- (107) Yates, J. R.; Cociorva, D.; Liao, L.; Zabrouskov, V. *Analytical Chemistry* **2006**, *78*, 493-500.
- (108) Ong, S.-E.; Mann, M. *Nat Chem Biol* **2005**, *1*, 252-262.
- (109) Picotti, P.; Aebersold, R. *Nat Meth* **2012**, *9*, 555-566.
- (110) Lange, V.; Picotti, P.; Domon, B.; Aebersold, R. *Molecular Systems Biology* **2008**, *4*.
- (111) de Leenheer, A. P.; Thienpont, L. M. *Mass Spectrometry Reviews* **1992**, *11*, 249-307.
- (112) Abraham, Y.; Zhang, X.; Parker, C. N. *Journal of biomolecular screening* **2014**, *19*, 628-639.
- (113) Gibb, S.; Strimmer, K. *Bioinformatics* **2012**, *28*, 2270-2271.
- (114) Coombes, K. R.; Tsavachidis, S.; Morris, J. S.; Baggerly, K. A.; Hung, M.-C.; Kuerer, H. M. *PROTEOMICS* **2005**, *5*, 4107-4117.
- (115) Perez-Riverol, Y.; Wang, R.; Hermjakob, H.; Müller, M.; Vesada, V.; Vizcaíno, J. A. *Biochimica et Biophysica Acta* **2014**, *1844*, 63-76.
- (116) May, D.; Law, W.; Fitzgibbon, M.; Fang, Q.; McIntosh, M. *J Proteome Res* **2009**, *8*, 3212-3217.
- (117) Wang, R.; Perez-Riverol, Y.; Hermjakob, H.; Vizcaíno, J. A. *PROTEOMICS* **2015**, *15*, 1356-1374.
- (118) Gatto, L.; Breckels, L. M.; Naake, T.; Gibb, S. *Proteomics* **2015**, *15*, 1375-1389.

- (119) Polpitiya, A. D.; Qian, W.-J.; Jaitly, N.; Petyuk, V. A.; Adkins, J. N.; Camp, D. G.; Anderson, G. A.; Smith, R. D. *Bioinformatics (Oxford, England)* **2008**, *24*, 1556-1558.
- (120) Taverner, T.; Karpievitch, Y. V.; Polpitiya, A. D.; Brown, J. N.; Dabney, A. R.; Anderson, G. A.; Smith, R. D. *Bioinformatics* **2012**, *28*, 2404-2406.
- (121) Ihaka, R.; Gentleman, R. *Journal of Computational and Graphical Statistics* **1996**, *5*, 299-314.
- (122) <https://www.rstudio.com/products/RStudio/>
- (123) Wickham, H. In *ggplot2: Elegant Graphics for Data Analysis*; Springer New York: New York, NY, 2009, pp 1-7.
- (124) Sievert, C.; Parmer, C.; Hocking, T.; Chamberlain, S.; Ram, K.; Corvellec, M.; Despouy, P. *R package version* **2016**, *4*.
- (125) Wickham, H. *2007* **2007**, *21*, 20.
- (126) Dowle, M.; Short, T.; Lianoglou, S.; Saporta, R.; Srinivasan, A.; Antonyan, E. *data.table: Extension of data.frame*, 2014.
- (127) Winston Chang, Joe Cheng, JJ Allaire, Yihui Xie and Jonathan McPherson (2017). shiny: Web Application Framework for R. R package version 1.0.0. <https://CRAN.R-project.org/package=shiny>
- (128) Winston Chang (2016). shinydashboard: Create Dashboards with 'Shiny'. R package version 0.5.3. <https://CRAN.R-project.org/package=shinydashboard>
- (129) Kolde, R. *R package version* **2012**, *61*.
- (130) Stacklies, W.; Redestig, H.; Scholz, M.; Walther, D.; Selbig, J. *Bioinformatics* **2007**, *23*, 1164-1167.
- (131) Adler, D.; Nenadic, O.; Zucchini, W. In *Proceedings of the 35th Symposium of the Interface: Computing Science and Statistics, Salt Lake City*, 2003.
- (132) John W. Tukey (1977). *Exploratory Data Analysis*. Addison-Wesley.
- (133) Wilkinson, L.; Friendly, M. *The American Statistician* **2009**, *63*, 179-184.
- (134) Jain, A. K.; Murty, M. N.; Flynn, P. J. *ACM Comput. Surv.* **1999**, *31*, 264-323.
- (135) Nugent, R.; Meila, M. *Methods in molecular biology (Clifton, N.J.)* **2010**, *620*, 369-404.
- (136) Ringner, M. *Nat Biotech* **2008**, *26*, 303-304.

# Paper I





## Multiplexed MALDI-MS arrays for screening of MIP solid phase extraction materials



Kishore Kumar Jagadeesan<sup>a,\*</sup>, Celina Wierzbicka<sup>b</sup>, Thomas Laurell<sup>a</sup>, Börje Sellergren<sup>b</sup>, Sudhirkumar Shinde<sup>b</sup>, Simon Ekström<sup>a</sup>

<sup>a</sup> Department of Biomedical Engineering, Lund University, Lund, Sweden

<sup>b</sup> Department of Biomedical Sciences, Faculty of Health and Society, Malmö University, Sweden

### ARTICLE INFO

#### Article history:

Received 25 March 2015

Received in revised form 19 October 2015

Accepted 22 October 2015

Available online 30 October 2015

#### Keywords:

Solid-phase extraction

Mass spectrometry

Proteomics

MALDI MS

ISET

### ABSTRACT

Technology that facilitates rapid investigation of solid phase extraction protocols using very small amounts of sorbent can save both time and money. The microfabricated ISET (Integrated Selective Enrichment Target) interfaced with MALDI mass spectrometry is able to provide an efficient, economic and generic optimization process for SPE sample preparation. The SPE is performed in a rapid and parallel fashion, with a processing time off only 2 h per ISET with 96 samples. Each of the 96 wells on the ISET can hold 600 nL of SPE sorbent. The ability to work with small amounts of sorbent and samples in the ISET platform provides a big advantage when developing affinity sorbents, such as molecularly imprinted polymers (MIPs). Here it is demonstrated that an amount of 25 mg phosphoserine imprinted MIP (pS-MIP) sorbent can allow for analysis of more than 500 ISET nanovials using a multitude of different conditions. In the presented case, the multiplexed experiments allowed for early discovery of unspecific interactions and subsequent minimization of these, resulting in a protocol that provided improved enrichment of phosphopeptides.

© 2015 Elsevier B.V. All rights reserved.

### 1. Introduction

Solid-phase extraction (SPE) is one of the most commonly used sample preparation technique in many laboratories. The flexibility and through-put of SPE has facilitated applications in many different fields such as; environmental, drug analysis, proteomics, and DNA analysis for a multitude of purposes e.g., purification, enrichment, desalting and fractionation [1]. Optimization of the SPE sample preparation step is crucial for high-sensitivity detection, as well as analysis robustness and reproducibility. The SPE optimization process for a certain analyte usually starts with screening for a suitable extraction phase or if the appropriate extraction phase is known with the fine tuning of the sample preparation conditions, i.e., the loading, washing and elution steps. Due to the ever increasing number of available SPE phases the development of efficient

methods that allows for rapid parallel screening and optimization of SPE sample preparation is of great importance.

Over the years a wide variety of functionalized polymeric sorbents and highly cross-linked polymers that can be used for SPE have been developed, both in the form of broad generic solid phase materials (RP, IEX, HILIC) and in the form of novel affinity SPE sorbents. These affinity phases can be based on inorganic small molecules (salts/IMAC), organic molecules (dyes/cibaron, inhibitors) or biomolecules (antibodies, proteins, sugars, nucleic acids). Especially immunosorbents, where an antibody is coupled to the solid phase have found widespread use for both small molecule and biomolecule SPE [2,3]. One of the biggest drawbacks associated with antibody based SPE methods is the cost, stability and sometimes cumbersome coupling to the solid phase. This has led to an interest in developing antibody mimics such as aptamers [4–6] and molecularly imprinted polymers (MIPs) [7,8]. In the case of MIPs the most successful applications have been developed for low molecular weight targets in non-aqueous systems, but recent developments have seen an increased effort to expand this technology to encompass biomolecule affinity applications [9,10]. An example of this is the development of MIPs having affinity for phosphopeptides [11–13]. Many of these new SPE phases can be

Abbreviations: ISET, integrated selective enrichment target; DRIE, deep reactive ion etching; MIP, molecularly imprinted polymer.

\* Corresponding author at: Lund University, Department of Biomedical Engineering, Div. Nanobiotechnology, Box 118, 221 00 Lund, Sweden. Fax: +46 462224527.

E-mail addresses: [kishore.jagadeesan@bme.lth.se](mailto:kishore.jagadeesan@bme.lth.se), [jkishore85@gmail.com](mailto:jkishore85@gmail.com) (K.K. Jagadeesan).

<http://dx.doi.org/10.1016/j.jchromb.2015.10.033>  
1570-0232/© 2015 Elsevier B.V. All rights reserved.



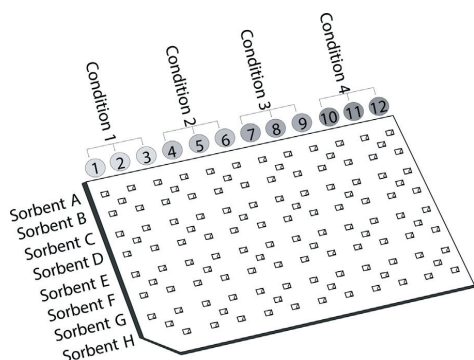


**Fig. 1.** Integrated selective enrichment target (ISET) with labelling illustrating how an experimental set-up for SPE optimization can be facilitated. In the drawing 8 different sorbents (A–H row wise) can be tested in triplicate under four different conditions (1–12 column wise).

produced using combinatorial techniques, thereby generating huge number of materials that needs to be characterized.

Current methods used for SPE screening and optimization are often based on any of the four widely available SPE formats; [14] (1) SPE Disks, in which sorbent is immobilized; (2) cartridges in which sorbents are filled in a small, plastic or glass open-ended containers [15,16]; (3) 96 well microtiter plate configurations, that mimics the standard 96 well microtiter plate [17] and (4) SPE pipette tips, where the sorbent is immobilized inside a pipette tip [18,19]. The process of screening SPE sample preparation in these commercially available formats can be quite time consuming and expensive, due to the large amounts of SPE phase required and limited options for filling with different materials.

As a solution, we have here applied our microfabricated SPE sample preparation platform, the Integrated Selective Enrichment Target, (ISET) that interfaces directly with MALDI mass spectrometry for analysis [20–22], for rapid and parallel investigation of the SPE process using minute amounts of sample. The ISET–SPE platform has previously been demonstrated in SPE applications such as purification of immuno-captured analytes [23], aptamer capture [24] and screening of recombinant proteins [25]. The ISET sample preparation platform is manufactured in silicon, having 96 pyramidal array positions, each of which can be filled with 0.6  $\mu$ L of a selected SPE sorbent. The small bead volume required for filling the nanovials allows for very economic SPE optimization, as more than 500 samples can be subjected to SPE on the ISET platform using as little as 25 mg of stationary phase, i.e., less than the amount present in an ordinary 1 mL SPE cartridge. At the same time the parallelization provided by the ISET platform (96 samples/chip) facilitates multiplexed analysis of different SPE materials or sample preparation conditions with enough replicates to ensure the validity of the developed SPE protocol. For example, multiplexing by using different solution conditions column-wise with respect to different SPE sorbents row-wise in the ISET arrays enables easy high-throughput optimization of the sample preparation protocol, Fig. 1.

Here the usefulness of the multiplexed MALDI MS SPE optimization is demonstrated using a molecularly imprinted polymer (MIP) developed for selective enrichment of phosphoserine (pS) containing peptides. The SPE optimization study was conducted, using different loading, washing and elution conditions. The collected data provided an optimized protocol maximizing the specificity while minimizing background, thereby allowing for specific capture of phosphopeptides from 1:10 mixture of BSA. In addition the

data from the multiplexed screening experiments could also be used to draw conclusions about the interactions of the MIP material.

## 2. Materials and methods

### 2.1. Proteins and reagents

Proteolytic enzyme, trypsin, from Promega (Madison, WI, USA) was used in the digestion step of all proteins. Pure phosphopeptides such as Bovine  $\beta$ -casein-monophospho (FQ-pS-EEQQQTEDELQDK), PKA Regulatory Proteins/peptides Subunit II Substrate (DLDVPIPGRFDRRV-pS-VAEE), Phosphorylated PKC Substrate-1 (KRP-pS-QRHGSKY-NH<sub>2</sub>), DAM1 [221–241] peptide (SFVLNPTNIGM-pS-KSSQGHVTK) and Kinase Domain of Insulin Receptor (TRDIYETDpYpYRK), Kinase Domain of Insulin Receptor (TRDIpYETDpYpYRK) were bought from AnaSpec (Fremont, CA, USA). Stock solutions of 2  $\mu$ M were prepared for each of these phosphopeptides in 100% ACN. All other chemicals and reagents were purchased from Sigma–Aldrich (St. Louis, MO, USA). Hydrophilic interaction chromatography beads 20  $\mu$ m (HILIC) were from Merck Millipore (Billerica, MA, USA), strong anionic exchange (SAX) Poros 50HQ from Life Technologies and magnetic TiO<sub>2</sub> beads from PerkinElmer.

Bovine serum albumin (BSA) and  $\beta$ -casein was digested with trypsin in a 1:100 ratio (enzyme:protein) at 37 °C. The digested proteins were diluted with 0.1% TFA and frozen to stop the digestion process. Stock solutions of 4  $\mu$ M were used to prepare samples by dilution with 100% acetonitrile (ACN).

### 2.2. Chemicals

Acrylamide and pentaerythritoltriacylate (PETA) were Aldrich products obtained from Sigma–Aldrich (Milwaukee, USA); 1,2,2,6,6-pentamethylpiperidine was from Fluka (Buchs, Switzerland); *N,N*-azo-bis(2,4-dimethyl) valeronitrile (ABDV) was from Wako Chemicals GmbH (Neuss, Germany); THF was from Acros (Geel, Belgium); The functional monomer *N*-3,5-bis(trifluoromethyl)-phenyl-*N'*-4-vinylphenylurea was synthesized as reported previously [26].

### 2.3. MIP SPE phase preparation

Imprinted polymer pS-MIP was prepared in the following manner: The template: bis-pentamethylpiperidine (PMP) salt of Fmoc-pSerOEt (template; 0.5 mmol), *N*-3,5-bis (trifluoromethyl)-phenyl-*N'*-4-vinylphenylurea (functional monomer, 1 mmol), acrylamide (1 mmol), and pentaerythritol triacrylate (PETA) (13, 3 mmol) were dissolved in THF (5.6 mL). The initiator 2,2'-azo-bis (2,4-dimethyl) valeronitrile (ABDV) (1% w/w of total monomer) was added to the solution. The solution was transferred to a glass ampoule, cooled to 0 °C, and purged with a flow of dry nitrogen for 10 min. The tubes were then flame-sealed while still cooling, and the polymerization was initiated by placing the tubes in a thermostatted water bath at 50 °C. The tubes were broken after 24 h and the polymers lightly crushed. Next polymers were subjected to template removal in a Soxhlet apparatus with MeOH/1N HCl (80:20 v/v). This process was followed by further crushing and sieving, whereafter the fraction of 25–36  $\mu$ m MIP sorbent particles was used for ISET SPE. Nonimprinted polymer (NIP) was prepared in the same manner as described above, but with the omission of the template molecule in the prepolymerization solution.

### 2.4. ISET

The ISET chips were manufactured by anisotropic wet etching and deep reactive ion etching (DRIE) by GeSiM (Großberkmannsdorf,

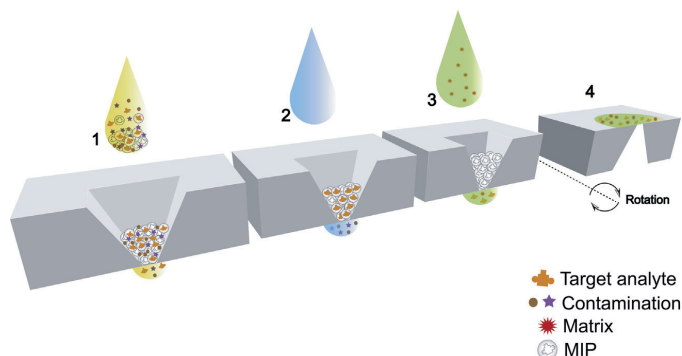


**Fig. 2.** Steps involved in the solid phase extraction utilizing the ISET platform with the molecularly imprinted polymer (MIPs) sorbent. In the ISET SPE sample preparation samples incubated with MIP material were transferred to ISET nanovials (1) followed by a wash step to remove undesired components (2). The captured analytes were then displaced by the elution step (3) and addition of MALDI matrix on the backside at low vacuum. Subsequently the ISET was turned over (4) and inserted into mass spectrometry for analysis.

Germany) from 780  $\mu\text{m}$  thick 4" silicon wafers. During the sample preparation steps the ISET chip was placed into a vacuum fixture made from an ordinary 384 microplate, which facilitates use with commercial liquid handling robots and vacuum manifolds. Before insertion in the MALDI instrument the ISET was secured in a milled steel adaptor using tape (3M, 7955 MLP), providing the same spot positioning as a normal MALDI target.

### 2.5. ISET–MIP sample preparation

All the SPE steps were performed using vacuum to enable liquid transport. Prior to loading the ISET nanovials the MIP particle concentration was adjusted in a test ISET so that a 2  $\mu\text{L}$  MIP slurry addition to a sample resulted in a final nanovial packing volume of 500–600 nL. During the final sample elution the vacuum was lowered in order to allow surface tension to retain the analytes in a small spot around the outlet hole, this facilitated a confined crystallized MALDI spot on the underside of the ISET after matrix addition. The ISET was subsequently turned up-side down and used as a MALDI target plate. Fig. 2 depicts the general steps of the ISET sample preparation.

### 2.6. The ISET MIP SPE protocol

1. MIP material corresponding to an SPE volume of 500–600 nL was added to each sample in a microplate or standard eppendorf tube and incubated for 90 min.
2. The captured analytes were transferred to the ISET by aspiration of sample/MIP from the bottom of the container and then loaded into the ISET using a high vacuum (10–15 in Hg).
3. Wash with  $5 \times 2 \mu\text{L}$  washing buffer (95% ACN, 5%  $\text{H}_2\text{O}$ , 0.1% TFA) using high vacuum (10–15 in Hg).
4. Turn off vacuum and remove the ISET chip from the vacuum fixture and rinse the entire underside of the chip with MQ water and ethanol. Dry the underside with a clean tissue.
5. Elution of the analytes to the underside of the ISET chip with  $2 \times 1 \mu\text{L}$  elution buffer (90% MeOH, 10%  $\text{H}_2\text{O}$ , 0.1%  $\text{H}_2\text{KPO}_4$ ) using low vacuum (1.5–2 in Hg).
6. Addition of 500 nL matrix solution: 2.5 mg dihydroxybenzoic acid (DHB) (10 mg/ml DHB in 80% MeOH), 1%  $\text{H}_3\text{PO}_4$  using low vacuum (1.5–2 in Hg).
7. The ISET was subsequently removed from the vacuum fixture turned over with matrix spots facing upwards and placed in a MALDI adaptor plate for MS analysis.

### 2.7. MALDI analysis

MALDI analysis was made using a Waters M@LDI-TOF MS (Milford, MA, USA). The MALDI-TOF instrument was used in reflector mode, MCP 1950 V and reflector voltage of 2000 V. Prior to data acquisition the MALDI settings were optimized to provide the best possible resolution and a three point calibration was made on each plate. All the spectra were acquired manually and approximately 100 shots were averaged. Resulting spectra were processed by MassLynx software v4.1 (Waters Corporation, Milford, MA, USA).

## 3. Results and discussion

Molecularly imprinted polymers developed to have specificity toward the phosphotyrosine (pY-MIP) group have been previously shown to allow for enrichment of tyrosine phosphorylated peptides [11–13]. The affinity for this type of material is quite complex and with a heterogeneous population of binding sites, a larger amount of sites in the  $10^4 \text{ M}^{-1}$  range and a 10–100 times less abundant population of high energy binding sites at  $10^{5-6} \text{ M}^{-1}$  [11]. Enrichment factors of 35 for the pY-MIP compared to 5.5 for the same a non-imprinted polymer (NIP) have been reported for a mixture of phosphorylated/unphosphorylated angiotensin 2. Although, when challenged with a more complex sample a triply tyrosine-phosphorylated peptide was out-competing a singly phosphorylated, and some binding of serine and threonine, as well as unphosphorylated peptides was also observed [12]. This type of complex behavior is expected in any affinity based SPE protocol, and as the complexity of a sample increases it becomes even more important to have an optimized SPE protocol. A suitable parallel can be drawn to the  $\text{TiO}_2$ -based affinity purification of phosphopeptides, where a huge amount of work and progress have been made in understanding and minimizing background from non-phosphorylated peptides [27].

Here the ISET platform was used in order to quickly screen a large number of conditions for optimization of the SPE conditions for a newly developed pS-MIP in order to minimize observed background and find out if the platform could facilitate large scale studies of MIP sorbents. As the affinity constant of the phospho-specific MIP material was expected to be in the  $\mu\text{M}$  range, some initial experiments were conducted in order to decide if the binding was time dependent. This was done by incubation of samples with the MIP material followed by transfer to the ISET for wash and elution at regular intervals. The sample solution was composed of

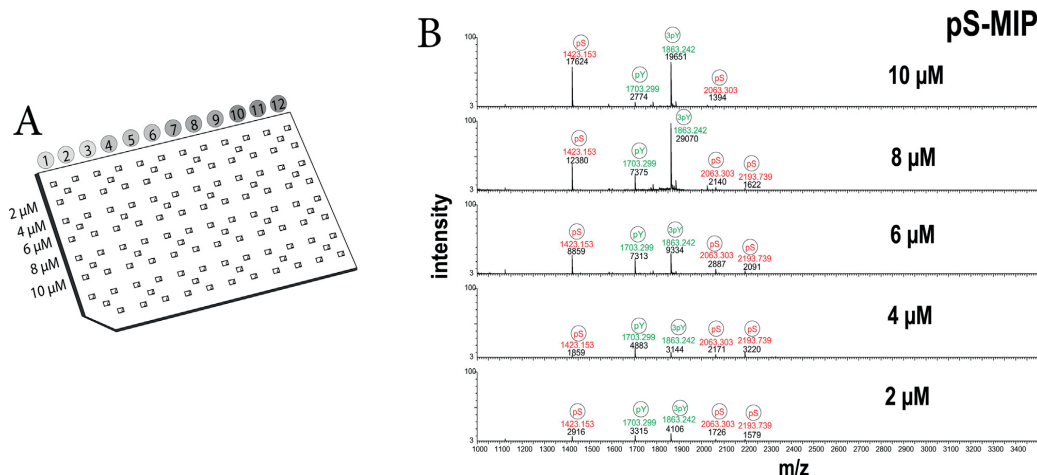


**Fig. 3.** Investigation of the selectivity and capacity of the pS-MIP sorbent. Using increasing concentrations (2, 4, 6, 8, 10  $\mu$ M) of a standard phosphopeptide mixture composed of singly phosphorylated peptides (3 pS and 1 pY) and one triply phosphorylated phosphotyrosine peptide (3pY) in different rows of the ISET. B. Mass spectra after the capture with the pS-MIP, as the capacity of the pS-MIP material in a ISET nanovals becomes limited (at 4–6  $\mu$ M) the triply phosphorylated phosphotyrosine peptide (3 pY) outcompetes the singly phosphorylated peptides.

four phosphoserine peptides and two phosphotyrosine peptides. Triplicate samples were prepared at time points of 30, 60, and 90 min of incubation. The resulting MS data revealed that binding was time dependent, with a maximum binding of phosphopeptides observed after 60–90 min (Supporting information, Fig. S1). In order to ensure maximum sensitivity and no differences due to binding time, 90 min incubation was used for all further experiments.

In a similar manner, the elution protocol was optimized using the same standard phosphopeptide mixture. A number of different conditions were investigated and it was found that the highest average signal intensities could be observed after elution using 90% MeOH, 10% H<sub>2</sub>O, 0.1% H<sub>2</sub>KPO<sub>4</sub> and a matrix solution of 2,5-dihydroxybenzoic acid containing 1% H<sub>3</sub>PO<sub>4</sub>. The addition of phosphoric acid to the matrix has previously been demonstrated to improve detection of phosphopeptides [28].

The capacity of the high affinity sites for pS-peptides in this type of MIP materials can be estimated to be in the order of 10 pmol/mg [12], and as the approximate amount of SPE material in one ISET nanoval is 50  $\mu$ g this would correspond to a 0.5 pmol capacity of high affinity sites/ISET position and a total capacity (including low affinity sites) in the range 5–50 pmol. To investigate if the pS-MIP material exhibited any preferential binding multi-phosphorylated peptides at limited capacity, a standard phosphopeptide mixture with increasing concentrations was processed. The standard phosphopeptide mixture was composed of two singly phosphorylated peptides (3 pS and 1 pY) and one triply phosphorylated tyrosine peptide (3pY). Identical amounts of pS-MIP sorbent was incubated in 10  $\mu$ l samples with increasing concentration (2, 4, 6, 8, 10  $\mu$ M) and transferred into ISET nanovals for wash and elution (corresponding to total loads ranging from 20 to 100 pmol). From the resulting MALDI mass spectra, Fig. 3, it was evident that as the concentration increased above 4–6  $\mu$ M the signal intensity did not increase in a predictable manner. Above 6  $\mu$ M the triply phosphorylated tyrosine peptide (1863 Da) and one of the singly serine phosphorylated peptides (1423 Da) showed a marked increase in signal intensity while the other peptide signals remained unchanged or decreased. This indicates that the binding capacity for the amount of pS-MIP sorbent in one ISET well is in close agreement with the theoretical value of 5–50 pmol. The

preferential binding of multi-phosphorylated peptides at under-capacity has also been observed for TiO<sub>2</sub> and is attributed to the stronger binding provided by multivalent interactions [29]. The increased signal for the singly phosphorylated serine peptide at 1423 Da could either be a result of the pS affinity provided by the MIP or a result of preferential ionization, as this peptide has a positive net charge and 2 lysine residues [30,31]. From the experiments it was evident that selectivity of the pS-MIP is affected by the capacity.

In order to investigate the impact of unspecific binding the pS-MIP SPE sample preparation was compared to too some standard phosphopeptide SPE sorbents, i.e., hydrophilic interaction chromatography (HILIC), strong anionic exchange (SAX) and TiO<sub>2</sub>, using samples consisting of trypsin digested  $\beta$ -casein. The tryptic digestion of  $\beta$ -casein results in 2 pS peptides and a number of non-phosphorylated peptides (background). Samples of 10  $\mu$ l at a concentration of 2  $\mu$ M were incubated for 90 min with each different sorbent and loaded into separate rows of ISET nanovals for wash, elution and analysis. Evaluation of the resulting mass spectra showed that the pS-MIP sorbent captured both phosphorylated peptides with a similar signal intensity and non-specific background as observed for the HILIC and SAX sorbents, Fig. 4. It is important to note that the signal intensities of the phosphopeptides are not used to draw conclusions, due the differences in capturing capacity for the different SPE materials (due to varying size and porosity), instead the relationship of phosphopeptide and background in combination with knowledge of binding mechanism for the SPE sorbents was used. In fact for all of the SPE phases unspecific binding of a non-phosphorylated acidic peptide at 2187.5 Da is observed, this acidic peptide has a pI of 4.07 and contains one glutamate as well as one aspartate residue with C-terminal carboxyl group. The phosphopeptide capture for the generic SPE materials can be explained by the fact that phosphopeptides are amongst the most acidic peptides due to their negatively charged phosphate group and are able to interact with different materials by many different ways, i.e., electrostatic interactions, Lewis acid–base and bidentate bonds [27]. The zwitter ionic HILIC material also provided high signals for both phosphopeptides and acidic peptides [32]. The SAX material captured the acidic peptide but to a

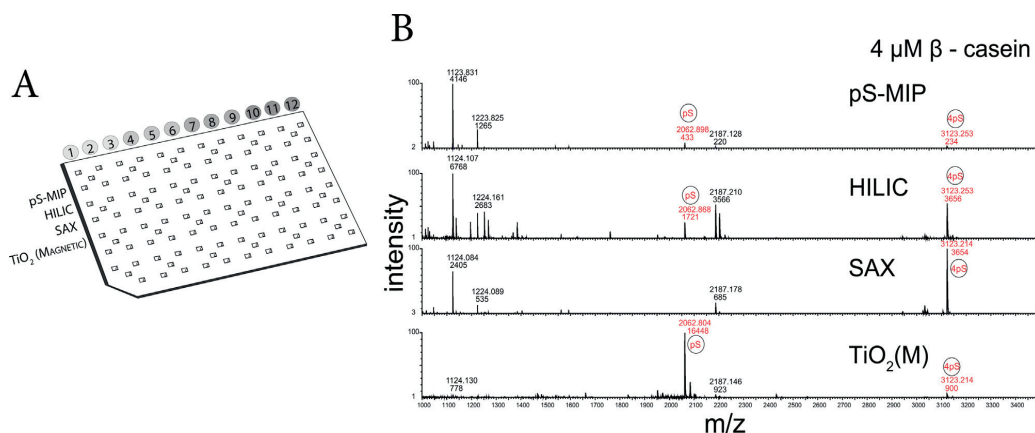


**Fig. 4.** Comparison of the MIP SPE with HILIC, SAX and magnetic  $\text{TiO}_2$ , using a standard  $\beta$ -casein sample. A. Each row of the ISET is loaded with different SPE materials. B. The resultant spectra show that MIP sorbent have similar non-specific background binding as the HILIC and SAX. Due to differences in size and porosity the capacity is higher for the HILIC, SAX and  $\text{TiO}_2$  SPE.

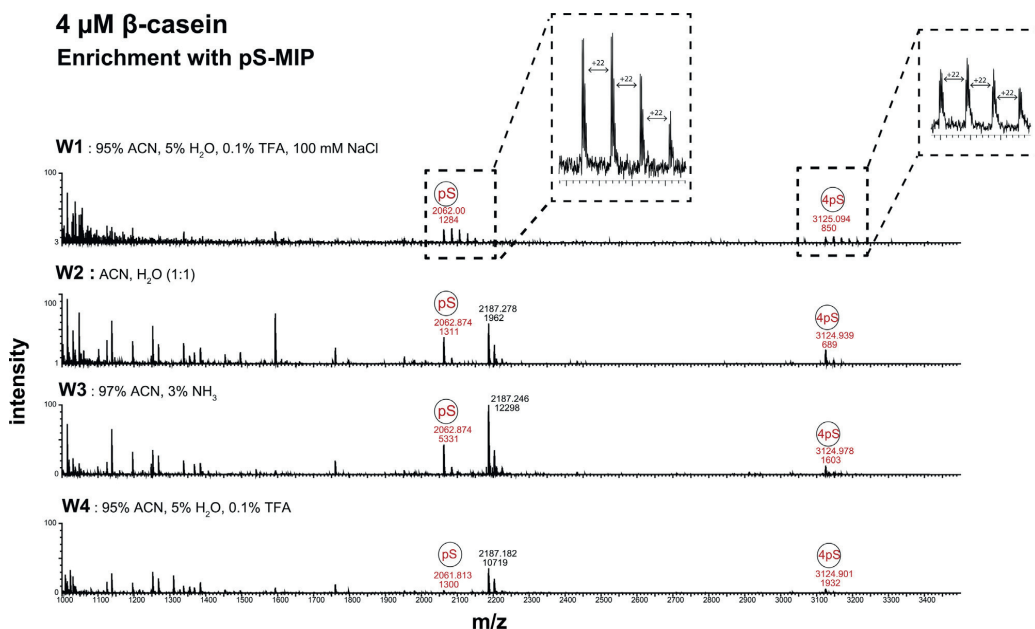


**Fig. 5.** Investigation of the presence of unspecific electrostatic interactions was performed by pS-MIP enrichment of a trypsin digested  $4 \mu\text{M}$   $\beta$ -casein sample using different washing buffers in the SPE protocol. The incubated sample/MIP mixture are loaded into the ISET and each wash buffer is used row wise. The following washing buffers were used in this experiment; W1–95% ACN, 5%  $\text{H}_2\text{O}$ , 0.1% TFA, 100 mM NaCl, W2–ACN: $\text{H}_2\text{O}$  (1:1), W3–97% ACN, 3%  $\text{NH}_3$ , W4–95% ACN, 5%  $\text{H}_2\text{O}$ , 0.1% TFA. The resultant spectra shows that addition of NaCl (W1) in the washing buffer reduces the un-specific binding, although at the cost of adduct formation ( $\text{M} + \text{Na}^+$ ).

lower extent and the singly phosphorylated peptide at 2062.8 Da was not observed at all, while the tetra-phosphorylated peptide at 3123.25 Da showed very strong binding [33,34]. The gold standard phosphopeptide capture sorbent,  $\text{TiO}_2$  displayed the highest intensities for the mono-phosphorylated peptide, a well-known behavior [35] and low signal for the acidic unspecific peptides. Nonspecific binding of acidic peptides containing aspartic acid and glutamic acid residues is also commonly seen with  $\text{TiO}_2$  and IMAC materials, and it has been extensively investigated [27,35]. Thus

for  $\text{TiO}_2$  there are many different methods for minimizing background available, such as the use of acidic loading buffers and weak competitive binders such as DHB [36] and lactic acid [37] or methylation of carboxyl groups [38].

In the case of the pS-MIP no significant difference in observed background could be seen when using acidic loading conditions (Supporting information, Fig. S2), neither did addition of DHB decrease the background (data not shown). The similarity in observed background for the pS-MIP and the HILIC and SAX phase

## pS-MIP

 $\beta$ -casein:BSA = 1:10 $\beta$ -casein:BSA = 1:5 $\beta$ -casein:BSA = 1:1

BSA

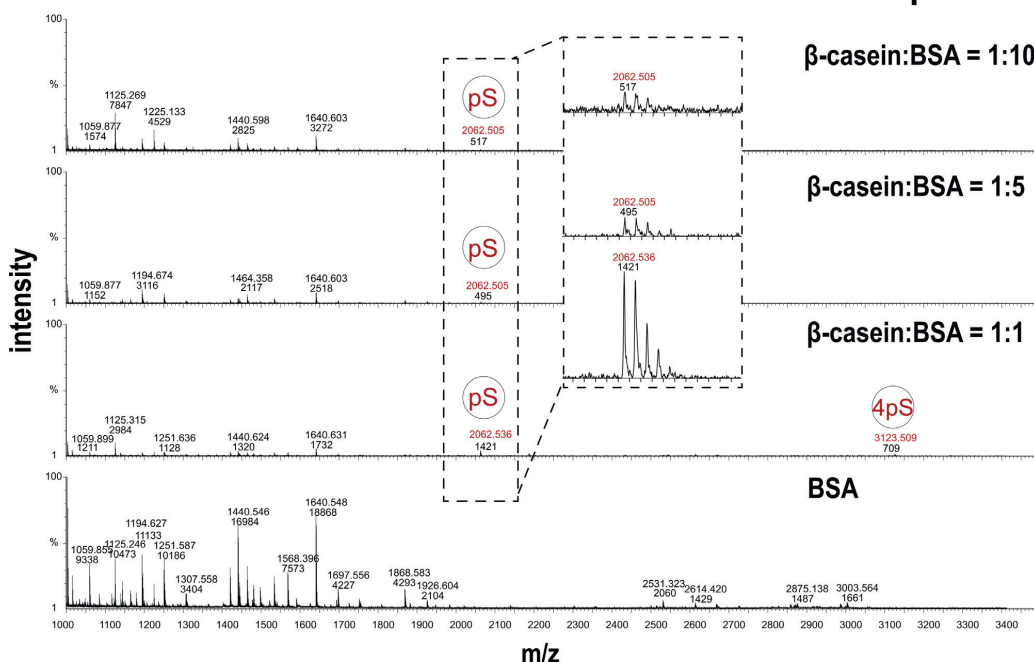


**Fig. 6.** Each row of the ISET are loaded with incubated sample/MIP mixture containing different ratios (1:1, 1:5, 1:10) of  $\beta$ -casein and BSA. The observed MALDI spectra of pS-MIP enriched  $\beta$ -casein spiked in BSA at different ratios (1:1, 1:5, 1:10). Under these optimized conditions the pS-MIP could capture both of the phosphopeptides at 1:1 and 1:5 and one phosphopeptide at 1:10 ratio of  $\beta$ -casein and BSA with very low background.

in combination with the fact that the phosphopeptides were also observed with the NIP material indicates that there might be other electrostatic interactions in the MIP material in addition to the specific phosphopeptide imprinting. The observed unspecific binding for the MIP sorbent could be due to interactions between peptide carboxyl groups with the urea moieties of the MIP/NIP materials.

In order to investigate how the unspecific background could be minimized different washing buffers were tested using the ISET platform. Four different washes were used; W1—95% ACN, 5%  $\text{H}_2\text{O}$ , 0.1% TFA, 100 mM NaCl, W2—97% ACN, 3%  $\text{NH}_3$ , W3—ACN: $\text{H}_2\text{O}$  (1:1), W4—95% ACN, 5%  $\text{H}_2\text{O}$ , 0.1% TFA, Fig. 5. The original washing protocol (W4) shows the same background as observed previously, while the wash containing only 50% ACN (W3) leads to an even higher background as some of the hydrophobic peptides are no longer washed away. In the wash using basic conditions (W2) the peak for the acidic peptide at 2186.6 Da becomes even more pronounced, as the negative net charge increases. Among the different washing buffers, W1 including 100 mM NaCl resulted in much less background compared to the other washing solutions. NaCl is commonly used in ion exchange protocols to enable elution and was added to W1 in order to minimize unspecific interactions of electrostatic nature and provide increased selectivity. In addition an improved selectivity was also observed when the pS-MIP was compared with NIP material, especially for the mono-phosphorylated peptide (Supporting information, Fig. S3).

This supports the hypothesis of unspecific electrostatic interactions on the surface of the pS-MIP material that can bind both phosphorylated and unphosphorylated peptides. Although it should be noted that while the addition of NaCl in the washing buffer reduced un-specific binding, the presence of salt in the final

elution lead to  $(\text{M} + \text{Na}^+)$  adduct formation and a lower sensitivity in the MALDI MS analysis.

As the use of NaCl in the washing step was both beneficial (reduced background) and detrimental (adducts, lower sensitivity), a new SPE protocol with NaCl added in the loading buffer and an extra wash step without NaCl was implemented in order to maintain sensitivity and low background while avoiding the adduct formation in the MS analysis step. This protocol was tested using samples containing different ratios of  $\beta$ -casein and BSA (1:10, 1:5, 1:1). The different samples of trypsin digested  $\beta$ -casein and BSA were incubated with the pS-MIP for 90 min in a loading buffer with 100% ACN, 100 mM NaCl. The incubated sample-MIP mixture was then transferred to the ISET and subjected to a SPE protocol using an extra wash without NaCl followed by elution and MALDI-MS analysis. From the resultant spectra, Fig. 6, it was clear that the background generated by the BSA peptides in the sample could be effectively reduced while avoiding the detrimental effects of Na adducts. Using this optimized SPE protocol, allowed for pS-MIP capture of one phosphopeptide (2062.5  $m/z$ ) even when the ratio of  $\beta$ -casein and BSA was 1:10.

In the case of many MIP systems the exact recognition mechanism is not clearly understood and even for a well-studied system like the used phosphopeptide MIP the specificity is very complex [11,39]. Due to the polymeric nature of the MIP material it is very difficult to discern between unspecific binding and specific binding. While  $\text{TiO}_2$  material presents a fairly homogeneous surface for binding, MIP sorbent consists of a polymer network with a mix of high affinity, low affinity binding sites and a multitude of chemical groups (from the monomers used) available for interaction. In this respect MIPs are more similar to their biological counterpart



the antibody, which exhibits even more diverse chemical makeup. Therefore, many fundamental properties of the MIPs affinity needs to be systematically studied, e.g., the dependence of the cross-linker concentration, functional monomer concentration, buffer composition, ionic strength, pH and temperature. This also makes it important to develop technologies that allows for optimization of the sample preparation protocol, both for taking full advantage of the selectivity provided by MIPs and for understanding of the underlying binding mechanisms.

#### 4. Conclusion

It is demonstrated that the ISET platform facilitates rapid investigation of different solid phase extraction protocols with low sorbent and sample usage. An amount of 25 mg MIP sorbent allowed for SPE sample preparation in more than 500 ISET wells. With a processing time of 2 h/ISET with 96 samples excluding sample incubation, the generic miniaturized format provides both multiplexed analysis and high-throughput. This makes the ISET platform an efficient screening step for newly prepared sorbent materials especially when time and cost are a concern. In the case of the investigated pS-MIP the multiplexed experiments allowed for discovery of unspecific interactions and subsequent minimization of these, resulting in a protocol that provided improved enrichment of phosphopeptides. The ability to develop optimized sample preparation protocols that maximizes the selectivity of MIPs is key aspect for successful applications using real clinical samples. In the near future this screening platform will be used for discovery of improved phosphopeptide specific MIPs from libraries made by combinatorial techniques, involving up to 96 different MIP sorbents.

#### Acknowledgment

This work has been performed as part of the 'Robust affinity materials for applications in proteomics and diagnostics' (PEP-MIP) project, supported by the Seventh Research Framework Programme of the European Commission. Grant agreement number: 264699.

#### Appendix A. Supplementary data

Supplementary data associated with this article can be found, in the online version, at <http://dx.doi.org/10.1016/j.jchromb.2015.10.033>.

#### References

- [1] C.F. Poole, New trends in solid-phase extraction, *TrAC Trends Anal. Chem.* 22 (2003) 362–373.
- [2] D. Stevenson, Immuno-affinity solid-phase extraction, *J. Chromatogr. B Biomed. Sci. Appl.* 745 (2000) 39–48.
- [3] N. Delaunay, V. Pichon, M.C. Hennion, Immunoaffinity solid-phase extraction for the trace-analysis of low-molecular-mass analytes in complex sample matrices, *J. Chromatogr. B Biomed. Sci. Appl.* 745 (2000) 15–37.
- [4] A.B. Iliuk, L. Hu, W.A. Tao, Aptamer in bioanalytical applications, *Anal. Chem.* 83 (2011) 4440–4452.
- [5] S. Kraemer, J.D. Vaught, C. Bock, L. Gold, E. Katilius, T.R. Keeney, N. Kim, N.A. Saccomano, S.K. Wilcox, D. Zichi, G.M. Sanders, From SOMAmer-based biomarker discovery to diagnostic and clinical applications: a SOMAmer-based, streamlined multiplex proteomic assay, *PLoS One* 6 (2011) e26332.
- [6] B. Madru, F. Chapuis-Hugon, E. Peyrin, V. Pichon, Determination of cocaine in human plasma by selective solid-phase extraction using an aptamer-based sorbent, *Anal. Chem.* 81 (2009) 7081–7086.
- [7] A. Moradian, K. Mosbach, Preparation of a functional, highly selective polymer by molecular imprinting. A demonstration with L-p-aminophenylalanine anilide as a template molecule allowing multiple points of attachment, *J. Mol. Recognit.* 2 (1989) 167–169.
- [8] G. Vlatakis, L.I. Andersson, R. Muller, K. Mosbach, Drug assay using antibody mimics made by molecular imprinting, *Nature* 361 (1993) 645–647.
- [9] N.W. Turner, C.W. Jeans, K.R. Brain, C.J. Allender, V. Hlady, D.W. Britt, From 3D to 2D: a review of the molecular imprinting of proteins, *Biotechnol. Prog.* 22 (2006) 1474–1489.
- [10] D.E. Hansen, Recent developments in the molecular imprinting of proteins, *Biomaterials* 28 (2007) 4178–4191.
- [11] M. Emgenbroich, C. Borrelli, S. Shinde, I. Lazrag, F. Vilela, A.J. Hall, J. Oxelbark, E. De Lorenzi, J. Courtois, A. Simanova, J. Verhage, K. Irgum, K. Karim, B. Sellergren, A phosphotyrosine-imprinted polymer receptor for the recognition of tyrosine phosphorylated peptides, *Chem. Eur. J.* 14 (2008) 9516–9529.
- [12] S. Helling, S. Shinde, F. Brosse, A. Schnabel, T. Müller, H.E. Meyer, K. Marcus, B.R. Sellergren, Ultratrace enrichment of tyrosine phosphorylated peptides on an imprinted polymer, *Anal. Chem.* 83 (2011) 1862–1865.
- [13] S. Shinde, A. Bunschoten, J.A. Kruijtz, R.M. Liskamp, B. Sellergren, Imprinted polymers displaying high affinity for sulfated protein fragments, *Angew. Chem. Int. Ed.* 51 (2012) 8326–8329.
- [14] A. Zwir-Ferenc, M. Biziuk, Solid phase extraction technique—trends, opportunities and applications, *Polish. J. Environ. Stud.* 15 (2006) 677–690.
- [15] R. Keci, J. Billing, D. Nivhede, B. Sellergren, E. Rees, Fast identification of selective resins for removal of genotoxic aminopyridine impurities via screening of molecularly imprinted polymer libraries, *J. Chromatogr. A* 1339 (2014) 65–72.
- [16] W. Ji, X. Ma, H. Xie, L. Chen, X. Wang, H. Zhao, L. Huang, Molecularly imprinted polymers with synthetic dummy template for simultaneously selective removal and enrichment of ginkgolic acids from *Ginkgo biloba* L. leaves extracts, *J. Chromatogr. A* 1368 (2014) 44–51.
- [17] C. Chassaing, J. Stokes, R.F. Venn, F. Lanza, B. Sellergren, A. Holmberg, C. Berggren, Molecularly imprinted polymers for the determination of a pharmaceutical development compound in plasma using 96-well MISPE technology, *J. Chromatogr. B* 804 (2004) 71–81.
- [18] H. Yan, C. Yang, Y. Sun, K.H. Row, Ionic liquid molecularly imprinted polymers for application in pipette-tip solid-phase extraction coupled with gas chromatography for rapid screening of dicofol in celery, *J. Chromatogr. A* 1361 (2014) 53–59.
- [19] T. Du, J. Cheng, M. Wu, X. Wang, H. Zhou, M. Cheng, Pipette tip-based molecularly imprinted monolith for selective micro-solid-phase extraction of methomyl in environmental water, *Anal. Methods* 6 (2014) 6375–6380.
- [20] S. Ekström, L. Wallman, J. Malm, C. Becker, H. Lilja, T. Laurell, G. Marko-Varga, Integrated selective enrichment target—a microtechnology platform for matrix-assisted laser desorption/ionization-mass spectrometry applied on protein biomarkers in prostate diseases, *Electrophoresis* 25 (2004) 3769–3777.
- [21] S. Ekström, L. Wallman, D. Hok, G. Marko-Varga, T. Laurell, Miniaturized solid-phase extraction and sample preparation for MALDI MS using a microfabricated integrated selective enrichment target, *J. Proteome Res.* 5 (2006) 1071–1081.
- [22] B. Adler, T. Laurell, S. Ekström, Optimizing nanovial outlet designs for improved solid-phase extraction in the integrated selective enrichment target—ISET, *Electrophoresis* 33 (2012) 3143–3150.
- [23] A. Ahmad-Tajudin, B. Adler, S. Ekström, G. Marko-Varga, J. Malm, H. Lilja, T. Laurell, MALDI-target integrated platform for affinity-captured protein digestion, *Anal. Chim. Acta.* 807 (2014) 1–8.
- [24] S.J. Lee, B. Adler, S. Ekström, M. Rezeli, A. Vegvari, J.W. Park, J. Malm, T. Laurell, Aptamer/ISET-MS: a new affinity-based MALDI technique for improved detection of biomarkers, *Anal. Chem.* (2014), <http://dx.doi.org/10.1021/ac501488b>.
- [25] B. Adler, T. Bostrom, S. Ekström, S. Hober, T. Laurell, Miniaturized and automated high-throughput verification of proteins in the ISET platform with MALDI MS, *Anal. Chem.* 84 (2012) 8663–8669.
- [26] A.J. Hall, P. Manesiotis, M. Emgenbroich, M. Quaglia, E. De Lorenzi, B. Sellergren, Urea host monomers for stoichiometric molecular imprinting of oxyanions, *J. Org. Chem.* 70 (2005) 1732–1736.
- [27] J. Fila, D. Hony, Enrichment techniques employed in phosphoproteomics, *Amino Acids* 43 (2012) 1025–1047.
- [28] S. Kjellström, O.N. Jensen, Phosphoric acid as a matrix additive for MALDI MS analysis of phosphopeptides and phosphoproteins, *Anal. Chem.* 76 (2004) 5109–5117.
- [29] L.D. Rogers, L.J. Foster, Phosphoproteomics—finally fulfilling the promise? *Mol. Biosyst.* 5 (2009) 1122–1129.
- [30] S. Gauci, B. Van Breukelen, S.M. Lemeer, J. Krijgsveld, A.J.R. Heck, A versatile peptide pI calculator for phosphorylated and N-terminal acetylated peptides experimentally tested using peptide isoelectric focusing, *Proteomics* 8 (2008) 4898–4906.
- [31] L.-N. Xu, L.-P. Li, L. Jin, Y. Bai, H.-W. Liu, Guanidyl-functionalized graphene as a bifunctional adsorbent for selective enrichment of phosphopeptides, *Chem. Commun.* 50 (2014) 10963–10966.
- [32] D.E. McNulty, R.S. Annan, Hydrophilic interaction chromatography reduces the complexity of the phosphoproteome and improves global phosphopeptide isolation and detection, *Mol. Cell. Proteomics* 7 (2008) 971–980.
- [33] S. Liu, C. Hughes, G.A. Lajoie, Recent advances and special considerations for the analysis of phosphorylated peptides by LC–ESI–MS/MS, *Curr. Anal. Chem.* 8 (2012) 35–42.
- [34] G. Han, M. Ye, H. Zhou, X. Jiang, S. Feng, X. Jiang, R. Tian, D. Wan, H. Zou, J. Gu, Large-scale phosphoproteome analysis of human liver tissue by enrichment and fractionation of phosphopeptides with strong anion exchange chromatography, *Proteomics* 8 (2008) 1346–1361.

- [35] K. Engholm-Keller, M.R. Larsen, Titanium dioxide as chemo-affinity chromatographic sorbent of biomolecular compounds—applications in acidic modification-specific proteomics, *J. Proteomics* 75 (2011) 317–328.
- [36] M.R. Larsen, T.E. Thingholm, O.N. Jensen, P. Roepstorff, T.J.D. Jørgensen, Highly selective enrichment of phosphorylated peptides from peptide mixtures using titanium dioxide microcolumns, *Mol. Cell. Proteomics* 4 (2005) 873–886.
- [37] N. Sugiyama, T. Masuda, K. Shinoda, A. Nakamura, M. Tomita, Y. Ishihama, Phosphopeptide enrichment by aliphatic hydroxy acid-modified metal oxide chromatography for Nano-LC–MS/MS in proteomics applications, *Mol. Cell. Proteomics* 6 (2007) 1103–1109.
- [38] E.S. Simon, M. Young, A. Chan, Z.-Q. Bao, P.C. Andrews, Improved enrichment strategies for phosphorylated peptides on titanium dioxide using methyl esterification and pH gradient elution, *Anal. Biochem.* 377 (2008) 234–242.
- [39] J. Hu, X. Mao, S. Cao, X. Yuan, Recognition of proteins and peptides: rational development of molecular imprinting technology, *Polym. Sci. Ser. A* 52 (2010) 328–339.

# Paper II





# Filter Plate–Based Screening of MIP SPE Materials for Capture of the Biomarker Pro-Gastrin-Releasing Peptide

SLAS Discovery

1–9

© 2017 Society for Laboratory Automation and Screening  
DOI: 10.1177/2472555216689494  
journals.sagepub.com/home/jbx

Kishore Kumar Jagadeesan<sup>1\*</sup>, Cecilia Rossetti<sup>2\*</sup>,  
Abed Abdel Qader<sup>3</sup>, Léon Reubsæet<sup>2</sup>, Börje Sellergren<sup>4</sup>,  
Thomas Laurell<sup>1</sup>, and Simon Ekström<sup>1</sup>

## Abstract

Affinity-based solid-phase extraction (SPE) is an attractive low-cost sample preparation strategy for biomarker analysis. Molecularly imprinted polymers (MIPs) as affinity sorbents offer unique opportunities for affinity SPE, due to their low manufacturing cost and high robustness. A limitation is the prediction of their affinity; therefore, screening of analyte recovery and specificity within a large range of SPE conditions is important in order to ensure high-sensitivity detection and assay reproducibility. Here, a  $\mu$ -SPE method for screening of the MIP-SPE materials using a commercial 384-well filter plate is presented. The method allows for rapid and automated screening using 10–30  $\mu$ L of packed SPE sorbent per well and sample volumes in the range of 10–70  $\mu$ L. This enables screening of many different SPE sorbents while simultaneously identifying optimal SPE conditions. In addition, the 384-well format also facilitates detection with a multitude of analytical platforms. Performance of the  $\mu$ -MIP-SPE method was investigated using a series of MIPs designed to capture pro-gastrin-releasing peptide (ProGRP). Fractions coming from sample load, cartridge wash, and elution were collected and analyzed using mass spectrometry (MS). The top-performing MIPs were identified, together with proper SPE conditions.

## Keywords

sample preparation, mass spectrometry, separations or chromatography, protein chemistry, protein labeling, proteomics, biomarkers

## Introduction

Recent developments of traditional generic solid-phase extraction (SPE) sorbents have provided new high-performing varieties, like mixed-mode polymeric sorbents<sup>1,2</sup> and nanostructured materials.<sup>3,4</sup> While many of these SPE materials are excellent when applied for removal of contaminants, the reduction of sample complexity is often lacking, especially in the case of low abundant biomarker analytes in complex matrixes, such as blood, serum,<sup>5</sup> plasma,<sup>6</sup> or urine.<sup>7,8</sup> Thus, there is a need for new SPE sample preparation materials with high selectivity and specificity toward targeted analytes, preferably with a high specific surface area and enhanced chemical/physical stability.<sup>9,10</sup> In order to enable high-sensitivity detection in complex samples, affinity sorbents based on molecular recognition, such as immunosorbents,<sup>11</sup> aptamer-based sorbents,<sup>12</sup> and molecularly imprinted polymers (MIPs),<sup>13</sup> are finding increased use. Among them, SPE sorbents based on immobilized antibodies are usually highly specific to their target.<sup>14</sup> Many successful biomarker assays have been developed by combining immunoaffinity SPE and MS,<sup>15,16</sup> but their broad application has been limited by issues

such as antibody stability, variability, availability, cost, and challenging sample preparation (e.g., mismatched solvents).<sup>17</sup> MIPs represent a possible alternative to antibody-based SPE, as MIPs have a low manufacturing cost, can be tailor-made with functionalities complementary to the target analyte, and

<sup>1</sup>Department of Biomedical Engineering, Lund University, Lund, Sweden

<sup>2</sup>Department of Pharmaceutical Chemistry, School of Pharmacy, University of Oslo, Oslo, Norway

<sup>3</sup>Department of Environmental Chemistry and Analytical Chemistry, Institute for Environmental Research (INFU), Technical University of Dortmund, Dortmund, Germany

<sup>4</sup>Department of Biomedical Sciences, Faculty of Health and Society, University of Malmö, Malmö, Sweden

\*These authors contributed equally to this work

Received Oct 14, 2016, and in revised form Dec 24, 2016. Accepted for publication Dec 27, 2016.

Supplementary material is available online with this article.

## Corresponding Author:

Kishore Kumar Jagadeesan, Department of Biomedical Engineering, Lund University, Box 118, Lund 221 00, Sweden.

Email: jkkishore85@gmail.com

can work even under extreme conditions (pH, temperature, and organic solvents).<sup>18,19</sup> Generally, the manufacturing of MIP sorbents involves a preorganization of the target molecule to be imprinted with the functional monomers, followed by a polymerization step with a cross-linker to lock the monomers into a polymer network and create the affinity sorbent.<sup>20,21</sup> Traditionally, MIP-SPE sorbents have been developed and applied for capture of small molecular targets,<sup>22,23</sup> but the development of MIPs for capture of biomolecules has been growing with the increased scientific understanding of imprinting.<sup>24,25</sup> Currently, MIPs targeting peptides or proteins cannot match the high affinity of the best antibodies, although the recent progress in MIP synthesis and the ever-increasing sensitivity and dynamic range of new analytical instruments could very well provide ample opportunities for new affinity SPE assays using MIPs.

In a typical development of a MIP SPE method, several parameters need to be screened, comprising those related to the synthesis of the sorbent, as well as those related to its use in SPE, that is, load, wash, and elution conditions. The performance is commonly evaluated by packing the imprinted polymer (15–50 mg) into SPE cartridges, and then measuring the recovery of the target compound in the fractions obtained after cartridge load, wash, and elution.<sup>10</sup>

Here, an automated, high-throughput SPE screening method is presented and used for screening of molecularly imprinted sorbents in order to identify promising candidates. The method is based on 384-well filter plates and is comparable to the previously presented ISET platform.<sup>26</sup> This type of platform greatly facilitates the screening of different phases with simultaneous investigation of diverse solvent/buffer conditions. Compared with the ISET, the 384-well filter plate format provides increased bed volume, and thus binding capacity (needed to enable use of low-affinity materials), and can be used with analysis techniques other than matrix-assisted laser desorption/ionization (MALDI), for example, liquid chromatography–electrospray ionization mass spectrometry (LC ESI-MS). The molecularly imprinted materials used for development and validation were designed to selectively capture a proteotypic peptide of pro-gastrin-releasing peptide (ProGRP), NLLGLIEAK, as previously reported.<sup>27</sup>

Although the 384-well format has been extensively utilized for immunoassays and *in vitro* receptor binding studies, its use in SPE is relatively new.<sup>28</sup> The presented method has been automated using liquid handling robotics, for the addition of the different solvents during the SPE process. The eluents resulting after the SPE experiments were analyzed on two different analytical platforms (ESI-triple quadrupole and MALDI-Orbitrap), allowing for quantification of NLLGLIEAK and evaluation of the different MIP sorbents based on recovery and removal of background.

The collected multiplexed experimental data on the ProGRP-specific MIP and non-imprinted polymer (NIP) phases provided both mechanistic information concerning

analyte binding and an improved protocol for the specific enrichment of NLLGLIEAK with reduced non-specific binding.

## Materials and Methods

### Protein and Peptide Samples

Internal standard (IS) NLLGLIEA[K-<sup>13</sup>C<sub>6</sub><sup>15</sup>N<sub>2</sub>] (95% purity, Thermo Fisher Scientific, Braunschweig, Germany) was diluted according to the AQUA peptide storage and handling guidelines and stored at –20 °C. Stock solutions of IS and NLLGLIEAK of 5 μM were used to prepare samples by dilution with 50 mM ammonium bicarbonate (ABC) buffer solution.

β-Casein (Sigma-Aldrich, St. Louis, MO) was digested overnight with trypsin (Promega, Madison, WI) in a 1:100 ratio (enzyme–protein) at 37 °C. The digested protein was diluted with 0.1% trifluoroacetic acid (TFA) and frozen to stop the digestion process. Stock solutions of 4 μM were used to prepare samples by dilution with 50 mM freshly prepared ABC buffer.

### μ-SPE in the 384-Filter Plate Format

μ-SPE was performed using 384-well filter plates filled with MIPs imprinted to capture the ProGRP signature peptide NLLGLIEAK. NIPs were used as controls to assess the MIP imprinting efficiency.

The MIPs were prepared as described previously with minor modifications<sup>27</sup> (see Supporting Information). Briefly, P<sub>MIP</sub>-1 and P<sub>MIP</sub>-2 were prepared by ethylene glycol dimethacrylate (EDMA) copolymerized with methacrylic acid (MAA), and P<sub>MIP</sub>-3 and P<sub>MIP</sub>-4 polymers were prepared from hydrophobic divinylbenzene (DVB) copolymerized with 2-amino ethyl methacrylamide (EAMA). For all MIPs, an N-terminally Z-protected peptide was used as a template for generating the surface imprint (**Suppl. Table S1**). The NIPs were prepared by the same synthetic protocol without the initial addition of the template molecule. The SPE platform used either MultiScreen HTS 384-well filter plates from Millipore made of styrene acrylonitrile (SAN) with polyvinylidene fluoride (PVDF) membrane/polyester support or AcroPrep 384-well filter plates from Pall Life Sciences made of polypropylene (SAN) with glass fiber (borosilicate glass, 1.0 μm) membrane. Thermo Scientific (Waltham, MA) Nunc plates made of polystyrene were used as collection plates. A Millipore MultiScreen HTS Vacuum Manifold coupled to a vacuum pump (0–6 g/cm<sup>2</sup>, Nerliens Meszansky, Oslo, Norway) was used to carry out the SPE protocol. A Biomek 3000 Laboratory Automation Workstation (Beckman Coulter, Fullerton, CA) was used to enable automated sample preparation. Control of the robot was governed directly by Biomek automation software v3.3 (Beckman Coulter).

The MIP- $\mu$ -SPE protocol consisted of the following steps;

1. A fixed vacuum of 10–15 Hg was used for filling the wells with 20  $\mu$ L of MIP/NIP material.
2. Wash, 2  $\times$  60  $\mu$ L of acetonitrile (ACN), was subsequently pulled through the wells.
3. Conditioning with 2  $\times$  60  $\mu$ L of methanol (MeOH), followed by 2  $\times$  60  $\mu$ L of 50 mM ABC buffer.
4. A 20  $\mu$ L sample in loading buffer was added to each well.
5. 80  $\mu$ L of wash buffer was added to each well.
6. For elution of the bound analytes, 80  $\mu$ L of elution solution was added.
7. During the transfer of washing and elution buffers, the vacuum was turned off and then turned on after the addition in order to facilitate a homogeneous wetting of the SPE bed.
8. MS analysis was performed on the collected fractions.

### Liquid Chromatography–Tandem Mass Spectrometry Analysis

The chromatographic system consisted of LPG-3400 M pumps with integrated degasser, a WPS-3000TRS autosampler, and an FLM-3000 flow manager (Dionex, Sunnyvale, CA). Chromatographic separation was carried out on a Hypersil GOLD aQ analytical column (Thermo Scientific, 100 Å, 3  $\mu$ m, 50  $\times$  1 mm) preceded by a Hypersil GOLD aQ Drop-In Guard Cartridge (Thermo Scientific, 100 Å, 3  $\mu$ m, 10  $\times$  1 mm). Sample (40  $\mu$ L) was injected in mobile phase A (20 mM formic acid [FA] and ACN 99:1, v/v) and eluted with a 30 min linear gradient from 1% to 85% of mobile phase B (20 mM FA/ACN 1:99, v/v) at a flow of 40  $\mu$ L/min. After each gradient run, the column was washed for 3 min with 90% mobile phase B and reequilibrated with mobile phase A. Column temperature was kept constant at 30 °C. For the MS (TSQ Quantum Access, Thermo Fisher Scientific) quantification, the standard peptide NLLGLIEA-[K-<sup>13</sup>C<sub>6</sub><sup>15</sup>N<sub>2</sub>] was spiked into the samples, and using selected reaction monitoring (SRM), the transitions pairs 489.9  $\rightarrow$  638.3 and 489.9  $\rightarrow$  751.4 were monitored (qualifier and quantifier, respectively). TSQ data were processed by Xcalibur's QualBrowser (Thermo Scientific), and the analyte peak area was automatically extracted by the genesis peak detection algorithm. Only peaks with a signal-to-noise (S/N) ratio above 10 and retention times corresponding to those of the reference samples were used. All collected fractions were diluted 1:10 with a 0.001% polyethylene glycol (PEG) + 0.1% FA solution before injection into the liquid chromatography–tandem mass spectrometry (LC-MS/MS) system, in order to reduce ACN concentration, maximize the ESI ionization, and minimize the absorption of peptides to the vials walls.<sup>29</sup>

The recovery of NLLGLIEAK for each analyzed fraction ( $R\%_{EF}$ ) was calculated based on the peak area generated by the NLLGLIEAK in the extracted fraction ( $A_{EF}$ ), and the peak area of NLLGLIEA[K-<sup>13</sup>C<sub>6</sub><sup>15</sup>N<sub>2</sub>] peptide ( $A_{IS}$ ), according to eq 1:

$$R\%_{EF} = (A_{EF}/A_{IS}) \times 100 \quad (1)$$

The recovery was normalized by setting the sum of all the observed peak areas for all fractions, that is, the sample flow-through, wash, and elution, as equation eq 2:

$$\text{Recovery percentage } (R\%) = \frac{R\%_{EF}}{(R\%_{\text{sample flow-through}} + R\%_{\text{wash}} + R\%_{\text{elution}})} \times 100 \quad (2)$$

### Nano-LC-MS/MS Analysis

For nano-LC-MS/MS analysis, sample fractions were mixed with 2  $\mu$ M heavy standard NLLGLIEA[K-<sup>13</sup>C<sub>6</sub><sup>15</sup>N<sub>2</sub>] in a 1:1 ratio by volume and diluted 1:10 with a solution of 0.1% FA. Thereafter, 5  $\mu$ L of the diluted sample was injected into the nano-LC-MS/MS system. Analysis was performed on an EASY-nLC (Thermo Scientific) running with a 75  $\mu$ m  $\times$  150 mm fused silica column packed in-house with ReproSil C18 (3  $\mu$ m, 120 Å from Dr. Maisch, Ammerbuch-Entringen, Germany) as an analytical column, preceded by a 0.1  $\times$  20 mm, 5  $\mu$ m EASY C18-A1 precolumn (Thermo Scientific) at 300 nL/min. The mobile phases consisted of (A) 20 mM FA and ACN (99:1, v/v) and (B) 20 mM FA and ACN (1:99, v/v). A linear gradient was run from 10% to 50% B in 15 min. Between samples, the B content was increased to 95% over 2 min and left constant for 5 min. The total analysis time per run was 22 min. The LC setup was connected to a TSQ Vantage instrument equipped with a nano-ESI ion source operated in positive ionization mode, spray voltage was set at 1.7 kV, and the heated capillary was kept at 270 °C. The mass spectrometer was operated in SRM mode and using the following transitions: 485.8  $\rightarrow$  347.2, 485.8  $\rightarrow$  460.3, 485.8  $\rightarrow$  573.4, 485.8  $\rightarrow$  630.4, and 485.8  $\rightarrow$  743.5 for the target peptide NLLGLIEAK and 489.8  $\rightarrow$  355.2 and 489.8  $\rightarrow$  468.3 for the IS NLLGLIEA-[K-<sup>13</sup>C<sub>6</sub><sup>15</sup>N<sub>2</sub>] (IS). TSQ data were processed using Skyline software v3.1 (MacCoss Lab, Seattle, WA).

The ratio of the peak area of the target peptide (NLLGLIEAK) from the extracted fraction (EF) to the peak area of the NLLGLIEA[K-<sup>13</sup>C<sub>6</sub><sup>15</sup>N<sub>2</sub>] peptide (IS) was used for quantification of NLLGLIEAK in samples, according to eq 1.

### MALDI-MS

For the MALDI-MS analysis, 1  $\mu$ L of SPE fraction was mixed with 1  $\mu$ L of 2  $\mu$ M labeled standard NLLGLIEA[K-<sup>13</sup>C<sub>6</sub><sup>15</sup>N<sub>2</sub>] and 1  $\mu$ L of alpha-cyano cinnamic acid matrix solution and spotted onto a MALDI target plate for analysis.

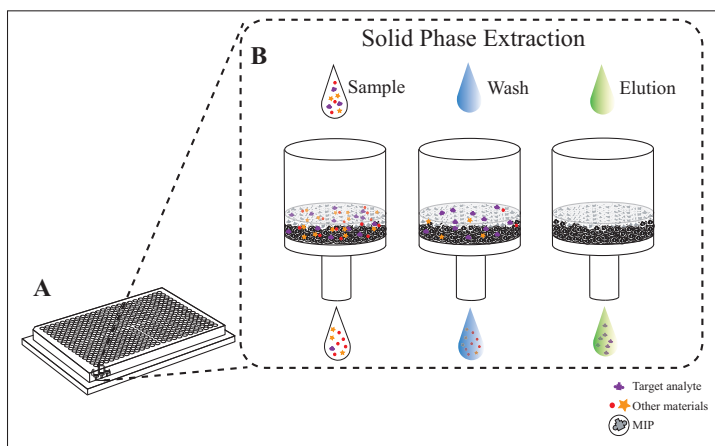


**Figure 1.** Schematic representation of the 384-well filter plates and the workflow of the SPE step in the microwell. **(A)** 384-well filter plate. **(B)** SPE sample preparation, where the sample is transferred to the microwell loaded with SPE material (1), followed by a wash step to remove undesired components (2), and the captured analytes are then displaced by the elution step (3).

Analysis was performed on a hybrid MALDI LTQ Orbitrap XL (Thermo Fisher Scientific) instrument. Full MS spectra for each spot were obtained as the average of 10 mass scans in positive mode, mass range 700–2000 Da at 60,000 mass resolution. The selective ion monitoring (SIM) spectra were obtained in positive mode, mass range 880–990 Da using 60,000 mass resolution. The peak intensities were extracted using Xcalibur (Thermo Scientific), and the data were analyzed with the statistical software package R.<sup>30</sup>

The intensity ratio (Intensity Ratio %) of each sample fraction was calculated from the intensity of the target peptide (NLLGLIEAK) observed in the sample fraction ( $I_{EF}$ ) and the intensity of the heavy IS ( $I_{IS}$ ), according to eq 3:

$$\text{Intensity Ratio \%} = (I_{EF} / I_{IS}) \times 100 \quad (3)$$

## Results and Discussion

The workflow of the method is illustrated in **Figure 1**, where the MIPs are prepacked into wells of a 384-well filter plate; (1) sample is drawn through the SPE bed, and after washing, (2) the captured analyte is eluted and (3) the collected eluents are analyzed using LC-MS and/or MALDI for the quantification of recovery and evaluation of the background removal (i.e., spiked peptides added to the sample) (**Fig. 2**).

### 384-Well Filter Plate: SPE Setup and Development

During SPE, unspecific absorption to surfaces can lead to sample losses and false results. Therefore, the retention of analyte contributed by unspecific absorption in the

384-well filter plate setup was investigated. Briefly, 20  $\mu\text{L}$  of a 5 nM NLLGLIEAK peptide in 50 mM ABC buffer was loaded into the filter plate wells without any MIP/NIP phase, followed by running an SPE protocol using 5% ACN as washing buffer and 80% MeOH + 3% FA as the elution buffer. The collected eluents were analyzed with LC-MS/MS for detection of binding of the target peptide. The analysis (**Suppl. Fig. S5**) showed that approximately 10% of the loaded peptide was bound to surfaces of the well (membrane absorption, dead volumes in the tip) and recovered during the elution step. At this quite low concentration (5 nM), the total loss due to adsorption was approximately 25% of the loaded analyte.

Chemical compatibility of the microplates and filter plates was checked with different conditions. Prolonged exposure of ACN resulted in warping of MultiScreen HTS 384-well filter plates and cross talk in the collection plates. This problem was addressed by changing the filter plates to AcroPrep 384-well filter plates, which are made of polypropylene (SAN) with glass fiber (borosilicate glass, 1.0  $\mu\text{m}$ ) membrane. The latter was inert to the all buffer conditions used in the described experiments.

### High-Throughput Screening of MIPs Using LC-MS

In the initial development of the 384-well filter plate SPE platform, only  $P_{MIP-4}$  and its nonimprinted counterpart  $P_{NIP-2}$  were used. These two sorbents had been previously investigated for SPE of the NLLGLIEAK peptide, using a reversed-phase-like SPE protocol with a low amount of organic modifier in the wash solution.<sup>27</sup> Thus, the 384-well filter plate SPE platform should provide the same results as the previous investigation. The impact of increasing organics in

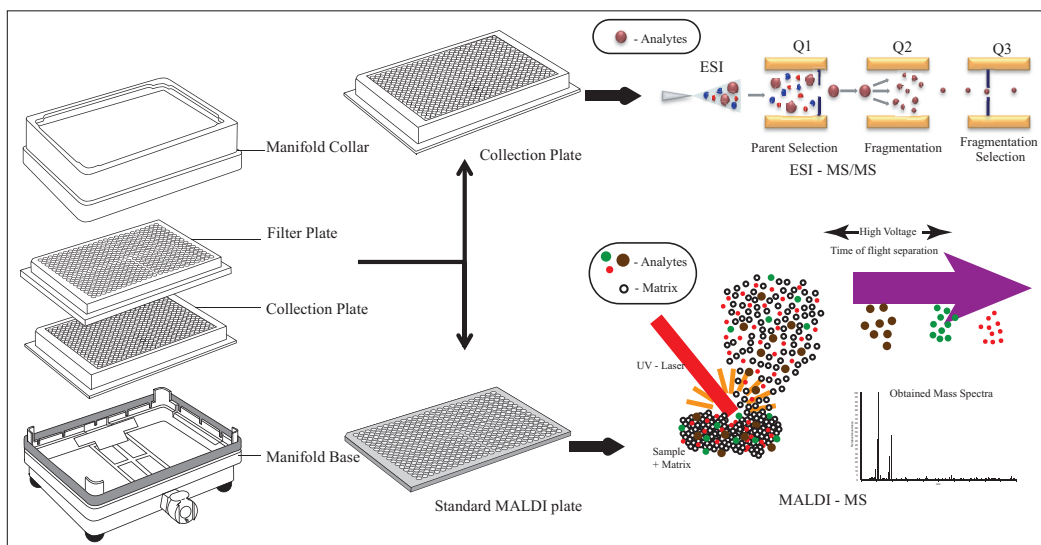


**Figure 2.** Schematic representation of the dual (MALDI and ESI)-analysis readout facilitated by the 384-well filter plate SPE method.

the washing buffer on the SPE sample preparation was therefore investigated using increasing ACN% (5, 10, 15, 30, 50, and 95). **Supplemental Figure S6** shows the recovery (R%) in the elution plotted against the ACN concentration used in the wash step. As expected, the data showed that a wash buffer with 5% ACN provides a higher recovery than the washes with higher ACN. This trend is also seen for the NIP, albeit with a lower recovery in the elution step. This effect can be explained by considering the nature of the peptide and the polymer. NLLGLIEAK is a 0.8 kDa proteolytic digest product dominated by a hydrophobic pentapeptide segment (55% hydrophobic residues); the polymeric sorbents were in this case based on DVB as the main constituent. In agreement with our recent report, this leads to a reversed-phase retention mechanism with a strong non-specific hydrophobic contribution. To suppress this effect, a careful optimization of the wash conditions is required. Indeed, at an increased ACN%, that is, at 30% and 50%, more significant imprinting-related differences in the elution recoveries were observed. However, as high content of ACN in the wash step resulted in lower recoveries, there is an obvious trade-off between recovery and specificity.

A second screening was performed to narrow down the optimal organic content in the wash step. For this experiment, wash buffers containing 5%, 7.5%, 10%, and 12.5% ACN were used. Samples of 5 nM NLLGLIEAK peptide in 50 mM ABC buffer were loaded onto the MIP/NIP materials, followed by wash and elution using 80% MeOH/3% FA. Recovery (R%) of the analyte in the wash and elution

fractions was calculated and plotted against the ACN concentration (**Suppl. Fig. S7**).

Analysis of the wash fraction (**Suppl. Fig. S7A**) shows that using 7.5% ACN as wash buffer leads to 34% of the analyte loss, whereas usage of 10% ACN as wash buffer increases the analyte loss to 48%. Based on the recovery observed in the elution step (**Suppl. Fig. S7B**), it appears that the most selective MIP retention, for this particular SPE protocol, could be found when using 7.5%–10% of ACN. At 7.5%, a total recovery of 50% was observed for the MIP, compared with 25% for its NIP counterpart. At 10% ACN, the recovery was a bit lower (40%), but the discrimination versus the NIP, showing only 8%, was significantly better. Wash with 12.5% ACN displayed lower recovery and diminished the affinity of the MIP compared with NIP. The 384-well filter plate-based SPE method thus provided the same results as the previously reported 1 mL cartridge for a NLLGLIEAK-specific MIP phase.<sup>27</sup>

### Verification by the MALDI-MS Method

The 384-well filter plate platform can in many situations be “too fast” for analysis readout with LC-MS; that is, 384 samples would take days to weeks to analyze. Therefore, MALDI-MS was investigated as an option for rapid readout in order to achieve a better match between the SPE-screening and the MS analysis time. While MALDI-MS can easily provide a qualitative answer, the multiplexed testing is much more useful if quantitative data from the samples can be obtained. The



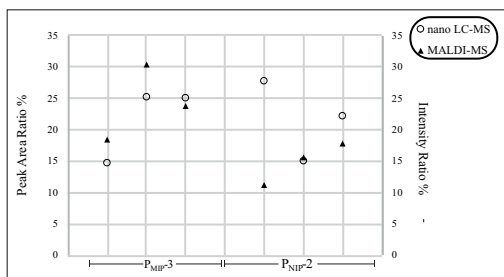


**Figure 3.** Quantitative comparison using nano-LC-MS (peak area ratio %) with the MALDI (intensity ratio %) samples of 20  $\mu\text{L}$  of 1  $\mu\text{M}$  NLLGLIEAK peptide in 50 mM ABC buffer, followed by 7.5% ACN wash and elution with 80% MeOH/3% FA.

feasibility of a quantitative MALDI-MS method was investigated by direct comparison with nano-LC-MS analysis. The previous LC-MS experiments showed an optimal reversed-phase-based SPE with 7.5% ACN in the wash buffer. These conditions were used for performing SPE with  $P_{\text{MIP-3}}$  (MIP) and its counterpart  $P_{\text{NIP-2}}$  (NIP). Samples of 1  $\mu\text{M}$  NLLGLIEAK peptide in 50 mM ABC buffer were used, and the concentration was increased to improve detection with MALDI. The collected SPE eluent fractions were subjected to analysis with both MALDI-MS and nano-LC-MS.

The observed peak area ratio (%) from the nano-LC-MS experiment was compared with the observed intensity ratio (%) from the MALDI experiment (Fig. 3). The intrasample variation of the MALDI and LC-MS provided a relative standard deviation (RSD) of <10%, excluding one “outlier” for  $P_{\text{NIP-2}}$ , although the intersample variation was somewhat higher (10%–15%).

The reproducibility of the sample preparation was investigated by comparing duplicates in the SPE and MS process, as shown in **Supplemental Figure S8**. The deviation is very low in the MS analysis,  $\leq 1\%$  (**Suppl. Fig. S8B**). However, variations arising from different SPE replicates (**Suppl. Fig. S8A**) are not entirely surprising, and can be attributed to flow variations and variations in bed volume. The variations in the SPE process make it extra important to at least employ relative quantitation and large number of replicates.

## High-Throughput Screening of the Polymer Library Using MALDI-MS

Using the MALDI-MS method, the ProGRP affinity of six different MIP/NIP ( $P_{\text{MIP-1-4}}$  to  $P_{\text{NIP-1-2}}$ ) phases was investigated. In order to see if additional modes of selectivity could be identified, additional SPE conditions, as depicted in **Table 1**, were evaluated using samples of 4  $\mu\text{M}$  NLLGLI-EAK. Briefly, after equilibration of the sorbents, 20  $\mu\text{L}$  of 4  $\mu\text{M}$  NLLGLIEAK peptide in loading buffers ABC + 0.5% FA (L1), ABC + 0.8% NaOH (L2), ABC (L3), and 100% ACN (L4) was added to each  $\mu$ -well. The  $\mu$ -SPE was carried out with 90  $\mu\text{L}$  of washing buffers 7.5% ACN + 0.5% FA (W1), 7.5% ACN + 0.8% NaOH (W2), 7.5% ACN (W3), and 100% ACN + 0.1% FA (W4), and 30  $\mu\text{L}$  of elution buffers 80% ACN + 3%  $\text{NH}_3$  (E1), 80% ACN + 3% FA (E2), and 50% MeOH + 5% FA (E3). The collected SPE fractions were then spotted in triplicate on a MALDI target plate with 1  $\mu\text{L}$  of an IS 10 nM NLLGLIEA[ $\text{K}_{-13}\text{C}_6^{15}\text{N}_2$ ] and 1  $\mu\text{L}$  of alpha-cyano cinnamic acid for analysis using SIM mode MALDI-MS.

The MALDI-MS peak intensity for NLLGLIEAK of different MIP ( $P_{\text{MIP-1-4}}$ ) and NIP ( $P_{\text{NIP-1-2}}$ ) phases in four different conditions—condition 1, L1W1E1; condition 2, L2W2E2; condition 3, L3W3E2; and condition 4, L4W4E3 is plotted in **Figure 4**. The data indicate that conditions 1 and 2 result in lower peak intensity than conditions 3 and 4. Imprinting-related effects in condition 3 are small, possibly a consequence of the relatively high sample load. However, the use of condition 3, corresponding to the condition selected in our previous report, MIPs  $P_{\text{MIP-3}}$  and  $P_{\text{MIP-4}}$ , showed increased analyte peak intensities corresponding to enhanced recoveries exceeding the NIP ( $P_{\text{NIP-2}}$ ).

## Investigation of MIP Selectivity

A further investigation of the selectivity at lower sample load was carried out by repeating the same experiment with samples of 40 nM NLLGLIEAK mixed with 40 nM  $\beta$ -casein digest (1:1 ratio). These concentrations still allowed for analysis using MALDI-MS. **Figure 5** shows the mean intensities (six spots, two samples) for the NLLGLIEAK

**Table 1.** Different SPE Optimization Conditions Used for the Semiquantitative Method for Materials  $P_{\text{MIP-1-4}}$  to  $P_{\text{NIP-1-2}}$ .

SPE Condition	Load Buffer	Wash Buffer	Elution Buffer
L1W1E1	ABC + 0.5% FA	7.5% ACN + 0.5% FA	80% ACN + 3% $\text{NH}_3$
L2W2E2	ABC + 0.8% NaOH	7.5% ACN + 0.8% NaOH	80% ACN + 3% FA
L3W3E2	ABC	7.5% ACN	80% ACN + 3% FA
L4W4E3	100% ACN	100% ACN + 0.1% FA	50% MeOH + 5% FA

L1, L2, L3, and L4, loading buffers 1–4; W1, W2, W3, and W4, washing buffers 1–4; E1, E2, and E3, elution buffers 1–3.

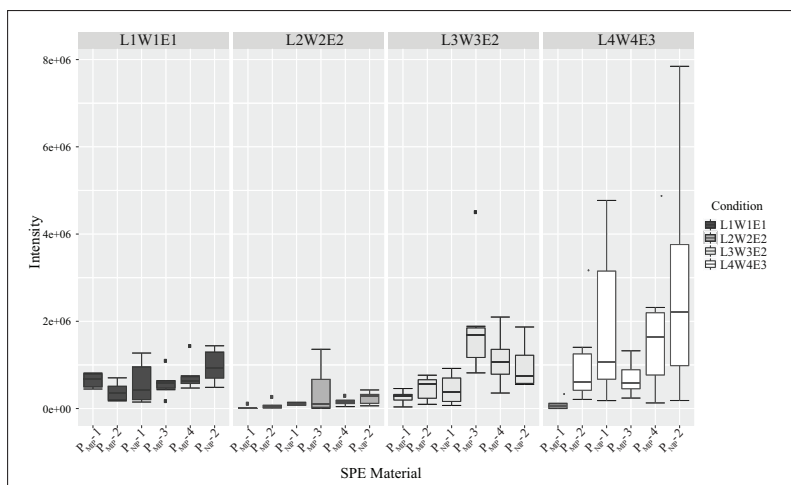


**Figure 4.** MALDI-MS analyte peak intensity observed for different MIP (i.e., P<sub>MIP</sub>-1–4) and NIP (P<sub>NIP</sub>-1–2) phases using four different conditions (L1W1E1, L2W2E2, L3W3E2, and L4W4E3). The box shows the MALDI-MS intensities generated by the replicates of the corresponding polymer, and the solid black line inside the box represents the median. Black dots above and below the boxes represent outliers.

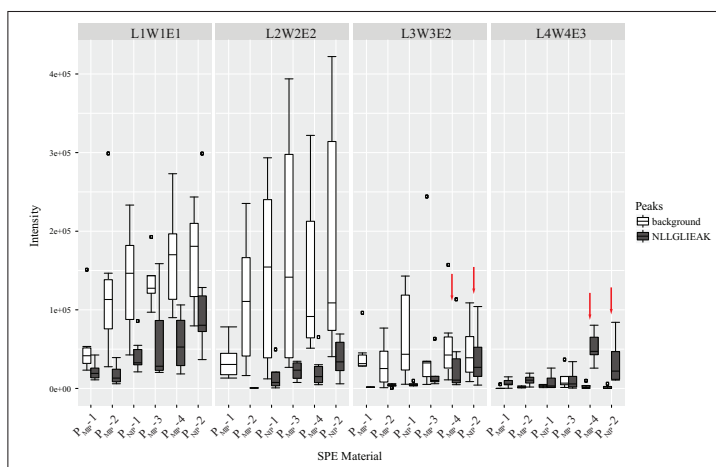


**Figure 5.** Intensity of the analyte peak (NLLGLEAK) and sum of the background peaks (i.e., sum of the intensity of the peptide peaks corresponding to the  $\beta$ -casein digest), corresponding to each SPE material in four different conditions using MALDI-MS analysis: condition 1, L1W1E1; condition 2, L2W2E2; condition 3, L3W3E2; and condition 4, L4W4E3. The box shows the MALDI-MS intensities generated by the replicates of the corresponding polymer, and the solid black line inside the box represents the median. Black dots above and below the boxes represent outliers.

peak (970 Da) (dark bars), and the white bars represent the summed intensity of the observed background peaks (i.e., sum of the intensity of the peptide peaks originating from the  $\beta$ -casein digest). Individual peptide intensities can be seen in **Supplemental Figure S9**. The data indicate that conditions 1 and 2 provide a generic SPE with high recovery observed for all peptides and have little to offer in terms of selectivity. Condition 3 provided two candidates showing selective retention, that is, P<sub>MIP</sub>-4 (MIP) and P<sub>NIP</sub>-2 (NIP). Both phases offered a reduced background and minor

selectivity, but with a low recovery. An interesting result was obtained using condition 4. The background in condition 4 was very low, and good selectivity could be observed using P<sub>MIP</sub>-4 (MIP) versus P<sub>NIP</sub>-2 (NIP).

In conclusion, the presented approach provides a convenient “all-in-one” experimental platform for performing high-throughput screening of synthetic polymer (MIP) libraries. Moreover, the method is also applicable to any generic SPE or affinity phases that can be packed in the filter plate. The 384-well filter plate method increases



sample preparation throughput significantly, that is, 15–20 min per sample (SPE and MALDI-MS analysis), compared with 60–90 min per sample (SPE and LC-MS analysis) for the standard off-line SPE cartridge method. Moreover, the highly parallelized method means that costs are reduced, for example, using a less solid phase (20  $\mu$ L) and smaller sample volume (both often available in limited amounts) and solvents, naturally facilitating considerable time savings, which scales with the increased sample numbers. It can be automated using basic liquid handling robotics and applied in different analytical workflows, leading in turn to greater consistency and reduced sample preparation time and effort. The issue of long analysis time as the LC-MS runs could be addressed using a MALDI readout, as demonstrated here. An entire plate can be run in 8 experiments (e.g., in our experiment, we used 8 different polymers with 4 SPE conditions in duplicate, for 48 samples in total for each experiment), and a partial analytical run of 144 samples on a MALDI-MS could be performed in approximately 15–20 min per sample (SPE and MALDI-MS analysis), with the cost of extraction sorbent for the screening made at a very low per sample cost (~0.5–1 USD/sample). The 384-well laboratory automation also minimizes the risk of mislabeling and sample handling errors. This makes the 384-well filter plate setup an efficient high-throughput screening platform for newly prepared sorbent materials using a MALDI-MS output.

In the case of the investigated ProGRP-specific MIP and NIP phases, the multiplexed experiments confirmed findings previously reported<sup>27</sup> with the identification of the optimal polymer sorbent for the hydrophobic retention of NLLGLIEAK. In addition, the presented platform allowed the identification of new SPE conditions with suppressed nonspecific binding. In the same settings, MIP sorbents showed enrichment toward the target peptide NLLGLIEAK, with the depletion of other peptides.

### Declaration of Conflicting Interests

The authors declared no potential conflicts of interest with respect to the research, authorship, and/or publication of this article.

### Funding

The authors disclosed receipt of the following financial support for the research, authorship, and/or publication of this article: This work has been performed as part of the ITN project PEPMIP (grant agreement no. 264699) supported by the Seventh Research Framework Programme of the European Commission under Marie Curie actions.

### References

- Fontanals, N.; Marcé, R. M.; Borrull, F.; et al. Mixed-Mode Ion-Exchange Polymeric Sorbents: Dual-Phase Materials That Improve Selectivity and Capacity. *Trends Analyt. Chem.* **2010**, *29*, 765–779.
- Lame, M. E.; Chambers, E. E.; Blatnik, M. Quantitation of Amyloid Beta Peptides A $\beta$ 1–38, A $\beta$ 1–40, and A $\beta$ 1–42 in Human Cerebrospinal Fluid by Ultra-Performance Liquid Chromatography–Tandem Mass Spectrometry. *Anal. Biochem.* **2011**, *419*, 133–139.
- Qiu, J.; Yan, Y.; Chang, H.; et al. Preparation of a Concentric Layered Structure of an Electrospun Nanofiber Column for Solid-Phase Extraction of Mass Viscous Crude Extracts. *Anal. Bioanal. Chem.* **2016**, *408*, 4425–4433.
- Ravelo-Pérez, L. M.; Herrera-Herrera, A. V.; Hernández-Borges, J.; et al. Carbon Nanotubes: Solid-Phase Extraction. *J. Chromatogr. A* **2010**, *1217*, 2618–2641.
- Jacobs, J. M.; Adkins, J. N.; Qian, W.-J.; et al. Utilizing Human Blood Plasma for Proteomic Biomarker Discovery. *J. Proteome Res.* **2005**, *4*, 1073–1085.
- Anderson, N. L.; Anderson, N. G. The Human Plasma Proteome: History, Character, and Diagnostic Prospects. *Mol. Cell. Proteomics* **2002**, *1*, 845–867.
- Decramer, S.; de Peredo, A. G.; Breuil, B.; et al. Urine in Clinical Proteomics. *Mol. Cell. Proteomics* **2008**, *7*, 1850–1862.
- Rodríguez-Suárez, E.; Siwy, J.; Zürlbig, P.; et al. Urine as a Source for Clinical Proteome Analysis: From Discovery to Clinical Application. *Biochim. Biophys. Acta* **2014**, *1844*, 884–898.
- Cruz-Vera, M.; Lucena, R.; Cárdenas, S.; et al. Highly Selective and Non-Conventional Sorbents for the Determination of Biomarkers in Urine by Liquid Chromatography. *Anal. Bioanal. Chem.* **2010**, *397*, 1029–1038.
- Plotka-Wasyłka, J.; Szczepańska, N.; de la Guardia, M.; et al. Modern Trends in Solid Phase Extraction: New Sorbent Media. *Trends Analyt. Chem.* **2016**, *77*, 23–43.
- Hennion, M.-C.; Pichon, V. Immuno-Based Sample Preparation for Trace Analysis. *J. Chromatogr. A* **2003**, *1000*, 29–52.
- Du, F.; Guo, L.; Qin, Q.; et al. Recent Advances in Aptamer-Functionalized Materials in Sample Preparation. *Trends Analyt. Chem.* **2015**, *67*, 134–146.
- Cheong, W. J.; Yang, S. H.; Ali, F. Molecular Imprinted Polymers for Separation Science: A Review of Reviews. *J. Sep. Sci.* **2013**, *36*, 609–628.
- Nevenen, T. K.; Simolin, H.; Suortti, T.; et al. Development of a High-Throughput Format for Solid-Phase Extraction of Enantiomers Using an Immunosorbent in 384-Well Plates. *Anal. Chem.* **2005**, *77*, 3038–3044.
- Parker, C. E.; Pearson, T. W.; Anderson, N. L.; et al. Mass-Spectrometry-Based Clinical Proteomics—A Review and Prospective. *Analyst* **2010**, *135*, 1830–1838.
- Stevenson, D. Immuno-Affinity Solid-Phase Extraction. *J. Chromatogr. B Biomed. Sci. Appl.* **2000**, *745*, 39–48.
- Buszewski, B.; Szultka, M. Past, Present, and Future of Solid Phase Extraction: A Review. *Crit. Rev. Anal. Chem.* **2012**, *42*, 198–213.
- Remcho, V. T.; Tan, Z. J. Peer Reviewed: MIPs as Chromatographic Stationary Phases for Molecular Recognition. *Anal. Chem.* **1999**, *71*, 248A–255A.

19. Sellergren, B. Imprinted Dispersion Polymers: A New Class of Easily Accessible Affinity Stationary Phases. *J. Chromatogr. A* **1994**, *673*, 133–141.
20. Haginaka, J. Molecularly Imprinted Polymers as Affinity-Based Separation Media for Sample Preparation. *J. Sep. Sci.* **2009**, *32*, 1548–1565.
21. Wackerlig, J.; Lieberzeit, P. A. Molecularly Imprinted Polymer Nanoparticles in Chemical Sensing—Synthesis, Characterisation and Application. *Sens. Actuators B Chem.* **2015**, *207* (Pt A), 144–157.
22. Shi, Y.; Zhang, J.-H.; Shi, D.; et al. Selective Solid-Phase Extraction of Cholesterol Using Molecularly Imprinted Polymers and Its Application in Different Biological Samples. *J. Pharm. Biomed. Anal.* **2006**, *42*, 549–555.
23. Andersson, L. I. Efficient Sample Pre-Concentration of Bupivacaine from Human Plasma by Solid-Phase Extraction on Molecularly Imprinted Polymers. *Analyst* **2000**, *125*, 1515–1517.
24. Turiel, E.; Martín-Esteban, A. Molecularly Imprinted Polymers for Sample Preparation: A Review. *Anal. Chim. Acta* **2010**, *668*, 87–99.
25. Cheong, W. J.; Ali, F.; Choi, J. H.; et al. Recent Applications of Molecular Imprinted Polymers for Enantio-Selective Recognition. *Talanta* **2013**, *106*, 45–59.
26. Jagadeesan, K. K.; Wierzbicka, C.; Laurell, T.; et al. Multiplexed MALDI-MS Arrays for Screening of MIP Solid Phase Extraction Materials. *J. Chromatogr. B* **2016**, *1021*, 213–220.
27. Rossetti, C.; Abdel Qader, A.; Halvorsen, T. G.; et al. Antibody-Free Biomarker Determination: Exploring Molecularly Imprinted Polymers for Pro-Gastrin Releasing Peptide. *Anal. Chem.* **2014**, *86*, 12291–12298.
28. Chang, M. S.; Kim, E. J.; El-Shourbagy, T. A. Evaluation of 384-Well Formatted Sample Preparation Technologies for Regulated Bioanalysis. *Rapid Commun. Mass Spectrom.* **2007**, *21*, 64–72.
29. Stejskal, K.; Potěšil, D.; Zdráhal, Z. Suppression of Peptide Sample Losses in Autosampler Vials. *J. Proteome Res.* **2013**, *12*, 3057–3062.
30. Ihaka, R.; Gentleman, R. R. A Language for Data Analysis and Graphics. *J. Comput. Graph. Stat.* **1996**, *5*, 299–314.



# Paper III



# **MALDI-Viz - A comprehensive informatics tool for MALDI-MS data visualization and analysis**

Kishore Kumar Jagadeesan and Simon Ekström

Department of Biomedical Engineering, Lund University, Sweden

## **Keywords:**

High-throughput screening, MALDI-MS, Data analysis, Data Visualization, R, Proteomics

**Abstract:**

High-throughput screening (HTS) is an important technique to profile a very large number of chemicals against the target(s) of interest rapidly. Recently, Mass spectrometry have emerged as an important tool in HTS, competing, fluorescent or colorimetric methodologies, due to its direct and label-free detection method. Among the various MS techniques, Matrix-assisted laser desorption/ionization mass spectrometry (MALDI-MS) fulfils the essential criteria, such as, speed and automation of a high-throughput analyses. However, integration, sorting and comparison of these datasets pose significant challenges, especially when analysing multiple experiments. In addition to the huge data quantities, the diversity of data corresponding to different sorbent phase, sorbent mass, and load, wash, and elution conditions makes manual data analysis difficult.

To address these challenges, a comprehensive informatics tool for MALDI is developed to facilitate visualization, statistical analysis, and high quality image and data export. This tool is a R-Shiny based Web application, accessible independently of the operating system and without the need to install program locally. It allows easy visualization of data, comparison of multiple experiments, and permits export to high quality images. This can be used to do quality checks, visualizations and analysis of mass spectrometry data, coming from proteomics experiments.

## Introduction

Scaled-down HTS methods applied for characterization of different separation phases has provided a breakthrough in the bioprocess development<sup>1,2</sup>. Development of new robotic based liquid handling techniques, labware concepts such as the 96/384/1536 well formats and software for rapid data analysis, have greatly advanced HTS technology<sup>3,4</sup>. Conventionally, many HTS assays are fluorescence-based<sup>5</sup>, however, the selectivity is not always sufficient, e.g. if the sample mixture consists of several proteins with similar structural features<sup>6</sup>. Also, the development of specific fluorescent probes or antibodies adds cost and time to the process. Recently, mass spectrometry (MS) has been recognised as an essential analysis tool in HTS for identification and characterization with the MS offering a label-free and direct-detection method<sup>6</sup>. Surface-based MS techniques such as desorption electrospray ionization (DESI) and matrix-assisted laser desorption/ionization (MALDI)<sup>7,8</sup>, have fast analysis times (around 1 s/sample) and very small sample volume requirements (typically nanoliter), have the potential to combine the label-free, interference-resistant readout with a throughput close to that of traditional fluorescence-based read-out<sup>8,9</sup>.

Three major miniaturized HTS formats have been demonstrated in recent times for investigation of different separation phases. The formats includes: (1) the microtiter filter plates<sup>10</sup>; (2) micropipette chromatography tips<sup>11</sup>; and (3) miniature packed columns<sup>12</sup>. Each of these uses phase volumes of around 500  $\mu$ L or lower, i.e. half of the normal laboratory scale SPE column volume (1 mL). These new formats facilitate screening of different separation phases with simultaneous investigation of diverse sample preparation conditions, to assess the conditions that are optimal for efficient separation of a target analyte. The MS based HTS, particularly if performed in parallel and on a daily basis will yield large amounts of raw data. Thus a major bottleneck in MS based HTS is the data analysis. Fast data analysis and trend identification in the generated information is also very important for design of further experiments.

The key challenge with multiparametric MS datasets is how to best organize, simplify, visualize and analyse the data while retaining the relationships among the different samples/parameters<sup>13</sup>. Furthermore, data import and export functionality is required for future assignment and consistent interpretation of deduced results. There are few devoted software tools for analysis of HTS MS data, but more general tools such as R<sup>14</sup>, SPSS and Matlab<sup>15</sup> packages can be used. Several open source libraries and frameworks such as OpenMS, Proteowizard, MsInspect, Bioconductor have been developed to facilitate MS data analysis<sup>16</sup>. DanteR<sup>17</sup> and InfernoRDN<sup>18</sup> are user-friendly graphical interfaces to the R framework that



allow normalization, statistical analysis based on ANOVA and various multivariate analysis to be carried out. Perseus that is part of the MaxQuant package is also available stand alone<sup>19</sup>, offering tools similar to the ones of DanteR. Thus there are a great variety of software tools and techniques for analysis of MS based proteomic datasets, although most of these tools are intended for, or requires a certain knowledge bioinformatics and sometimes even programming skills.

Also there is a particular lack of specific tools that cover the MALDI data visualization and analysis. The fast generation of MALDI data needs to be visualized and analysed by different statistical techniques, compared to the in proteomics more common ESI MS. In this paper we present MALDIViz, a comprehensive informatics tool for MALDI that facilitate visualization, statistical analysis, and high quality image and data export. MALDIViz is a R-Shiny based Web application, accessible independently of operating system and without the need to install any program locally. It allows easy visualization of data, comparison of multiple experiments, and can be used to do quality checks, visualization and analysis of data from screening experiments.

## **Materials and Methods**

### **Built-in Analysis Functions**

MALDIViz App is a Shiny-based web application, accessible independently of the operating system and without the need to install the program locally. MALDIViz incorporates algorithms for multi-dimensional visualization, statistical analysis, and for creating publication quality images. It has been written entirely in the R language<sup>14</sup> (R version 3.2.3) and developed using Rstudio and Shiny framework. Rstudio is an open source interface for development of R applications, and Shiny is a package that allows to build interactive web applications directly from R.

MALDIViz uses several R packages internally, including `data.table`<sup>20</sup>, `reshape`<sup>21</sup>, `plyr`<sup>22</sup> packages for basic data manipulation capabilities such as filtering, and splitting into groups; `rgl`<sup>23</sup>, `plotly`<sup>24</sup> and `ggplot2`<sup>25</sup> packages for plotting; `d3heatmap`, `pheatmap`<sup>26</sup> packages for drawing heat map; `MALDIquant`<sup>27</sup> package for MALDI data pre-processing; `pcamethod`<sup>28</sup> package for principal component analysis calculations. MALDIViz is freely available at <https://jkkishore85.shinyapps.io/maldiviz/>.

### **Datasets**

Two different datasets were used in order to demonstrate the MALDIViz functionality.

#### *SPE Screening Dataset*

Data from a screening experiment with different molecularly imprinted SPE phases developed for selective enrichment of a proteotypic peptide from the protein Pro-GRP, a biomarker used for Small Cell Lung Cancer diagnosis. Briefly, 6 different polymers in 4 different conditions was processed in duplicate using a micro-SPE platform. Thereafter, the collected eluents were analysed in triplicates using MALDI-MS<sup>29</sup>.

### *Cancer Dataset*

Publicly available data from MALDI-based sample profiling using gold-nanoparticles to separate the proteins and peptides in human serum. The protocol described in this work divides each sample into two sub-samples: pellet and supernatant. The MALDI spectra of both sub-samples are grouped by their corresponding conditions using three-dimensional PCA. The dataset is composed of sera from 5 patients with lymphoma, sera from 5 patients with myeloma, and sera from 2 healthy donors<sup>30</sup>.

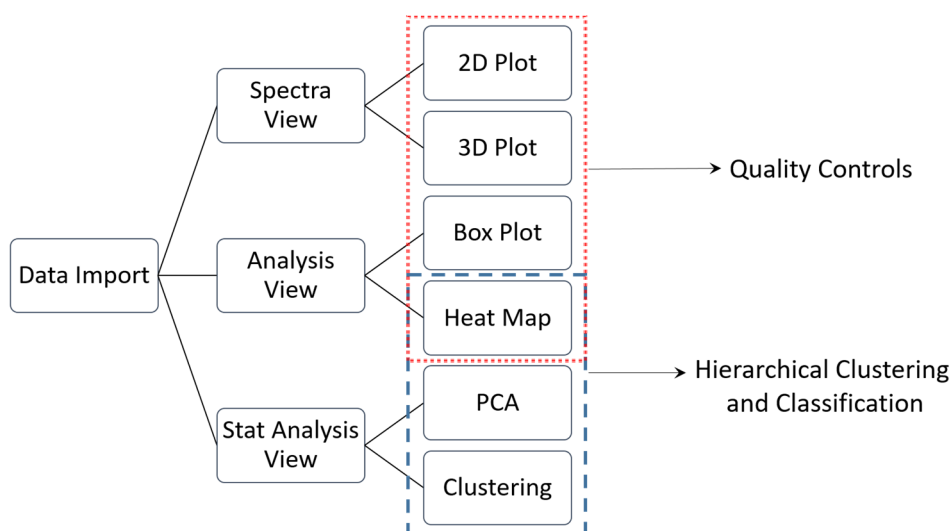


**Figure 1. The main workflows and operations that MALDIViz can perform**

### **Data Pre processing**

MALDIViz tracks contextual information using rows and columns in data tables. Input data for analysis can be any data table (crosstab) containing columns of mass and intensities, with additional columns corresponding to informational metadata from each experiment, such as, type of separation phase, buffer condition, replicate details, or clinical outcomes. At the present version of MALDIViz, up to four columns representing different metadata can be added by the user. In an interactive analysis the user might want to modify the sample groups for instance to include or exclude certain samples. To enable an efficient sample grouping, user can do sample selection based on the supplied metadata. The strategy is easy to use and particularly suited for batch processing.

Supported file formats are any file that stores tabular data, including flat files (either CSV or tab-delimited text files) and Microsoft Excel files. An example of how a typical dataset looks like, from the web app, is displayed in Figure 2.

The screenshot shows the MALDI Viz web application interface. On the left is a sidebar with navigation links: Introduction, Data Set, Dataset Type (Material Screening), Choose file to upload (Browse..., SPE\_dataset1.c, Upload complete), File delimiter, Spectra View, Analysis, and Stat Analysis. The main panel displays a dataset table with 21 rows and 7 columns. The first three columns are labeled 'Numeric Data' and the last four are labeled 'Meta data + Annotations for heatmap1'. The table is divided into two sections: 'Annotations for heatmap2' (columns 4-5) and 'Annotations for heatmap1' (columns 6-7). The data is as follows:

V1	m/z	intensity	material	condition	p.replicate	a.replicate
1	850.1798	2480.5	SPE1	Con1	1	1
2	850.2289	4470.1	SPE1	Con1	1	1
3	850.2506	4582.8	SPE1	Con1	1	1
4	850.2818	6009.0	SPE1	Con1	1	1
5	851.1799	2287.7	SPE1	Con1	1	1
6	851.2595	7091.7	SPE1	Con1	1	1
7	851.2801	7475.7	SPE1	Con1	1	1
8	852.1823	2623.5	SPE1	Con1	1	1
9	852.2219	2457.4	SPE1	Con1	1	1
10	852.2630	14160.7	SPE1	Con1	1	1
11	852.3240	1076.3	SPE1	Con1	1	1
12	853.2079	1088.1	SPE1	Con1	1	1
13	853.2574	5439.0	SPE1	Con1	1	1
14	853.2932	2136.3	SPE1	Con1	1	1
15	854.0602	3245.9	SPE1	Con1	1	1
16	854.1710	1209.1	SPE1	Con1	1	1
17	854.2403	11560.7	SPE1	Con1	1	1
18	854.2826	1548.4	SPE1	Con1	1	1
19	854.6602	305.8	SPE1	Con1	1	1
20	855.0589	8792.3	SPE1	Con1	1	1
21	855.2399	15263.0	SPE1	Con1	1	1

**Figure 2. A screenshot from the MALDIViz app showing a typical dataset loaded.**

## Data Visualization and Analysis Pipeline

MALDIViz provides visualization tools in the form of 2D plot, 3D plot, boxplot and heat map plots for quick data overview and control quality. Once the MALDI data features are extracted, data sets are imported into the MALDIViz for analysis, as shown in Figure 1.

### *Spectra View*

An important function of MALDIViz is its ability to interactively show information about specific sample specified by the user based on values in the metadata, for example, buffer conditions and separation phases. Figure 3 shows examples of the data visualization capabilities provided by MALDIViz. The user can inspect the data such as m/z, intensity, and sample details by moving the cursor along the spectrum.

2D visualization is efficient in showing many data points at the same time. However, it is difficult to visualise the data trends when there are large overlaps of samples. If one wishes to view intensity pattern of several spectra accurately, a better choice would be 3D visualization. In 3D visualization, horizontal axis, x represents m/z, the vertical axis, y represents intensity. And depth axis z represents different samples. In order to show 3D visualizations from a variable view point, the user can zoom and rotate the view around all axes. In addition, it is also possible to change scaling on the m/z value. Similar to the 2D plot, the user can see spectrum data, such as m/z, intensity, and sample details by moving the cursor along the spectrum. The spectra window also allows for colouring of the plots by user-defined groups,

which is useful for finding features and patterns across the experiment in one quick step instead of looking at all the individual spectra.

#### *Analysis view*

The analysis window allows for comparison of the experimental data using box and heatmap plots. Box plots provides a clear visual interpretation of the differences between groups and a measure of the within-group variation. The grouping can be accomplished based on user supplied values in the metadata. For example, a SPE material screening data can be plotted with grouping based on buffer condition to examine any significant differences between separation phases while varying buffer conditions (Figure 3C). Heatmap is plotted using `pheatmap`, `d3heatmap` R packages. Similar to the boxplot, the feature selection on the data is accomplished based on user supplied values in the metadata. Hierarchical clustering and annotation can also be applied to columns and/or rows based on the user inputs.

#### *Stat analysis View*

Stat analysis view offers more advanced, but still easy-to-use multivariate statistical analysis tools for data exploration and validation.

#### *Principal component analysis (PCA)*

MALDIViz can perform PCA for classification and identification of major sources of variation in the data. The ultimate goal of PCA is to reduce the dimensionality of a multivariate dataset while retaining most of the variation in the dataset.<sup>13, 31</sup> By reducing the dimensionality, each sample (spectra) can be represented by a point in a 2D or 3D coordinate system (score plot), in which, spectra with similar variation characteristics can be clustered together and the differences between sample groups can be readily visualized in the system.

PCA creates new variables, the principal components (PCs), which are linear combinations of the original variables (i.e.,  $m/z$  values). The first PC (PC1) is the direction along which the samples show the largest variation. The second PC (PC2) is the direction uncorrelated to the first component along which the samples show the largest variation. The first three of the orthogonal and linearly independent new coordinates (PC1, PC2, and PC3) are then used to visualize the data as dots in a 3-dimensional space<sup>32</sup>.

It can be estimated how much each of the original variables (e.g  $m/z$  values) contribute to each of the new PCs. These values are called loadings. The loading plots of the PCA analysis provide information regarding the contribution of each  $m/z$  value to the variance covered by each respective PC. MALDIViz also offers two types of data pre-processing, i.e., mean-centering and variance scaling prior to PCA<sup>33</sup>. By mean-centering, an average data spectrum is calculated and subtracted from each spectrum of the data set. Without mean-centering, the calculated PC1

will be the average of the data set and will not describe the variation in spectral content. Variance scaling can be used to ensure that all variables contribute equally during the PCA calculation.

#### *Cluster analysis*

Cluster analysis aims to identify which groups of objects are similar to each other but different (or distant) from objects in other groups. There are several ways to define dissimilarity (or distance), according to each particular goal<sup>34</sup>. Typical clustering methods include hierarchical clustering, k-means, neural network, and SPADE. MALDIViz provides hierarchical clustering analysis (HCA) and k-means clustering methods. HCA generates clusters by simply pairing individuals or sub-clusters that are the smallest distance apart in the space, with the original parameters as the coordinates (in our case, m/z values)<sup>35</sup>. MALDIViz allows user to choose between different distance measurement algorithms such as euclidean, maximum, manhattan, canberra, binary or minkowski distance, and select different linkage criteria functions such as complete, single, average, ward.D, ward.D2, mcquitty, median or centroid<sup>34</sup>. The results of the hierarchical clustering is presented in a dendrogram.

#### *Heatmap2*

Similar to heatmap1, heatmap2 is plotted with hierarchical clustering and annotation options to columns and/or rows based on the user inputs. Heatmap2 plots the heatmap for the all m/z values in the dataset, while heatmap1 plots heatmap only for the user defined m/z values.

## **Results and Discussion**

### **Case 1:**

We applied the MALDIViz analysis pipeline in order to analyse high-throughput screening experimental data and identify an optimal SPE phase for the retention of NLLGLIEAK, a proteotypic peptide of Pro-Gastrin Releasing Peptide<sup>29</sup>. In this experiment, 6 different SPE phases in duplicate were examined using 4 different SPE conditions, and MALDI-MS analysis of the SPE eluents was carried out in triplicates.

An example of MALDI-MS spectra resulting from eluent treated with two different SPE materials but the same condition is shown in Fig. 3 A. Without dedicated analysis software such as MALDIViz, user will have to compare these mass spectra one by one which is both tedious and very risky from an analytical perspective. Fig. 3 B shows a MALDIViz generated 3D visualization of MALDI-MS spectra profiles of four different SPE materials (SPE 2, 4, 5, and 6) using Condition 3 as the SPE condition. This way visualizations in combination with user defined sample grouping by colouring option provides a fast and convenient to identify experimental trends.

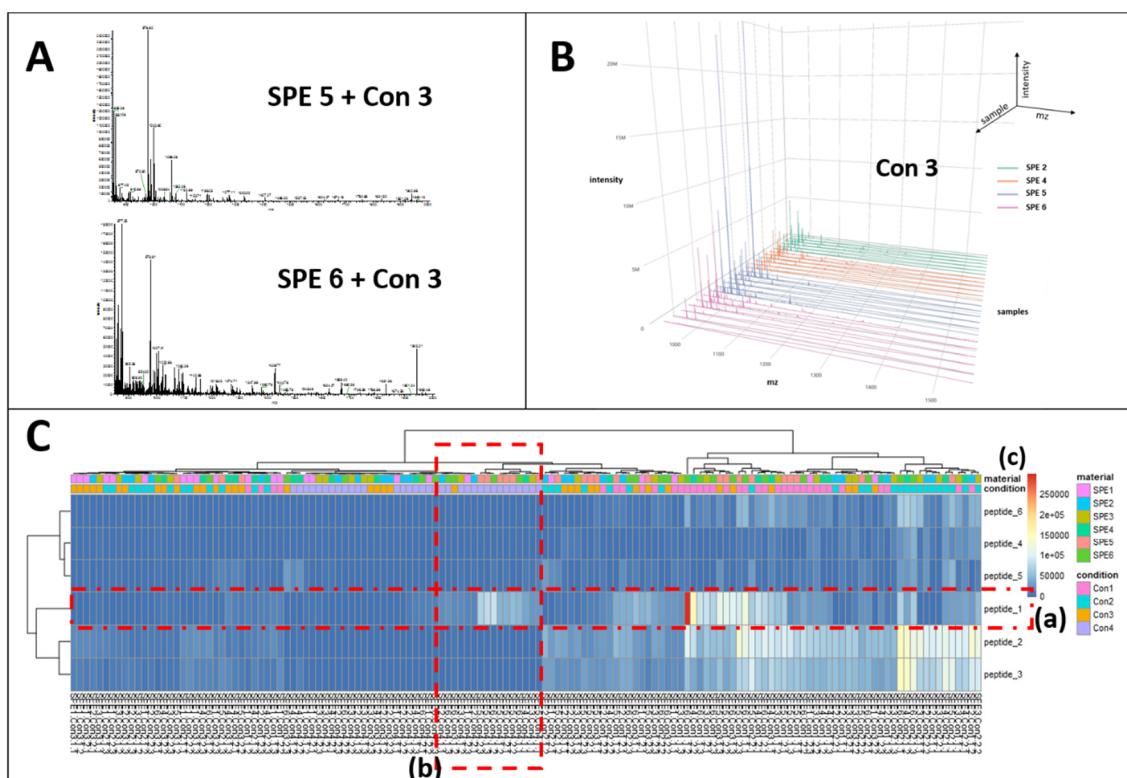


**Figure 3A.** MALDI-MS-based spectra profiles of eluent treated with two different SPE materials (SPE 5 and 6) in a same condition 3. **Figure 3B.** MALDIViz generated 3D visualization of MALDI-MS spectra profiles of four different SPE materials (SPE 2, 4, 5, and 6) using condition 3 as SPE condition. **3C.** Peptide intensity profiles, of the analyte peak (i.e., peptide 1), and the background peaks (i.e., the peptides peaks corresponding to the b-casein digest (i.e., peptide 2, peptide 3, peptide 4, peptide 5, peptide 6)), corresponding to 6 SPE materials in 4 different conditions using MALDI-MS analysis, displayed as a heat map. The upper dendrogram with annotations (c), shows the clustering of the samples, while the side dendrogram automatically groups the more similar peptides. Significant variations in the analyte peptide (a) intensity were observed in the SPE materials 4 and 5 at condition 4 (b).

Although this quick observation of the intensity distribution across the groups can be used to find features and patterns across the experiment, it is important to note that the MALDI signal intensities are not ideal for drawing conclusions, due to ion suppression and sweet spots. Furthermore, there might be experimental differences affecting the intensity, e.g. capacity differences in SPE materials. Instead the relationship of target and background in combination with knowledge of binding mechanism for the SPE sorbents should be assessed for the final conclusion.

To further assess experimental quality, Peptide intensity profiles, of the analyte peak (i.e., peptide 1), and the background peaks (i.e., peptide 2, peptide 3, peptide 4, peptide 5, peptide 6), resulting from the 6 SPE materials in 4 different conditions was plotted as a heat map (Figure 3C). In this heatmap the vertical axis represents the samples, and the horizontal axis represents the different peptides and the colours corresponding peptide intensities. The highest intensities are easy to find in these plots and the top performing SPE material and condition is given by the annotation available at the top of the plot. Optionally MALDIViz, hierarchical clustering can be applied to columns and/or rows. Users can choose which clustering method and linkage method to use. Similarly, users can select the annotation parameters based on the metadata. From the Figure 3C, condition 1 and 2 were identified as having a generic SPE affinity with high recovery observed for all peptides and low selectivity. While condition 4 provided 2 SPE materials (i.e. SPE material 5 and 6), showing selective retention. This significant phenomenon was also demonstrated with the box-plot analysis<sup>29</sup>. Summing up, MALDIViz provided a convenient “all-in-one” data analysis platform that was fundamental for performing high-throughput screening of SPE materials.

## **Case 2:**

In the second case study, a previously published and validated dataset from a MALDI-based sample profiling carried out with gold-nanoparticles as a separation phase is used for demonstration<sup>30</sup>. The dataset comprises observed MALDI peaks after analysis of serum from 5 patients with lymphoma, 5 patients with myeloma, and serum from 2 healthy donors. López-Cortés et al. demonstrated that the resulting MALDI spectra could be grouped by their corresponding cancer type using three-dimensional PCA.

Two separate classification methods, heatmap and PCA, were applied with MALDIViz, in order to ensure that the previously classification results could be reproduced. For distance measurement and linkage options in the heatmap, we used the most commonly used euclidean algorithm with Ward’s method<sup>34</sup>. The dendrogram and annotation on top of the heatmap shows (Figure 4B), a clear clustering of the samples into three groups (i.e., lymphoma, myeloma and healthy samples). Figure 4A shows the PCA plot generated by MALDIViz after processing the entire peak lists. The PCA classification also results in three distinct clusters representing lymphoma, myeloma and healthy samples, in a 3-dimensional subspace spun by the first three PCs. By assigning a different color to each group (i.e., lymphoma, myeloma and healthy), users can quickly visually identify the separate groups.

In conclusion, the herein presented MALDIViz, web application facilitates the analysis and visualization of MALDI-MS data and export of results as high quality images for

documentation and publication. MALDIViz incorporates various functions with focus on analysis of data from high-throughput MALDI screening experiments. The case studies provide some examples of the visual interpretation of differences between different sample groupings as well as a wide range of statistical tools with clustering and PCA, all with a user-friendly interface, designed to minimize the need of bioinformatics expertise and complicated client installations. The MALDIViz app has been and continuous to be a very important tool for analysing MALDI data in our laboratory, and we now would like to share this tool with the scientific community. The app is very generic and can surely be applied to many different analytical problems. we also would like to encourage anyone working with MALDI MS to try the tool, we recommend users to start with a dataset where the answers are known. Although designed specifically for analysing MALDI data, the web app can also be applied to analysis of data from microarray and other -omics data with a MALDIViz compatible data format.

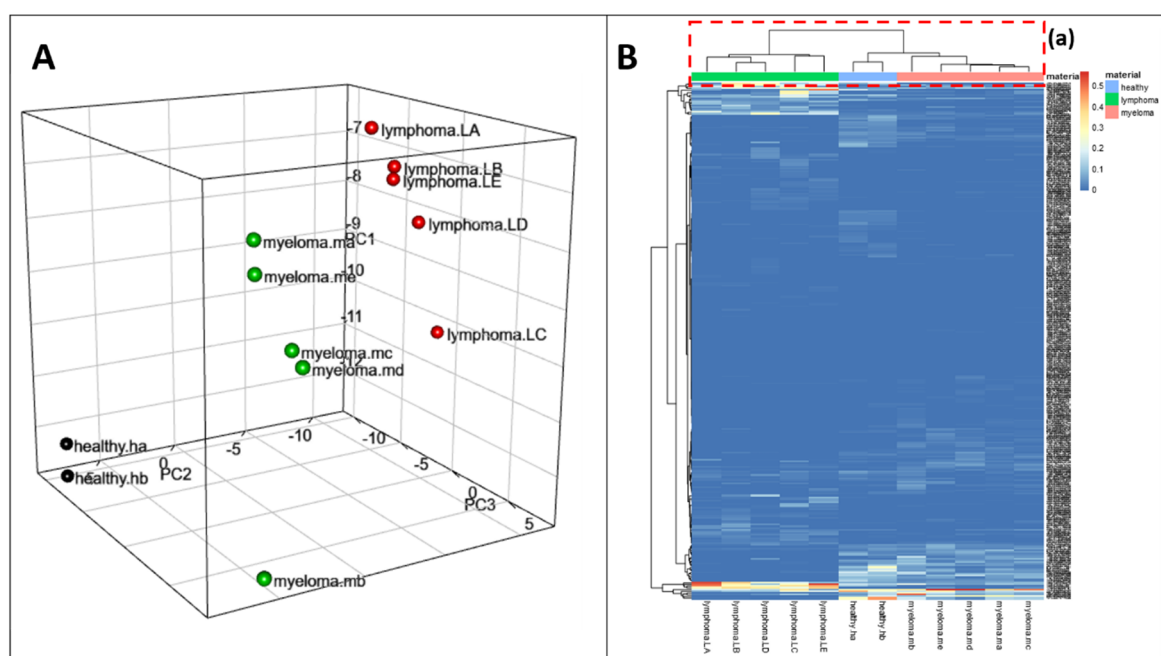


**Figure 4A. Principal component analysis (PCA) presenting three different clusters, one for each sample. Figure 4B. Heatmap of the cancer dataset. (a) Annotations on top of the heatmap show clustering of the samples.**

Currently MALDIViz limits the input file size and does not allow matrices of very high dimensionality. This is mainly due to the performance issues as the huge matrices take longer to upload and calculate, make the tool slower and inconvenient to use. These limits may be reconsidered in the next versions of MALDIViz. Efforts are also taken to add the relative quantitation analysis in the material screening studies, and will reflect in the next versions of MALDIViz.



## References

1. Chhatre, S.; Titchener-Hooker, N. J. Review: Microscale methods for high-throughput chromatography development in the pharmaceutical industry. *Journal of Chemical Technology and Biotechnology* **2009**, 84 (7), 927-940.
2. Welsh, J. Pushing the limits of high-throughput chromatography process development: current state and future directions. *Pharmaceutical Bioprocessing* **2015**, 3 (1), 1-3.
3. Lowe, C. R. Combinatorial approaches to affinity chromatography. *Current Opinion in Chemical Biology* **2001**, 5 (3), 248-256.
4. Bleicher, K. H.; Bohm, H.-J.; Muller, K.; et al. Hit and lead generation: beyond high-throughput screening. *Nat Rev Drug Discov* **2003**, 2 (5), 369-378.
5. Inglese, J.; Johnson, R. L.; Simeonov, A.; et al. High-throughput screening assays for the identification of chemical probes. *Nat Chem Biol* **2007**, 3 (8), 466-479.
6. Rathore, R.; Corr, J.; Scott, G.; et al. Development of an Inhibitor Screening Platform via Mass Spectrometry. *Journal of Biomolecular Screening* **2008**.
7. Jagadeesan, K. K.; Wierzbicka, C.; Laurell, T.; et al. Multiplexed MALDI-MS arrays for screening of MIP solid phase extraction materials. *Journal of Chromatography B* **2016**, 1021, 213-220.
8. Haslam, C.; Hellicar, J.; Dunn, A.; et al. The Evolution of MALDI-TOF Mass Spectrometry toward Ultra-High-Throughput Screening: 1536-Well Format and Beyond. *J Biomol Screen* **2016**, 21 (2), 176-86.
9. Pusch, W.; Kostrzewa, M. Application of MALDI-TOF Mass Spectrometry in Screening and Diagnostic Research. *Current Pharmaceutical Design* **2005**, 11 (20), 2577-2591.
10. Rege, K.; Pepsin, M.; Falcon, B.; et al. High-throughput process development for recombinant protein purification. *Biotechnology and Bioengineering* **2006**, 93 (4), 618-630.
11. Wenger, M. D.; DePhillips, P.; Price, C. E.; et al. An automated microscale chromatographic purification of virus-like particles as a strategy for process development. *Biotechnology and Applied Biochemistry* **2007**, 47 (2), 131-139.
12. Wierling, P. S.; Bogumil, R.; Knieps-Grünhagen, E.; et al. High-throughput screening of packed-bed chromatography coupled with SELDI-TOF MS analysis: monoclonal antibodies versus host cell protein. *Biotechnology and Bioengineering* **2007**, 98 (2), 440-450.
13. Abraham, Y.; Zhang, X.; Parker, C. N. Multiparametric Analysis of Screening Data: Growing Beyond the Single Dimension to Infinity and Beyond. *J Biomol Screen* **2014**, 19 (5), 628-39.
14. Ihaka, R.; Gentleman, R. R. A Language for Data Analysis and Graphics. *Journal of Computational and Graphical Statistics* **1996**, 5 (3), 299-314.
15. Coombes, K. R.; Tsavachidis, S.; Morris, J. S.; et al. Improved peak detection and quantification of mass spectrometry data acquired from surface-enhanced laser desorption and

- ionization by denoising spectra with the undecimated discrete wavelet transform. *PROTEOMICS* **2005**, 5 (16), 4107-4117.
16. Gatto, L.; Breckels, L. M.; Naake, T.; et al. Visualization of proteomics data using R and bioconductor. *Proteomics* **2015**, 15 (8), 1375-89.
  17. Polpitiya, A. D.; Qian, W.-J.; Jaitly, N.; et al. DAnTE: a statistical tool for quantitative analysis of -omics data. *Bioinformatics (Oxford, England)* **2008**, 24 (13), 1556-1558.
  18. Taverner, T.; Karpievitch, Y. V.; Polpitiya, A. D.; et al. DanteR: an extensible R-based tool for quantitative analysis of -omics data. *Bioinformatics* **2012**, 28 (18), 2404-6.
  19. Tyanova, S.; Temu, T.; Sinitcyn, P.; et al. The Perseus computational platform for comprehensive analysis of (prote)omics data. *Nat Meth* **2016**, 13 (9), 731-740.
  20. Dowle, M.; Short, T.; Lianoglou, S.; et al. *data.table: Extension of data.frame*. 2014.
  21. Wickham, H. Reshaping Data with the reshape Package. 2007 **2007**, 21 (12), 20.
  22. Wickham, H. The Split-Apply-Combine Strategy for Data Analysis. 2011 **2011**, 40 (1), 29.
  23. Adler, D.; Nenadic, O.; Zucchini, W. In *Rgl: A r-library for 3d visualization with opengl*, Proceedings of the 35th Symposium of the Interface: Computing Science and Statistics, Salt Lake City, 2003.
  24. Sievert, C.; Parmer, C.; Hocking, T.; et al. plotly: Create Interactive Web Graphics via 'plotly.js'. *R package version* **2016**, 4 (6).
  25. Wickham, H. Introduction. In *ggplot2: Elegant Graphics for Data Analysis*; Springer New York: New York, NY, 2009, pp. 1-7.
  26. Kolde, R. Pheatmap: pretty heatmaps. *R package version* **2012**, 61.
  27. Gibb, S.; Strimmer, K. MALDIquant: a versatile R package for the analysis of mass spectrometry data. *Bioinformatics* **2012**, 28 (17), 2270-1.
  28. Stacklies, W.; Redestig, H.; Scholz, M.; et al. pcaMethods--a bioconductor package providing PCA methods for incomplete data. *Bioinformatics* **2007**, 23 (9), 1164-7.
  29. Jagadeesan, K. K.; Rossetti, C.; Qader, A. A.; et al. Filter Plate-Based Screening of MIP SPE Materials for Capture of the Biomarker Pro-Gastrin-Releasing Peptide. *SLAS DISCOVERY: Advancing Life Sciences R&D* 0 (0), 2472555216689494.
  30. López-Cortés, R.; Oliveira, E.; Núñez, C.; et al. Fast human serum profiling through chemical depletion coupled to gold-nanoparticle-assisted protein separation. *Talanta* **2012**, 100, 239-245.
  31. Ringner, M. What is principal component analysis? *Nat Biotech* **2008**, 26 (3), 303-304.
  32. Cho, Y.-T.; Chiang, Y.-Y.; Shiea, J.; et al. Combining MALDI-TOF and molecular imaging with principal component analysis for biomarker discovery and clinical diagnosis of cancer. *Genomic Medicine, Biomarkers, and Health Sciences* **2012**, 4 (1-2), 3-6.

33. Weaver, E. M.; Hummon, A. B.; Keithley, R. B. Chemometric analysis of MALDI mass spectrometric images of three-dimensional cell culture systems. *Analytical Methods* **2015**, 7 (17), 7208-7219.
34. Nugent, R.; Meila, M. An overview of clustering applied to molecular biology. *Methods in molecular biology (Clifton, N.J.)* **2010**, 620, 369-404.
35. Quackenbush, J. Computational analysis of microarray data. *Nat Rev Genet* **2001**, 2 (6), 418-427.

# Paper IV



# Solid-phase extraction of the alcohol abuse biomarker phosphatidylethanol using newly synthesized polymeric sorbent materials containing quaternary heterocyclic groups

Mariana Duarte<sup>a,b</sup>, Kishore Kumar Jagadeesan<sup>a</sup>, Johan Billing<sup>b</sup>, Ecevit Yilmaz<sup>b</sup>, Thomas Laurell<sup>a</sup> and  
Simon Ekström<sup>a</sup>

a - Department of Biomedical Engineering, Lund University, Box 118, 221 00 Lund, Sweden

b - MIP Technologies AB, a subsidiary of Biotage AB, Box 737, 22007 Lund, Sweden

Corresponding author:

Ms. Mariana Duarte

[mariana.duarte@bme.lth.se](mailto:mariana.duarte@bme.lth.se)

Department of Biomedical Engineering, Lund University, Box 118, 221 00 Lund, Sweden

Keywords:

Solid-phase extraction

Polymer adsorbents

Ion-exchangers

Screening

Phosphatidylethanol

## Abstract

Phosphatidylethanol (PEth) is an interesting biomarker finding increased use for detecting long term alcohol abuse with high specificity and sensitivity. Prior to detection, sample preparation is an unavoidable step in the work-flow of PEth analysis and new protocols may facilitate it. Solid-phase extraction (SPE) is a versatile sample preparation method widely spread in biomedical laboratories due to its simplicity of use and the possibility of automation. In this work, a library of polymeric SPE materials with different surface functionalities was screened for PEth extraction in order to identify the surface characteristics that are important for PEth retention and recovery. The library of SPE materials was evaluated using samples of PEth spiked in human plasma and detection was done by LC-MS/MS. Finally, with the information obtained from the screening, four new SPE materials were formulated, synthesized and tested. A material based on quaternized 1-vinylimidazole with a poly(trimethylolpropane trimethacrylate) backbone was found suitable for PEth extraction in human blood.

## 1. Introduction

Phosphatidylethanol (PEth) belongs to a group of phospholipids that can be used to determine alcohol abuse[1-3]. In the erythrocytes membrane, phospholipase D catalyses the reaction of phosphatidylcholine with ethanol that leads to the formation of PEth, Fig. 1.

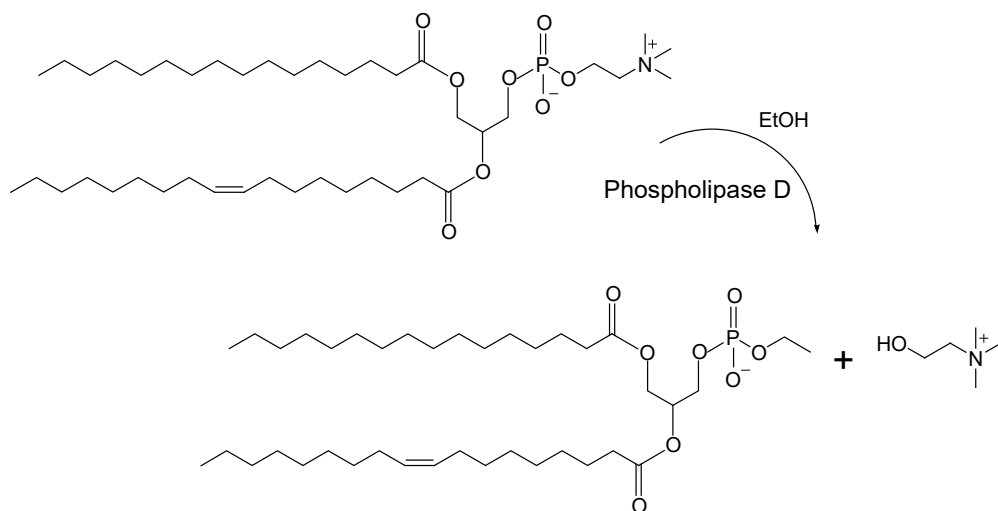


Figure 1. Schematic picture of the formation of PEth: PEth is formed from ethanol and phosphatidylcholine in the cell membrane by a transphosphatidyl transfer reaction catalysed by phospholipase D.

This group of phospholipids have a common polar head group, phosphoethanol, and long-chain fatty acid moieties typically containing 14 to 22 carbon atoms with 0 to 6 double bonds[4, 5]. Among the different forms, PEth-16:0/18:1 and PEth-16:0/18:2 (Nomenclature: 'PEth-16:0/18:1'; 16,18 - number of carbons and 0,1 - number of double bonds of the fatty acids) are the major species and account for more than 60% of the total PEth in blood[6]. PEth has been gaining ground in clinical analysis as an effective alcohol abuse marker, with a blood concentration reference value for alcohol overconsumption of 0.3  $\mu$ M and due to the long half-life of PEth in the blood, it can be detected even after 14 days without alcohol consumption. PEth has a higher sensitivity (94.5-100%)



and specificity (100%) compared to other established markers such as carbohydrate deficient transferrin, gamma-glutamyl transferase and mean corpuscular volume[7, 8].

Different analytical techniques have been utilized over the past few decades to detect and quantify PEth in blood, e.g thin-layer chromatography (TLC) [9], high-performance liquid chromatography (HPLC) [10-12], capillary electrophoresis (CE), non-aqueous capillary electrophoresis (NACE) [13, 14] and immunoassays targeting the head group[15]. In more recent years, mass-spectrometry-based (LC-MS) methods have brought high analytical sensitivity, shorter turnaround time and, above all, the ability to distinguish the different molecular forms of PEth[16-19].

An important practical aspect in the MS-based methods for PEth analysis is the sample preparation step, i.e. how to extract, isolate, clean-up and enrich PEth from its complex sample matrix (blood)[20]. By removing some of the endogenous background from the sample, matrix ion suppression[21, 22] can be minimized; additionally, a cleaner sample also provides improved robustness of the chromatographic separation. To date, liquid-liquid extraction (LLE) is the most widespread method for PEth extraction from blood[4, 13, 16, 18]. The LLE extraction is based on partition of lipids (where PEth is a small fraction) into an added organic phase[23]. The most popular method uses chloroform and methanol as solvents[13], but there are many alternative solvent systems[4, 16, 18] including a dispersive liquid-liquid micro extraction (DLLME) using dichloromethane as extraction solvent and acetone as the dispersive solvent[24].

Recently, solid phase extraction (SPE) has been suggested as a means to pre-separate target lipids from other sample matrix components[25]. Compared to LLE, an SPE sample preparation can potentially provide higher selectivity, allowing for a greater reduction of background, speed of extraction, easier automation and reduced use of organic solvents[26, 27]. In this respect a tailor

made SPE material targeting PEth may offer better clean-up than existing methods/materials. With the use of polymeric SPE sorbents, there is ample opportunity to control e.g. the hydrophobicity and surface functionality through the choice of the components. This work presents an SPE material development strategy based on an initial screening of a selected library of polymeric SPE materials with different surface functionalities and then, based on the gained information, formulating and synthesizing new SPE materials designed for improved PEth extraction.

## 2. Materials and methods

### 2.1. Materials

PEth-16:0/18:1 was obtained from Abcam (Cambridge, UK). Distilled water was purified using an ultra-pure water system from Elga (High Wycombe, UK). ABDV (2,2'-azo-bis(2,4-dimethylvaleronitrile) was obtained from Wako Chemicals (Neuss, Germany), Celvol 523 was from Celanese (Dallas, Texas, USA). All the other chemicals including lyophilized human plasma and HPLC-grade solvents were purchased from Sigma-Aldrich (Steinheim, Germany). The chemicals were used as received except for 4-vinylpyridine which was distilled before use. PEth free human blood was obtained from healthy volunteers. Elemental analysis was carried out by Mikroanalytisches Laboratorium Kolbe (Mülheim, Germany). Pore volumes and surface areas were obtained by N<sub>2</sub> adsorption analyses provided by the Department of Chemical Engineering, Lund University using a Micromeritics ASAP 2400 instrument. The samples were degassed overnight at 60 °C. The library of SPE materials and the ion-exchanger Evolute AX were kindly provided by MIP Technologies AB (Lund, Sweden).

## 2.2. LC–MS/MS analysis

The LC-MS/MS analysis of PEth was performed using a Shimadzu HPLC instrument with two HPLC pumps (LC-20AD), a vacuum degasser (DGU-20A3) and an autosampler (SIL-20AC) connected to an Applied Biosystems mass spectrometer (API3200) with an electro spray ionization interface. The chromatographic separation was carried out with a Thermo Scientific Hypersil HyPURITY C4 column (100 mm x 4.6 mm, 5  $\mu$ m particle size) in gradient mode with solvent A: 20% 2 mM NH<sub>4</sub>Ac + 80% MeCN, solvent B: 100% isopropanol. From sample injection until 2.0 min, isocratic elution with 90% A and 10% B was used; from 2.0 –3.0 min, a linear gradient to 50% B; from 3.0–6.0 min, a linear gradient to 100% B; from 6.0 –7.0 min, isocratic elution with 100% B; and from 7.0–8.0 min, a linear gradient back to 90% A and 10% B. The flow rate was 400  $\mu$ L/min and the sample injection volume 10  $\mu$ L. The column was reconditioned with 90% A and 10% B for 5 min after each injection.

The mass spectrometer was used in negative mode with the following settings: electrospray capillary voltage, 3500 V, ion source temperature 350°C, curtain gas (N<sub>2</sub>) 20 psi, collision gas (N<sub>2</sub>) 3 psi, nebulizer gas 15 psi, auxiliary gas 40 psi, de-clustering potential –80 V, focusing potential –350 V, entrance potential –9 V, and collision energy –45 V. Data was acquired through multiple reaction monitoring mode (MRM) to detect the major product ions (fatty acid fragments) from the deprotonated species of PEth-16:0/18:1 ( $m/z$  701.5 $\rightarrow$ 255.5 and 701.5 $\rightarrow$  281.5).

## 2.3. SPE materials library screening procedures

A library of 12 available SPE materials was screened against samples containing PEth, first in water and then spiked in human plasma to increase background complexity. All the used SPE phases were highly cross-linked polymeric beads in sizes of 20-70  $\mu$ m (see information in Table 1). For

each SPE phase, triplicate 3 mL polypropylene cartridges (Biotage AB, Sweden) were packed with 100 mg material held in place by 20  $\mu$ m pore size frits at the top and the bottom of the packed bed. The SPE protocol consisted of the following steps:

1. Conditioning: 1 mL of methanol and 1 mL of water
2. Loading: 1 mL of water or diluted human plasma (1:10 in water) spiked with PEth, flow rate < 1 mL/min
3. Washing 1 (W1): 1 mL water:acetonitrile 50:50 (v/v)
4. Washing 2 (W2): 1 mL water:acetonitrile 10:90 (v/v)
5. Elution 1 (E1): 1 mL 5% formic acid in water:acetonitrile 10:90 (v/v)
6. Elution 2 (E2): 1 mL 10% formic acid in water:acetonitrile 10:90 (v/v)

All fractions were collected and analysed using the LC–MS/MS method described above.

## 2.4 Synthesis of solid-phase extraction materials

### 2.4.1 Quaternized poly(TRIM-*co*-VI) (P1)

Celvol 523 (20 g) was dissolved in 980 mL water in a 2 L reactor at 80°C under stirring and the solution was allowed to cool down. Then, 1-vinylimidazole (51.3 g), trimethylolpropane trimethacrylate (TRIM) (184.8 g) and benzoyl peroxide (5.58 g, 75%, remainder water) were dissolved in toluene (325 mL) and added to the reactor at room temperature and the mixture was stirred at 300 rpm using an anchor stirrer. The temperature was increased to 75°C and maintained there for 24 h. The resulting beads were filtered off in a filter funnel and washed three times with warm water and once with methanol before wet sieving. The 32-90  $\mu$ m fraction was washed once with methanol, three times with ethyl acetate, three times with formic acid and three times with

methanol in a filter funnel before drying in a vacuum oven at 40°C. The nitrogen content of the resin was found to be 2.2% corresponding to an imidazole content of 0.8 meq/g.

A portion of the resin (5 g) was suspended in DMF (30 mL) and iodomethane (5 mL) was added. The mixture was stirred for 24 h at 40°C and then filtered off in a filter funnel. The resulting resin was washed three times with water and five times with methanol and then dried in a vacuum oven at 40°C.

#### 2.4.2 Quaternized poly(TRIM-*co*-4VP) (P2)

The polymer was prepared as P1 but using 4-vinylpyridine (57.3 g) instead of 1-vinylimidazole. The nitrogen content measured before quaternization of the resin was found to be 3.0% corresponding to a pyridine content of 2.1 meq/g.

#### 2.4.3 Quaternized poly(PETRA-*co*-VI) (P3)

Pentaerythritol triacrylate (PETRA) (32.2 g), 1-vinylimidazole (5.7 g) and ABDV (0.95 g) were dissolved in toluene (38 mL). The mixture was distributed equally in two 100 mL glass bottles and polymerized in a ventilated oven for 24 h at 50°C. After polymerization, the bottles were broken with a hammer and the polymer was crushed in a mortar into 5-10 mm size pieces. The polymer pieces were washed three times with methanol in a filter funnel and then dried in a vacuum oven at 40°C. After drying, the polymer was ground and wet sieved and the 32-90 µm fraction was washed once with methanol, five times with ethyl acetate and three times with methanol in a filter funnel before being dried again in the vacuum oven at 40°C. The nitrogen content of the resin was found to be 4.0% corresponding to an imidazole content of 1.4 meq/g.

The quaternization was carried out as for P1.

#### 2.4.4 Quaternized poly(PETRA-*co*-4VP) (P4)

The polymer was prepared as P3 but using 4-vinylpyridine (3.1 g) in methyl isobutyl ketone (MIBK) (66 mL). The nitrogen content measured before quaternization of the resin was found to be 2.0% corresponding to a pyridine content of 1.4 meq/g.

#### 2.5 PEth solid-phase extraction from human blood

The SPE materials synthesized were packed in 3 mL SPE cartridges (60 mg/cartridge) in triplicate and used for solid-phase extraction of spiked PEth in human blood according to the following protocol:

1. Conditioning: 1 mL of methanol and 1 mL of water
2. Loading: 1 mL of diluted human blood (1:10 in water) spiked with PEth (0.3  $\mu$ M), flow rate < 1 mL/min
3. Washing 1 (W1): 1 mL water
4. Washing 2 (W2): 1 mL 1% formic acid in water:acetonitrile 10:90 (v/v)
5. Elution (E): 1 mL 10% formic acid in water:acetonitrile 10:90 (v/v)

The elution fractions were collected, evaporated and reconstituted in 250  $\mu$ L of mobile phase A and analysed using the LC–MS/MS method described above.

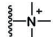
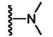
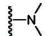
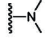
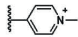
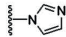
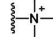
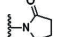
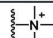
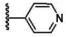
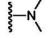
### 3. Results and discussion

#### 3.1. Screening of SPE libraries for extraction of PEth in water and human plasma

In order to identify material properties suitable for SPE of PEth, 12 different materials were chosen based on the structure of PEth and screened. The materials comprise backbones providing different levels of hydrophobicity and functional groups imparting either positive or neutral interaction

sites. The characteristics of each SPE material are presented in Table 1. The ligand density and surface area are also included as important measures for understanding possible interactions.

Table 1. Characteristics of the SPE materials used for the first screening step.

Material ID	Part No.	Surface chemistry			
		Functional group	Ligand Density [mmol/g]	Backbone	BET surface area (m <sup>2</sup> /g)
I	MH03-1124		0.76	poly(DEGDMA)	2
II	RM10-3131		0.64	poly(PETRA)	364
III	RM10-3133		0.64	poly(TRIM)	338
IV	RJ12-2442		0.65	poly(DVB)	73
V	RP03-3413		4.47	poly(TRIM)	23
VI	I3030		3.51	poly(DVB)	75
VII	RM06-3098		1.18	poly(EGDMA)	2
VIII	RL01-2827		1.80	poly(DVB)	182
IX	RJ05-2291	None	-	poly(DVB)	372
X	RK12-2772		0.09	poly(DVB)	91
XI	RM05-3053		1.33	poly(DVB)	580
XII	RM10-3134		0.64	poly(DVB)	548

DEGDMA: di(ethylene glycol) dimethacrylate; PETRA: pentaerythritol tetra-acrylate; TRIM: trimethylolpropane trimethacrylate; DVB: divinylbenzene ; EGDMA: ethylene glycol dimethacrylate

The SPE materials containing tertiary amine functional groups (II, III, IV and XII) are expected to behave as weak anion exchangers (pKa~9), while the materials containing quaternary amines and quaternary pyridine (I, V, VII and X) are strong anion exchangers i.e. exhibit permanently charged groups. Materials VI and XI, containing imidazole (pKa~7) and pyridine (pKa~5), should have none or only little charge under the current extraction conditions. Additionally, these functional groups, as well as the pyrrolidone group of material VIII, can provide sites for hydrogen bonding. The other retention mechanism to be considered is hydrophobic interaction between the fatty acid

chains of PEth and the hydrophobic backbone of the polymers. The hydrophobicity is to a large extent dependent on the polymer backbone; poly(DEGDMA) is the least hydrophobic one followed by poly(PETRA), poly(TRIM) and poly(EGDMA), which have similar properties, and finally poly(DVB) which provides the most hydrophobic backbone.

The SPE library (Table 1) was first screened using samples of 4  $\mu$ M PEth spiked in water. The applied SPE protocol used a high organic content (50-90%) in the wash steps and an acidic elution. Therefore, anion exchange should be the dominant mechanism responsible for PEth retention. The SPE flow-through and elution was collected and subjected to LC-MS/MS analysis, the observed signal (peak area) is plotted in Fig. 2.

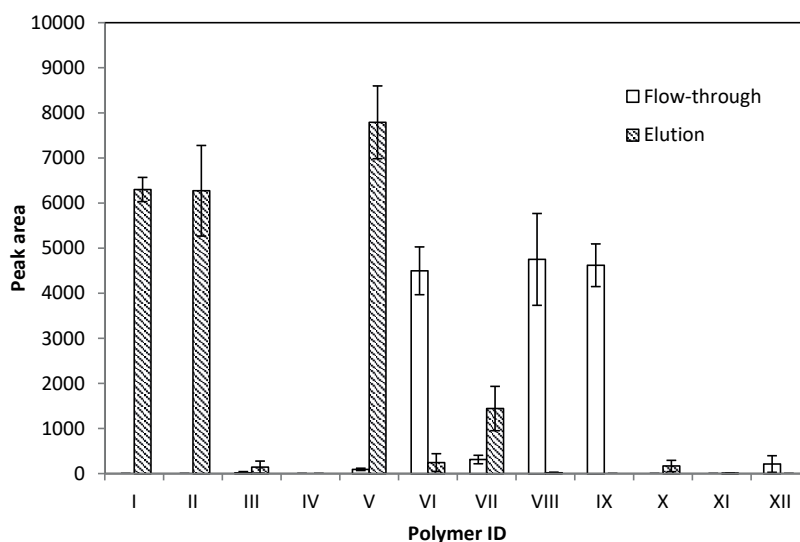


Figure 2. MS peak area of PEth resulting after analysis of the flow-through (white) and the elution step (striped). The best SPE materials I, II and V provided high signal for the elution and no signal of the analyte in the flow-through.

From the data in Fig. 2 and Table 1, it is evident that a purely hydrophobic retention as offered by the DVB based materials VI, VIII and IX was insufficient for retention, as high signal for PEth was observed in the flow-through. The SPE phases III, IV, X, XI and XII provided very high retention,



with little or no observed signal of PEth in either flow-through or elution. This overly strong retention is most likely due to a very hydrophobic backbone, e.g. DVB, in combination with anion exchange functionalities (IV, X and XII) and hence it appears that even under these conditions with a high organic content, hydrophobicity still plays a role. Another factor that also contributes to this strong retention is a high surface area (III, XI and XII). In order to improve the recovery for these materials, one could just increase the elution volume. However, large elution volumes are not a desirable feature in any SPE sample preparation method and hence these materials were not passed on to the second screening. Rather, the materials selected for the second screening step (I, II and V) displayed strong retention of PEth, with negligible or no signal observed in the flow-through, while still allowing for efficient elution. It may be noted that while material VII, containing a quaternary amine, also showed a signal for PEth in the elution, the recovery was quite low and therefore material VII was excluded from the second screening. All the high performing materials (I, II and V) possess a combination of a positively charged surface with an intermediate or low hydrophobicity backbone.

In the second screening step, using only SPE materials I, II and V, all the fractions from the sample preparation were analysed. Also, a more complex sample was used (0.5  $\mu$ M PEth spiked in diluted human plasma 1:10). The analysis revealed that material I and II suffer from losses during loading and wash (Fig. 3). Material V provided the highest observed signal for PEth in the elution and very low losses in the wash steps, W1 (50% acetonitrile) and in W2 (90% acetonitrile). The ability to use a high organic content in the wash should allow for removal of hydrophobic (proteins) contaminants during SPE.

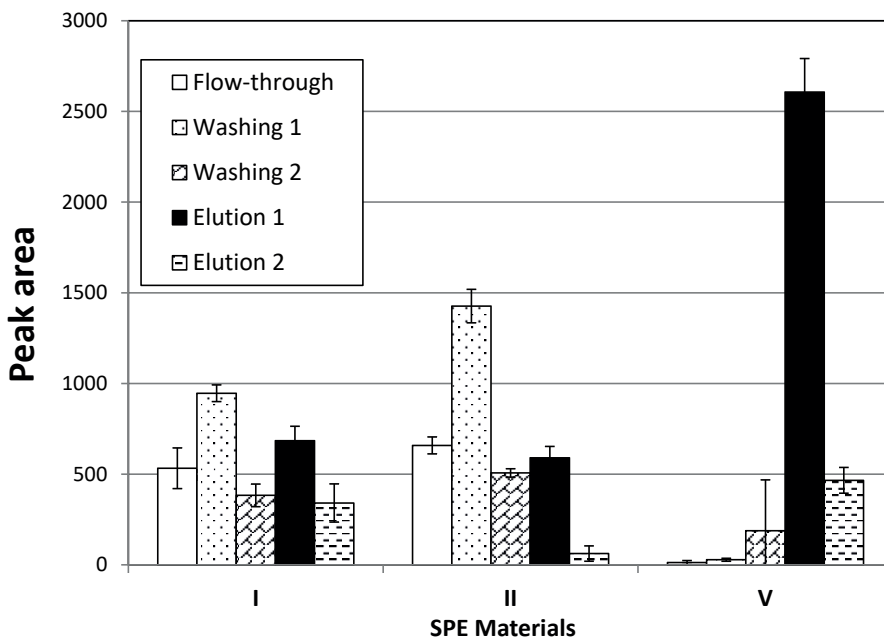


Figure 3. MS peak area in fractions collected after SPE of 0.5  $\mu\text{M}$  PETH spiked in plasma for the flow-through, washes (W1, W2) and elutions (E1, E2) using I, II and V. Here, material V provides the lowest PETH signal in the flow-through and washing and the highest response in the elution fraction.

In order to facilitate quantitative determination of the recovery for material V, with the used instrumentation and no isotope dilution, the PETH spike was increased to 5  $\mu\text{M}$  and the extraction repeated using the same protocol. The recovery was found to be  $1.05 \pm 0.22$ , as calculated from observed peak area for the eluted fractions divided by the peak area observed for external standards (5  $\mu\text{M}$  in mobile phase).

An unexpected isobaric compound(s) was observed in the XIC/SRM chromatogram for spiked plasma when analysed without SPE (i.e. injected directly), Fig. 4. It is noteworthy that after SPE purification, the unknown isobaric peak disappeared and a higher intensity of PETH at 7.2 min was observed. Although we did not manage to identify the offending peak, it is an example of why it is important to reduce sample complexity before analysis. Even if modern LC-MS methods have the

capability to handle quite complex samples, sample matrix variations in patient samples can sometimes lead to erroneous results. Another benefit of the SPE is that a cleaner sample leads to better assay/instrument robustness.

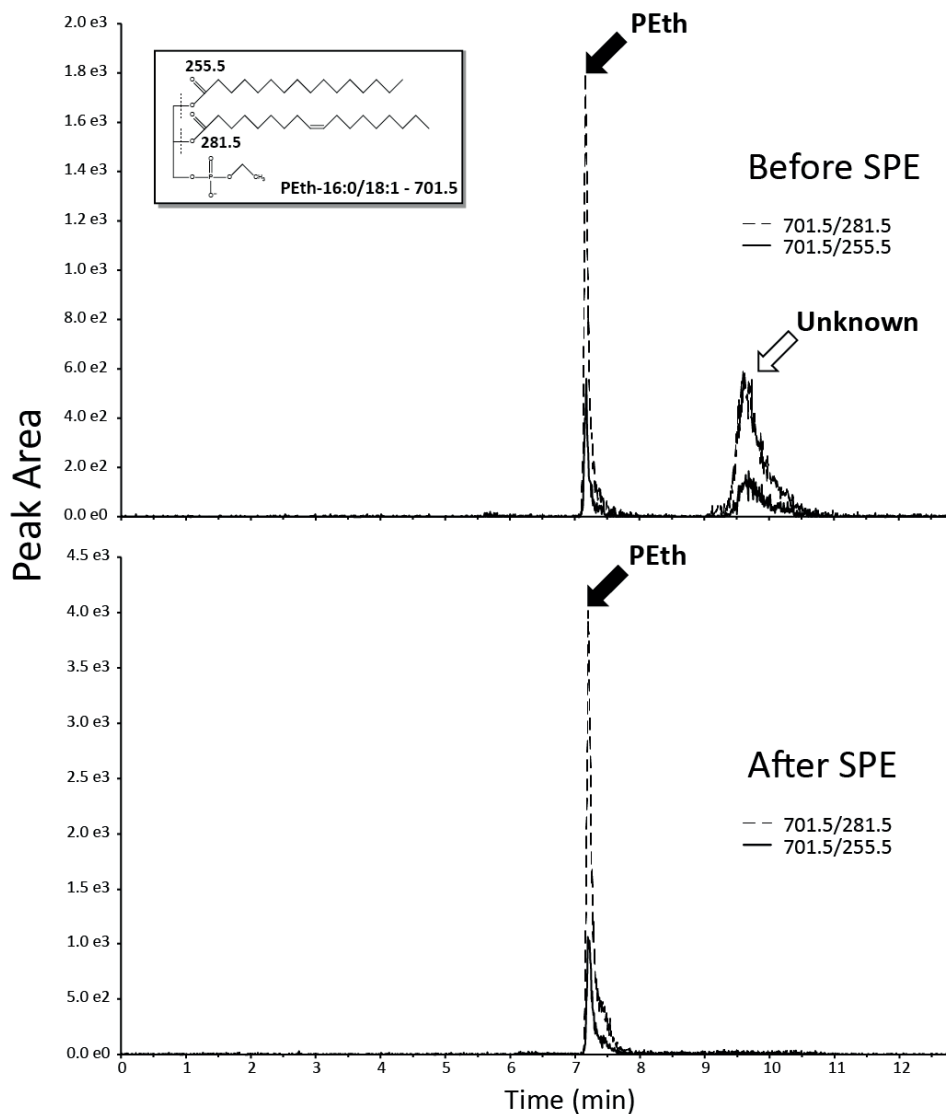


Figure 4. XIC/SRM chromatograms for 5  $\mu$ M PEth 16:0/18:1 (m/z 701.5/255.5 and m/z 701.5/281.5) spiked in human plasma, before SPE and after SPE using material V.

### 3.2. Synthesis of new solid phases for PEth extraction and evaluation with whole blood

From the initial screening, it was concluded that PEth required an SPE material with anion-exchange capability and that too hydrophobic backbones would be detrimental for the elution step. In particular, material V with the combination of a cross-linker of intermediate hydrophobicity and quaternized pyridine functionality seemed interesting. Based on this knowledge, a new set of related polymers was synthesized (Table 2).

Table 2. The new synthesized SPE materials for PEth extraction from human blood: chemical composition and porosity data. All polymers were quaternized with iodomethane after synthesis.

SPE material ID	Functional monomer	Crosslinker	BET surface area (m <sup>2</sup> /g)	Pore volume (mL)	Average pore size (Å)
P1	1-vinylimidazole	TRIM	419	0.67	64
P2	4-vinylpyridine	TRIM	300	0.66	89
P3	1-vinylimidazole	PETRA	305	1.01	132
P4	4-vinylpyridine	PETRA	344	0.90	105

TRIM and PETRA were chosen as cross-linkers as they provide intermediate hydrophobicity. We also decided to test another quaternized heterocyclic group, quaternary imidazole, by using the functional monomer 1-vinylimidazole for the synthesis of P1 and P3 instead of the 4-vinylpyridine monomer used in synthesis of P2 and P4. The quaternizations were carried out with iodomethane (see Fig. 5 for structures).

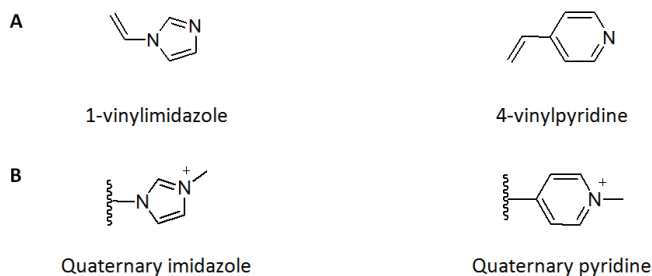


Figure 5. Monomers used in the synthesis of the polymers (A) and the resulting functional groups in the polymer after quaternization (B).

In the library screening, PEth was spiked into 1:10 diluted plasma and while this is a fairly complex sample, PEth is clinically extracted from whole blood. Blood is probably one of the most difficult matrices to work with as it is not only extremely complex but also very viscous. However, since it is the matrix of main interest, it was used for the evaluation of the new materials. For comparison, Evolute AX (Biotage AB) was included as a benchmark. This commercially available SPE product comprises quaternary amines on a modified polystyrene-based (PS) polymer (exchange capacity 0.7 mmol/g). This product is similar to the synthesized materials as it is a mixed-mode ion-exchanger offering both hydrophobic and strong anion exchange interactions.

In Fig. 6 we present the SPE recoveries of PEth in human blood samples. All the synthesized polymers exhibit satisfactory recoveries (28-49%). P1 shows the highest recovery in the elution, about 50% of PEth loaded onto the SPE column. The lowest recovery is obtained with P2 which has the most similar characteristics to material V (best performing material in the screening). Therefore, the newly develop material P1 represents an improvement compared to the composition originally found and it appears that the more polar imidazole moiety may be better suited for SPE

of PEth (in blood) than the more non-polar pyridine moiety (imidazole logP -0.02 compared to 0.65 for pyridine).[28, 29] The materials containing the slightly less hydrophobic crosslinker PETRA also perform well and all the synthesized materials outperform the commercial benchmark strong anion exchanger Evolute AX.

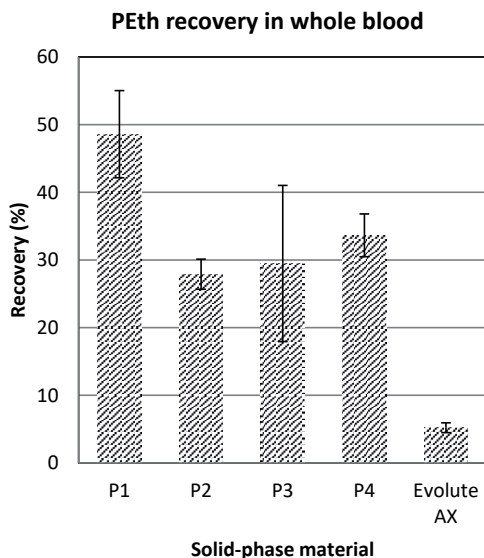


Figure 6. Recovery values of PEth extraction from whole blood using 4 new polymers and a commercial benchmark.

From the results of the initial SPE library screening, it is reasonable to believe that the low recovery for Evolute AX is due to the hydrophobicity of the PS backbone, causing this conventional mixed-mode ion-exchanger to be unsuitable for SPE of PEth, even though its modified backbone is less hydrophobic than a purely PS/DVB one.

The lower recoveries obtained from blood (50%) in comparison to the best performing material for SPE of PEth in human plasma (100%) can be expected due to the use of (lyzed) whole blood. This also forced the SPE procedure to be adapted to include a stronger wash step composition (W2), containing 90% acetonitrile and 1% formic acid. The recovery value of 50% obtained with this

protocol shows that unlike conventional materials, P1 can effectively retain and release PEth and provides a good starting point for the development of SPE methods for PEth extraction in clinical samples.

### 3. Concluding remarks

This paper introduces new SPE materials for PEth extraction from complex biological matrices such as blood. A series of screening procedures using different SPE materials were carried out and after identification of the core mechanism of retention, new polymers designed for PEth extraction were synthesized. Using this procedure we have developed an SPE material which possesses appropriate binding properties and allows for purification of PEth from human blood. We concluded that a good SPE material for PEth should include strong anion exchange capabilities and that a very hydrophobic backbone will be detrimental for recovery of PEth, making cross-linkers of intermediary hydrophobicity a better choice. Additionally, heterocyclic amino groups seem to perform better than alkyl amino groups. The best material synthesized in this study contains strong anion exchange functionalities in the form of quaternary imidazole groups with a cross-linker of intermediary hydrophobicity (TRIM). These findings constitute a first step towards a versatile SPE method for PEth analysis in the clinical lab which may bring advantages in terms of solvent use, automation, through-put and analysis time in comparison with traditional liquid-liquid extraction methods. Moreover, the findings of this study show that even though conventional mixed-mode ion-exchangers might be insufficient for more complex matrices, fine tuning of the solid-phase characteristics can make SPE an option for sample preparation in those cases.

## 5. Acknowledgments

The authors would like to acknowledge the financial support by the European Commission, under the 7th Framework programme, integrated in the PepMIP project: “Robust affinity materials for applications in proteomics and diagnostics”, grant # 264699.

## 6. References

1. Hansson, P., et al., *Blood Phosphatidylethanol as a Marker of Alcohol Abuse: Levels in Alcoholic Males during Withdrawal*. Alcoholism: Clinical and Experimental Research, 1997. 21(1): p. 108-110.
2. Torrente, M.P., W.M. Freeman, and K.E. Vrana, *Protein biomarkers of alcohol abuse*. Expert Rev Proteomics, 2012. 9(4): p. 425-36.
3. Varga, A., et al., *Phosphatidylethanol in Blood as a Marker of Ethanol Consumption in Healthy Volunteers: Comparison with Other Markers*. Alcoholism: Clinical and Experimental Research, 1998. 22(8): p. 1832-1837.
4. Helander, A. and Y. Zheng, *Molecular species of the alcohol biomarker phosphatidylethanol in human blood measured by LC-MS*. Clin Chem, 2009. 55(7): p. 1395-405.
5. Gnann, H., et al., *Identification of 48 homologues of phosphatidylethanol in blood by LC-ESI-MS/MS*. Anal Bioanal Chem, 2010. 396(7): p. 2415-23.
6. Isaksson, A., et al., *Phosphatidylethanol in blood (B-PEth): a marker for alcohol use and abuse*. Drug Test Anal, 2011. 3(4): p. 195-200.
7. Aradottir, S., et al., *PHosphatidylethanol (PEth) concentrations in blood are correlated to reported alcohol intake in alcohol-dependent patients*. Alcohol Alcohol, 2006. 41(4): p. 431-7.
8. Viel, G., et al., *Phosphatidylethanol in blood as a marker of chronic alcohol use: a systematic review and meta-analysis*. Int J Mol Sci, 2012. 13(11): p. 14788-812.
9. Alling, C., L. Gustavsson, and E. Anggard, *An abnormal phospholipid in rat organs after ethanol treatment*. FEBS Lett, 1983. 152(1): p. 24-8.
10. Aradottir, S. and B.L. Olsson, *Methodological modifications on quantification of phosphatidylethanol in blood from humans abusing alcohol, using high-performance liquid chromatography and evaporative light scattering detection*. BMC Biochem, 2005. 6: p. 18.
11. Gunnarsson, T., et al., *Determination of phosphatidylethanol in blood from alcoholic males using high-performance liquid chromatography and evaporative light scattering or electrospray mass spectrometric detection*. J Chromatogr B Biomed Sci Appl, 1998. 705(2): p. 243-9.
12. Tolonen, A., et al., *A method for determination of phosphatidylethanol from high density lipoproteins by reversed-phase HPLC with TOF-MS detection*. Analytical Biochemistry, 2005. 341(1): p. 83-88.
13. Nalesso, A., et al., *Analysis of the alcohol biomarker phosphatidylethanol by NACE with on-line ESI-MS*. Electrophoresis, 2010. 31(7): p. 1227-33.
14. Varga, A. and S. Nilsson, *Nonaqueous capillary electrophoresis for analysis of the ethanol consumption biomarker phosphatidylethanol*. Electrophoresis, 2008. 29(8): p. 1667-71.
15. Nissinen, A.E., et al., *Immunological Detection of in Vitro Formed Phosphatidylethanol—An Alcohol Biomarker—With Monoclonal Antibodies*. Alcoholism: Clinical and Experimental Research, 2008. 32(6): p. 921-928.



16. Zheng, Y., O. Beck, and A. Helander, *Method development for routine liquid chromatography–mass spectrometry measurement of the alcohol biomarker phosphatidylethanol (PEth) in blood*. Clinica Chimica Acta, 2011. 412(15–16): p. 1428-1435.
17. Gnann, H., et al., *Selective detection of phosphatidylethanol homologues in blood as biomarkers for alcohol consumption by LC-ESI-MS/MS*. J Mass Spectrom, 2009. 44(9): p. 1293-9.
18. Nalesso, A., et al., *Quantitative profiling of phosphatidylethanol molecular species in human blood by liquid chromatography high resolution mass spectrometry*. J Chromatogr A, 2011. 1218(46): p. 8423-31.
19. Marques, P., et al., *Detection of phosphatidylethanol (PEth) in the blood of drivers in an alcohol ignition interlock program*. Traffic Inj Prev, 2011. 12(2): p. 136-41.
20. Pawliszyn, J., *Sample Preparation: Quo Vadis?* Analytical Chemistry, 2003. 75(11): p. 2543-2558.
21. Cote, C., et al., *Matrix effect elimination during LC-MS/MS bioanalytical method development*. Bioanalysis, 2009. 1(7): p. 1243-57.
22. Fang, N., et al., *Matrix effects break the LC behavior rule for analytes in LC-MS/MS analysis of biological samples*. Exp Biol Med (Maywood), 2014.
23. Ferreira-Vera, C., F. Priego-Capote, and M.D. Luque de Castro, *Comparison of sample preparation approaches for phospholipids profiling in human serum by liquid chromatography–tandem mass spectrometry*. Journal of Chromatography A, 2012. 1240(0): p. 21-28.
24. Cabarcos, P., et al., *Application of dispersive liquid-liquid microextraction for the determination of phosphatidylethanol in blood by liquid chromatography tandem mass spectrometry*. Talanta, 2013. 111: p. 189-95.
25. Fauland, A., et al., *An improved SPE method for fractionation and identification of phospholipids*. J Sep Sci, 2013. 36(4): p. 744-51.
26. Ahmad, S., et al., *HybridSPE: A novel technique to reduce phospholipid-based matrix effect in LC-ESI-MS Bioanalysis*. J Pharm Bioallied Sci, 2012. 4(4): p. 267-75.
27. Murphy, C.M. and M.A. Huestis, *LC-ESI-MS/MS analysis for the quantification of morphine, codeine, morphine-3-beta-D-glucuronide, morphine-6-beta-D-glucuronide, and codeine-6-beta-D-glucuronide in human urine*. J Mass Spectrom, 2005. 40(11): p. 1412-6.

# Paper V



# Catalytic Formation of Disulfide Bonds in Peptides by Molecularly Imprinted Microgels at Oil/Water Interfaces

Xiantao Shen,<sup>\*,†,‡,||</sup> Chuixiu Huang,<sup>\*,‡,§,||</sup> Sudhirkumar Shinde,<sup>‡</sup> Kishore Kumar Jagadeesan,<sup>‡</sup> Simon Ekström,<sup>‡</sup> Emelie Fritz,<sup>#</sup> and Börje Sellergren<sup>\*,‡</sup>

<sup>†</sup>Key Laboratory of Environment and Health, Ministry of Education & Ministry of Environmental Protection, State Key Laboratory of Environmental Health (Incubation), School of Public Health, Tongji Medical College, Huazhong University of Science and Technology, Hangkong Road #13, Wuhan, Hubei 430030, China

<sup>‡</sup>Department of Biomedical Sciences, Faculty of Health and Society, Malmö University, SE20506 Malmö, Sweden

<sup>§</sup>School of Pharmacy, University of Oslo, P.O. Box 1068, 0316 Blindern Oslo, Norway

<sup>||</sup>G&T Septech AS, P.O. Box 33, 1917 Ytre Enebakk, Norway

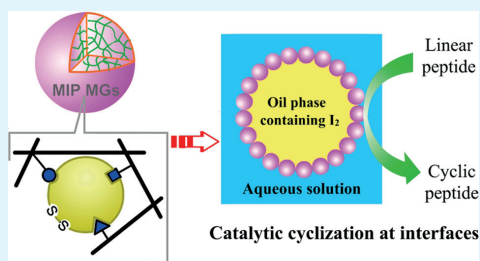
<sup>‡</sup>Department of Biomedical Engineering, Lund University, 221 00 Lund, Sweden

<sup>#</sup>INFU, Technische Universität Dortmund, 44221 Dortmund, Germany

## Supporting Information

**ABSTRACT:** This work describes the preparation and investigation of molecularly imprinted polymer (MIP) microgel (MG) stabilized Pickering emulsions (PEs) for their ability to catalyze the formation of disulfide bonds in peptides at the O/W interface. The MIP MGs were synthesized via precipitation polymerization and a programmed initiator change strategy. The MIP MGs were characterized using DLS analysis, SEM measurement, and optical microscopy analysis. The dry and wet MIP MGs showed a hydrodynamic diameter of 100 and 280 nm, respectively. A template rebinding experiment showed that the MIP MGs bound over two times more template (24 mg g<sup>-1</sup>) compared to the uptake displayed by a nonimprinted reference polymer (NIP) MG (10 mg g<sup>-1</sup>) at saturation. Using the MIP MGs as stabilizers, catalytic oxidation systems were prepared by emulsifying the oil phase and water phase in the presence of different oxidizing agents. During the cyclization, the isolation of the thiol precursors and the oxidizing reagents nonselectively decreased the formation of the byproducts, while the imprinted cavities on the MIP MGs selectively promoted the intramolecular cyclization of peptides. When I<sub>2</sub> was used as the oxidizing agent, the MIP-PE-I<sub>2</sub> system showed a product yield of 50%, corresponding to a nearly 2-fold increase compared to that of the nonimprinted polymer NIP-PE-I<sub>2</sub> system (26%). We believe the interfacial catalysis system presented in this work may offer significant benefits in synthetic peptide chemistry by raising productivity while suppressing the formation of byproducts.

**KEYWORDS:** molecularly imprinted polymers, disulfide-rich cyclic peptides, Pickering emulsions, interfacial catalysis, intramolecular cyclization



## INTRODUCTION

Disulfide-rich cyclic peptides discovered in a wide variety of plants and animals display a broad spectrum of biological activities and pharmaceutical applications.<sup>1–3</sup> These disulfide bridges play important roles in folding and stabilizing protein tertiary structure. Therefore, artificial introduction of disulfide bonds in peptides is of special interest.<sup>4</sup> For example, Berezhkovskiy et al. synthesized a nonobese diabetic (NOD) mouse MHC class II derived peptide, which was an efficient vaccine to prevent diabetes and insulinitis in NOD mice.<sup>5</sup> Wong et al. demonstrated a disulfide-rich cyclic peptide to be an attractive material serving as a drug design scaffold for the incorporation of active epitopes.<sup>6</sup> However, in a previous

review article, White et al. showed that cyclic peptides were difficult, and often impossible, to synthesize using traditional synthetic methods.<sup>7</sup> For the synthesis of disulfide-rich cyclic peptides, the traditional methods include both solution and solid-phase synthesis.<sup>8,9</sup> A crucial final step consists of the controlled intramolecular formation of disulfide bonds involving two strategically placed cysteine residues while suppressing side reactions such as dimerization or oligomerization.<sup>10,11</sup>

Received: August 12, 2016

Accepted: October 17, 2016

Published: October 17, 2016

Traditionally, intramolecular formation of disulfide bonds is achieved by oxidizing the thiols under strict conditions favoring intramolecular reactions at the expense of intermolecular reactions.<sup>11</sup> However, this reaction system has some drawbacks (e.g., low capacity, difficult separation of the excess oxidizing reagent). We present here an approach utilizing imprinting and reagent partitioning in Pickering emulsions (PEs) which successfully addresses these drawbacks. Pickering emulsions are solid particle stabilized emulsions which are now extensively used in colloid chemistry.<sup>12,13</sup> Particularly promising is their use in synthetic chemistry in order to enhance catalytic efficiency and for catalyst recycling in interfacial or biphasic catalysis.<sup>14–19</sup> We have previously demonstrated PE as a versatile tool for enhancing water compatibility and imprinting efficiency in molecularly imprinted polymers (MIPs).<sup>20,21</sup> Moreover, protein imprinting, cell imprinting, and Janus MIPs as self-propelled transporters have also been presented on the basis of PEs.<sup>22–24</sup>

Although numerous examples have been reported on the use of the molecular imprinting concept in molecular recognition, sensing, and separations,<sup>25–29</sup> the area of catalysis has been less exploited. Reactions previously investigated using imprinted enzyme mimics include dehydrofluorination, hydrolyses, selective photocatalysis, Diels–Alder, and aldol reactions.<sup>30–35</sup> To our knowledge the use of MIPs to control peptide disulfide bridge formation has not been reported.

Therefore, in this work we demonstrate that oxidizing agent partitioning in MIP microgel (MG) stabilized oil/water PE provides an effective means of promoting the cyclization of cysteine-rich peptides, in this case somatostatin (SST), a growth hormone inhibiting hormone composed of a cyclic 14 amino acid peptide (Figure 1a). The system design was guided by the following criteria and assumptions: (i) The thiol

precursors and the oxidizing agent will be dissolved in different phases of the PEs. This will reduce the collision concentration of reagents, which in turn will suppress peptide dimerization or oligomerization. (ii) The heterogeneous nature of the catalyst will facilitate product purification. (iii) The oxidation reaction will occur at the PE interface where the imprinted cavities of the MIP MGs will act as microreactors for directing the intramolecular cyclization of the peptides at the expense of intermolecular reactions.

## EXPERIMENTAL SECTION

**Materials.** *N,N,N,N*-Tetra-methyl-ethylenediamine (TEMED), ammonium persulfate (APS), dithiothreitol (DTT), acrylic acid (AA), *N*-isopropylacrylamide (NIPAm), *N*-tert-butylacrylamide (TBA), and *N,N'*-methylene bis(acrylamide) (MBA) were obtained from Sigma-Aldrich. Toluene, dimethyl sulfoxide (DMSO), acetonitrile (ACN), methanol (MeOH), and ethyl acetate were supplied from VWR International. Trifluoroacetic acid was from Acros (Geel, Belgium). Characteristic MSH-tetrapeptide (Sequence: H-His-Phe-Arg-Trp-OH, MSH) was obtained from BACHEM. Standard peptide H-NLLGLIEAK-OEt (molecular weight: 998) was purchased from Genscript (Piscataway, NJ). Somatostatin (H-Ala-Gly-Cys-Lys-Asn-Phe-Phe-Trp-Lys-Thr-Phe-Thr-Ser-Cys-OH, molecular weight: 1638), and desmopressin (Mpr-Tyr-Phe-Gln-Asn-Cys-Pro-D-Arg-Gly-NH<sub>2</sub>, molecular weight: 1069) were from Sigma-Aldrich. Reference somatostatin (Ser-Asn-Pro-Ala-Met-Ala-Pro-Arg-Glu-Arg-Lys-Ala-Gly-Cys-Lys-Asn-Phe-Phe-Trp-Lys-Thr-Phe-Thr-Ser-Cys, molecular weight: 2375) was purchased from WuHan Moon Biosciences Co., Ltd. Iodine, potassium ferricyanide(III), and ZnO nanoparticles (90 ± 10 nm in diameter) were purchased from Shanghai Aladdin Biochem Technology Co., Ltd. Other chemicals were of reagent grade or higher.

**Synthesis of MIP Microgels (MIP MGs).** In a previous work, a protocol for the synthesis of nanogels or microgels via aqueous surfactant-free radical precipitation copolymerization has been presented using a programmed temperature ramp from 45 to 65 °C during the nucleation stage of the polymerization.<sup>36</sup> To keep the stability of the template peptide at low temperature and hence to suppress unwanted methylenation through reaction of especially lysines with TEMED radicals,<sup>37</sup> the synthesis of MIP MGs employs a programmed initiator change method (change from single APS to a mixture of APS and TEMED) during the nucleation stage in this work. Here, AA, NIPAm, and TBA were used as functional monomers, and MBA was used as a cross-linker. Typically, 20.7 μL of AA, 217.3 mg of NIPAm, 61.0 mg of TBA, and 46.3 mg of MBA were dissolved in 20 mL of PBS buffer (pH 7.4, 20 mM). After dissolving 6.8 mg of SST into the monomer solution, the reaction mixture was filtered through a 0.45 μm filter to remove particles. In this solution, 120 μL of APS solution (10%) was added, and then nitrogen was bubbled through the reaction mixture for 15 min. The reaction mixture was shaken at 50 °C for 3 h.

Subsequently, 120 μL of APS solution (10% in weight) and 60 μL of TEMED were added into the clear reaction system. Following completion of initiator supplement, the polymerization was allowed to proceed at 50 °C for another 1 h. The polymeric MGs were purified by dialysis against 1 L of pure water (changing water more than 4 times/day) for 3 days, 1 L of water containing 3 mL of 4 mol L<sup>-1</sup> HCl (changing the solution more than 4 times/day) for 3 days, and 1 L of pure water (changing water more than 4 times/day) for 2 days, successively.

The leakage of target peptide from MIP MGs was investigated using a Spectamar Gemini EM made by Molecular Device (UK) with SoftMaxPro6.4 software. Typically, 0.5 mL of the MIP MG solution was mixed with 0.5 mL of PBS buffer (pH 7.4, 20 mM) and incubated in a 1.5 mL Eppendorf tube at 25 °C for 16 h. The MIP MGs were removed by centrifugation for 15 min with a speed of 14 000 rpm. After addition of 200 μL of the supernatant into a 96 well quartz plate (Hellma Analytics, Germany), the quartz plate was placed into the fluorescence reader. The excitation wavelength and the emission

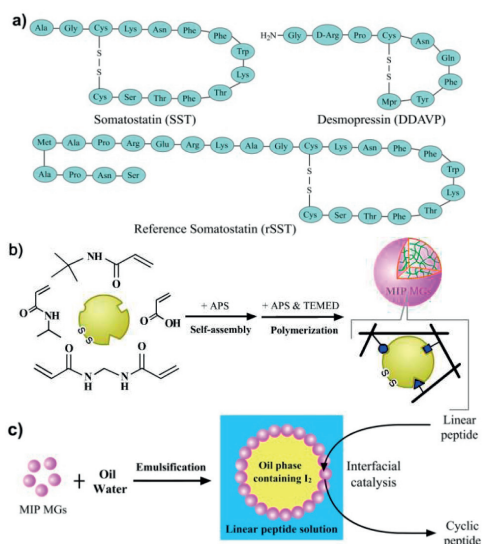


**Figure 1.** (a) Structure and amino acid sequence of the peptides used in the study. (b) Procedure used for synthesizing MIP MG. (c) Scheme depicting the procedure used for the preparation of MIP MG stabilized Pickering emulsion and its application in interfacial formation of cyclopeptide.

wavelength for SST were 280 and 356 nm, respectively. When no SST was observed in the supernatant, the washing step was terminated.

After removal of the template (SST), the weight of MIP MGs in the solution was measured by drying the MIP MG solution (1 mL) at 95 °C for 16 h and then at 100 °C for 1 h. For further application, the MIP MG solution was diluted with water to 9.0 mg mL<sup>-1</sup> (dry polymer) and stored at 25 °C. The NIP MG solution was prepared and washed in an identical way except that the templates were not added to the reaction mixture during the synthesis.

**Preparation of Pickering Emulsion.** Typically, 600  $\mu$ L of MG solution, 100  $\mu$ L of concentrated linear peptide solution, 300  $\mu$ L of ethyl acetate, and 100  $\mu$ L of toluene were mixed together. Nitrogen was bubbled through the emulsion for 5 min to remove O<sub>2</sub>. To obtain a stable Pickering emulsion, the mixture was shaken vigorously by hand. For the catalysis, 100  $\mu$ L of oxidizing reagent solution was also added after a 1-h equilibrium adsorption. After the addition of the oxidizing reagent solution, the emulsion was shaken vigorously by hand again. It is noted that the oxidizing reagent solution used in the experiments was pure DMSO, 2.5 mmol L<sup>-1</sup> potassium ferricyanide (III) solution, or 2.5 mmol L<sup>-1</sup> I<sub>2</sub> in methanol. The Pickering emulsions stabilized by MIP (or NIP) MGs in the presence of oxidant I<sub>2</sub>, potassium ferricyanide (III), and DMSO were named MIP-PE-I<sub>2</sub> (or NIP-PE-I<sub>2</sub>), MIP-PE-K<sub>3</sub>Fe(CN)<sub>6</sub> [or NIP-PE-K<sub>3</sub>Fe(CN)<sub>6</sub>], and MIP-PE-DMSO (or NIP-PE-DMSO), respectively. In control experiments, an unstable Pickering emulsion was observed when no MGs were used (see Figure S9a).

**Characterization.** The morphology of the MGs was observed using a scanning electron microscope (Inspect SEM F50, FEI Company). The wet MGs were cast onto a glass slide and dried at ambient temperature before SEM testing.

The size distribution of the wet MGs was measured using dynamic light scattering (DLS) with a Coulter LS230 instrument (Beckman-Coulter Co. Ltd.). The MG solution was diluted to a concentration of 0.1 mg mL<sup>-1</sup> during the measurement.

The optical images of Pickering emulsions were recorded with an inverted optical microscope with an HMX lamp house assembly (model TMS-F) made by Nikon Japan.

**Selectivity and Binding Test.** The selectivity test was conducted by incubation of 0.6 mL of the MIP MG solution (containing 5.4 mg of dry MGs) and 0.4 mL of PBS buffer (pH 7.4, 20 mM) containing different peptides (single or a mixture of DDAVP with LLS) in a 1.5 mL Eppendorf. After incubation at 25 °C for 16 h, the MIP MGs were removed by centrifugation for 15 min at a speed of 14 000 rpm. The concentration of the peptides in the supernatant was then determined. It is noted that when we investigated the effects of temperature on the MGs binding, the experiment was conducted at 25, 30, 35, 40, and 45 °C, respectively.

The concentration of DDAVP was determined using HPLC. The gradient for HPLC method used for analysis follows: 0 min 21% mobile phase B, 15 min 40% mobile phase B, 17 min 21% B, 20 min 21% B. Mobile phase A was prepared by diluting 11 mL of phosphoric acid with water, adjusting to pH 2.3 with triethylamine, and diluting to 1000 mL with water. Mobile phase B was acetonitrile 100%. Flow rate was 1.0 mL min<sup>-1</sup>, and UV detection was at 215 nm. Injection volume was 50  $\mu$ L. The column used is a Luna C18 (150 mm  $\times$  4.6 mm i.d., 5  $\mu$ m) HPLC column from Phenomenex (Torrance, CA).

The concentration of SST and L-SST was measured using a fluorescence reader (Gemini EM Microplate Reader). Typically, 200  $\mu$ L of the supernatant was added into a 96 well quartz plate (Hellma Analytics, Germany), and the quartz plate was placed into the fluorescence reader. The excitation wavelength and the emission wavelength were 287 and 356 nm, respectively. It is noted that the solution should be diluted when the SST (L-SST) concentration is higher than 400 mg L<sup>-1</sup>.

The rebinding test was conducted also by incubating 0.6 mL of the MIP/NIP MG solution (containing 5.4 mg of dry MGs) with 0.4 mL of PBS buffer (pH 7.4, 20 mM) containing different concentrations of peptides in a 1.5 mL Eppendorf tube. After incubation at 25 °C for 16 h, the MIP MGs were removed by centrifugation for 15 min at a speed

of 14 000 rpm. The concentration of the peptides in the supernatant was then determined.

**Langmuir Isotherm Model Study.** With the assumption that monolayer adsorption happened at binding cavities with homogeneous energy levels, no interactions between adsorbed molecules, and no transmigration of adsorbed molecules onto the polymeric surface, the equilibrium adsorption data were simulated using the Langmuir isotherm model as follows:

$$q_e = \frac{q_m k_l C_e}{1 + q_m k_l} \quad (1)$$

$$\frac{C_e}{q_e} = \frac{1}{k_l q_m} + \frac{C_e}{q_m} \quad (2)$$

Here  $C_e$  is the equilibrium concentration of the SST solution (mg L<sup>-1</sup>),  $q_e$  is the adsorption capacity at equilibrium (mg g<sup>-1</sup>),  $q_m$  is the maximum adsorption capacity at monolayer coverage (mg g<sup>-1</sup>), and  $k_l$  is the Langmuir constant (L mg<sup>-1</sup>). For the calculation of the coefficients in eq 1, eq 1 was changed into eq 2.

**Interfacial Catalysis study.** MIP-PE-I<sub>2</sub>/NIP-PE-I<sub>2</sub> (using iodine as oxidizing agent), MIP-PE-K<sub>3</sub>Fe(CN)<sub>6</sub>/NIP-PE-K<sub>3</sub>Fe(CN)<sub>6</sub> (using K<sub>3</sub>Fe(CN)<sub>6</sub> as oxidizing agent), and MIP-PE-DMSO/NIP-PE-DMSO (using DMSO as oxidizing agent) were monitored at 25 °C with respect to the transformation of linear to cyclic peptide. For comparison, a suspension system containing 600  $\mu$ L of MG solution, 100  $\mu$ L of concentrated linear peptide solution, and 100  $\mu$ L of oxidizing agent served as negative controls.

To test the catalytic activities and the conversion of linear to cyclic peptide in these systems, the concentration of thiol groups in L-SST was measured using Ellman's reagent. Typically, aliquots of the reaction solution were sampled at given time intervals. The samples were centrifuged to remove the MGs in the solution. The MGs were further washed with 0.1 mol L<sup>-1</sup> HCl solution (0.5 mL) 3 times. The sample solution and the washing solutions were mixed and filtered through 0.45  $\mu$ m filters; the concentrations of thiol groups in L-SST were then measured by Ellman's reagent. A 0.5 mL portion of the sample and 50  $\mu$ L of Ellman's reagent stock solution were mixed and allowed to react at 25 °C for 3 min. After the reaction, the UV-vis adsorption (at 410 nm) of the mixture was measured using a Varian Cary 50 UV-vis spectrophotometer.

## RESULTS AND DISCUSSION

**Preparation and Characterization of MGs.** MIP MGs were prepared via aqueous surfactant-free radical precipitation copolymerization of acrylic acid (AA), *N*-*tert*-butylacrylamide (TBA), *N*-isopropylacrylamide (NIPAm), and *N,N'*-methylene bis(acrylamide) (MBA) initiated by ammonium persulfate (APS)/*N,N,N,N*-tetra-methyl-ethylenediamine (TEMED) and in the presence of the template (SST) based on a previously reported procedure (Figure 1 b).<sup>38,39</sup> In view of our recent findings concerning TEMED induced peptide methenylations, the protocol was slightly modified by delaying the addition of the accelerator TEMED.<sup>39</sup> As a control, the corresponding nonimprinted MGs were prepared in the absence of the template.

The hydrodynamic diameter of the MGs was measured by scanning electron microscope (SEM) and dynamic light scattering (DLS). It is seen that the dry MIP MGs were easily aggregated (Figure 2b) and had a hydrodynamic diameter of  $\sim$ 100 nm (Figure S7). The increase in diameter from  $\sim$ 100 nm of the dry MIP MGs to 280 nm of the wet MGs (Figure 2a) demonstrates the gel-like character of the lightly cross-linked beads.

**Binding Study.** Template rebinding to the MIP and NIP MGs was then investigated by fluorescence spectrometry. From the results shown in Figure 3a, it is seen that the MIP MGs

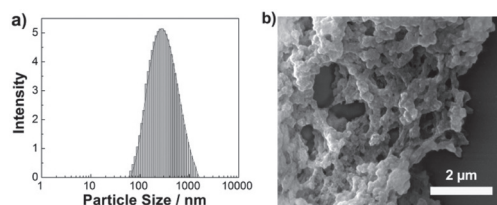


**Figure 2.** (a) DLS analysis of MIP MGs in water. (b) SEM image of MIP MGs casted on a glass slide.

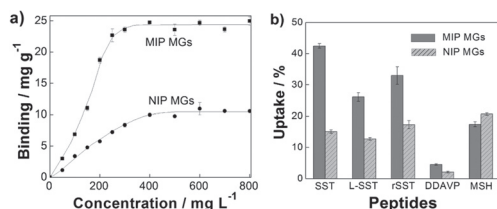


**Figure 3.** (a) Binding isotherms of SST on MIP and NIP MGs. (b) Uptake of different peptides ( $183 \mu\text{mol L}^{-1}$ ) by MIP and NIP MGs. The MG concentration was  $5.4 \text{ mg mL}^{-1}$ .

bound more than two times more template ( $24 \text{ mg g}^{-1}$ ) compared to the uptake displayed by a nonimprinted reference polymer (NIP) MG ( $10 \text{ mg g}^{-1}$ ) at saturation. Therefore, the specific uptake of SST at saturation on MIP MGs was estimated to be ca.  $14 \text{ mg g}^{-1}$ , which is in the same range as the binding capacity of the traditional thermoresponsive imprinted hydrogels.<sup>40</sup>

Figure S16 shows that the adsorption of SST on the MGs was fitted well to the Langmuir isotherm model ( $R \geq 0.93$ ), suggesting a relatively homogeneous distribution of imprinted sites. The additional uptake at saturation on MIP MGs ( $14 \text{ mg g}^{-1}$ ) corresponds to nearly 71% of the nominal capacity assuming a quantitative template utilization (see SI). In order to probe whether the excess binding was selective, the MGs were challenged with other peptides including linear somatostatin (L-SST), reference somatostatin (rSST), desmopressin (DDAVP), and melanocyte stimulating hormone (MSH) (Figure 3b). As anticipated, the MIP MGs showed

the highest template selectivity and notably a clear preference for the cyclic versus the linear form. A competitive binding experiment further confirmed the MIP MGs enhanced affinity for SST (Figure S14). It is noted in Figure 3b that the MIP MGs also show preferential binding to L-SST (template analogue), which will play an important role when the MIP MGs are used as catalysts for the cyclization of L-SST.

The thermoresponsiveness and related rebinding characteristics of the MIP MGs were also investigated in this work. It is known that thermal phase transition temperature (also known as the lower critical solution temperature, LCST) is one of the important characteristic of a temperature responsive polymer. Therefore, we first investigated the optical absorbance of the MIP MGs ( $0.5 \text{ mg mL}^{-1}$ , approximately) at different temperatures. As seen in Figure 4a the transition from a clear to an opaque solution occurred in the interval  $20\text{--}40^\circ\text{C}$ , approximately. The thermoresponsiveness was further confirmed by the photographs of MIP MGs dispersed in water at different temperatures ( $20$  and  $50^\circ\text{C}$ ) and the measurement of the temperature-dependent average diameter. Using a  $^1\text{H}$  NMR study, Chen et al. demonstrated that the thermoresponsiveness of this kind of MGs is due to temperature-dependent interchain hydrogen bonding.<sup>41</sup> Interestingly, as seen in Figure 4b the selectivity of the MIP MGs was preserved in a wide temperature range (from  $25$  to  $45^\circ\text{C}$ ) with the highest nonspecific binding observed at  $40^\circ\text{C}$  near the LCST. This indicates that the hydrophilicity/hydrophobicity balance of the polymer might also influence the nonspecific binding affinity with respect to the target peptide.<sup>42</sup>

The oil/water Pickering emulsion was generated by emulsifying the aqueous phase (pH 7.4 PBS buffer containing the linear peptide substrate) and organic phase (a mixture of toluene and ethyl acetate) using the polymeric MGs as solid stabilizers (Figure 1c). The morphology (stability) of the Pickering emulsions was observed visually (Figure 5a) and by optical microscopy (Figure 5b and Figure S9). The data showed that the Pickering emulsions consisted of round spherical droplets in a size range  $5\text{--}70 \mu\text{m}$  (with an average diameter of  $35 \pm 14 \mu\text{m}$ ) and that the emulsions were stable during the reaction.

**Catalysis Study.** The catalytic performance of the PEs was then investigated with respect to the cyclization of linear SST and DDAVP (Table 1). It is noted that the linear peptide concentration was  $183 \mu\text{mol L}^{-1}$  in all of the following catalytic

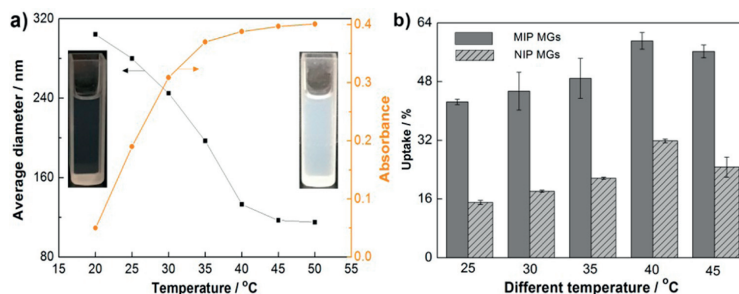


**Figure 4.** (a) Average diameter and optical absorbance of the MIP MGs at different temperatures. The absorbance was measured at  $700 \text{ nm}$ . The inset is the photographs of MIP MGs dispersed in water at  $20^\circ\text{C}$  ( $T < \text{LCST}$ ) and  $50^\circ\text{C}$  ( $T > \text{LCST}$ ). (b) Uptake of SST by MIP MGs and NIP MGs at different temperatures. The peptide concentration was  $183 \mu\text{mol L}^{-1}$ , and the MG concentration was  $5.4 \text{ mg mL}^{-1}$ .



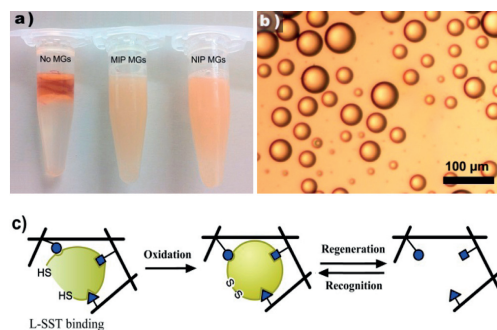


**Figure 5.** (a) Macroscopic view of different emulsions after a 30 min reaction period. (b) Optical microscopy image of the MIP-PE-I<sub>2</sub> droplets. For the Pickering emulsion, the water phase was a mixture of 600 μL of MG solution and 100 μL of concentrated L-SST solution, and 100 μL of 2.5 mmol L<sup>-1</sup> I<sub>2</sub> in methanol solution; the oil phase was a mixture of 300 μL of ethyl acetate and 100 μL of toluene. (c) Scheme showing the catalytic process of cyclopeptide formation.

studies. This concentration has been confirmed to be appropriate according to the disassociation constants toward MIP MGs (see SI). In the literature, it is well-known that the oxidizing agent plays an important role in the formation of the disulfide bond in peptides.<sup>43</sup> To achieve the interfacial catalysis, I<sub>2</sub> which partitioned preferentially into the oil phase of the PEs (see Figure S11) was selected as the main oxidizing agent in this study. As a control, potassium ferricyanide(III) (see Figure S12) and DMSO (see Figure S13) which partitioned preferentially into the water phase were also chosen. When I<sub>2</sub> was used, the reactions were monitored over sufficient time for nearly quantitative conversions (>93%) to be achieved (Table 1). Compared to I<sub>2</sub>, DMSO and potassium ferricyanide (III) were shown as less efficient oxidizing agents (see Table S1).

We first investigated the effect of MIP-PE-I<sub>2</sub> systems on the extent of byproduct formation. Two control experiments were performed for this purpose: (1) a mixture system containing MIP MGs, PBS buffer, methanol, oxidizing agent, and the linear peptide, and (2) a homogeneous solution system containing

PBS buffer, methanol, oxidizing agent, and linear peptide in absence of MGs.

As confirmed by MALDI analysis, peptide dimers were identified as the main byproducts during the cyclization of L-SST (Figure 6). For L-DDAVP (see Figure S19), the ion complex (between cyclic peptides and I<sup>-</sup>) was dominating.<sup>44</sup> Interestingly, the byproducts of the ion complex between L-SST were not observed in all the catalytic system. It is seen in Figure 1a that the ring of the SST molecule contains 12 amino acids, whereas the ring of the DDAVP molecule contains only 6 amino acids. The different phenomenon (formation of ion complex) for L-DDAVP and L-SST might be due to the distinct size of the host cavities of DDAVP and SST.<sup>45</sup>

The yield of cyclic product was further investigated. For L-DDAVP the product yields for the PE systems (>26% for L-DDAVP) were considerably higher than that for the control systems (not detected). This conclusion was also confirmed when L-rSST and L-SST were used as the linear peptide (Table 1). For example, it is seen in Table 1 that the interfacial MIP-PE-I<sub>2</sub> system showed a product yield of 50%, which is considerably higher than the yields obtained using the traditional homogeneous system (11%). These data indicate that the PE catalyzed peptide cyclization at the oil/water interface was more efficient than the traditional homogeneously catalyzed reactions (Table 1 and Table S1).

The catalytic performance of the MIP-PE-I<sub>2</sub> system and the NIP-PE-I<sub>2</sub> system for L-SST was then carefully investigated. In comparison with the NIP-PE-I<sub>2</sub> system, the MIP-PE-I<sub>2</sub> system gave rise to a higher product yield and less dimerization (Table 1 and Table S2). These data suggest that I<sub>2</sub> acted as effective oxidizing agent with a pronounced effect on the cyclization of L-SST (Figure 6). The inhibition of the dimerization in the catalytic system might be attributed to the specific binding of SST and L-SST to the MIP MG binding sites. Interestingly, in the MIP-PE-I<sub>2</sub> system, the product yield for L-rSST (38%) agreed with the binding results shown in Figure 3b, indicating that the MIP MGs also possessed some affinity for the template analogue rSST (although L-rSST has a large molecular size). The MIP-MGs in general showed a low affinity for L-DDVAP (although L-DDVAP has also two cysteine), whereas the MIP MGs lacked affinity toward DDVAP (Figure 3b). After the

**Table 1.** Effect of Reaction Conditions on the Conversion and Yield in the PE Catalyzed Cyclization of Linear Cysteine Containing Peptides

entry	peptide	oxidizing agent/its partition	MGs	catalytic system	conversion (%)	cyclopeptide yield (%)
1	L-DDAVP	I <sub>2</sub> /water	no	homogenous	>95 <sup>b</sup>	nd <sup>c</sup>
2		I <sub>2</sub> /water	MIP	mixture	>93 <sup>b</sup>	nd <sup>c</sup>
3		I <sub>2</sub> /oil	NIP	emulsion	>95	26.2
4		I <sub>2</sub> /oil	MIP	emulsion	>95	29.8
5	L-rSST	I <sub>2</sub> /water	no	homogenous	>95 <sup>b</sup>	<5
6		I <sub>2</sub> /water	MIP	mixture	>95 <sup>b</sup>	13.8 ± 0.1
7		I <sub>2</sub> /oil	NIP	emulsion	>95	25.5 ± 0.5
8		I <sub>2</sub> /oil	MIP	emulsion	>95	38.4 ± 0.7
9	L-SST	I <sub>2</sub> /water	no	homogenous	>95 <sup>b</sup>	10.7 ± 0.2
10		I <sub>2</sub> /water	MIP	mixture	>95 <sup>b</sup>	15.1 ± 0.3
11		I <sub>2</sub> /oil	ZnO <sup>a</sup>	emulsion	>95	26.3 ± 2.6
12		I <sub>2</sub> /oil	NIP	emulsion	>95	25.7 ± 0.4
13		I <sub>2</sub> /oil	MIP	emulsion	>95	49.9 ± 1.7

<sup>a</sup>Nanoparticles. <sup>b</sup>The I<sub>2</sub> in the homogeneous mixture was removed by a mixture of 300 μL of ethyl acetate and 100 μL of toluene before the measurement using Ellman's reagent. <sup>c</sup>nd: not detected. For Pickering emulsion, the oil phase was a mixture of 300 μL of ethyl acetate and 100 μL of toluene. The oxidizing reagent was 100 μL of 2.5 mmol L<sup>-1</sup> I<sub>2</sub> in methanol solution. The time length of the reaction was 30 min.



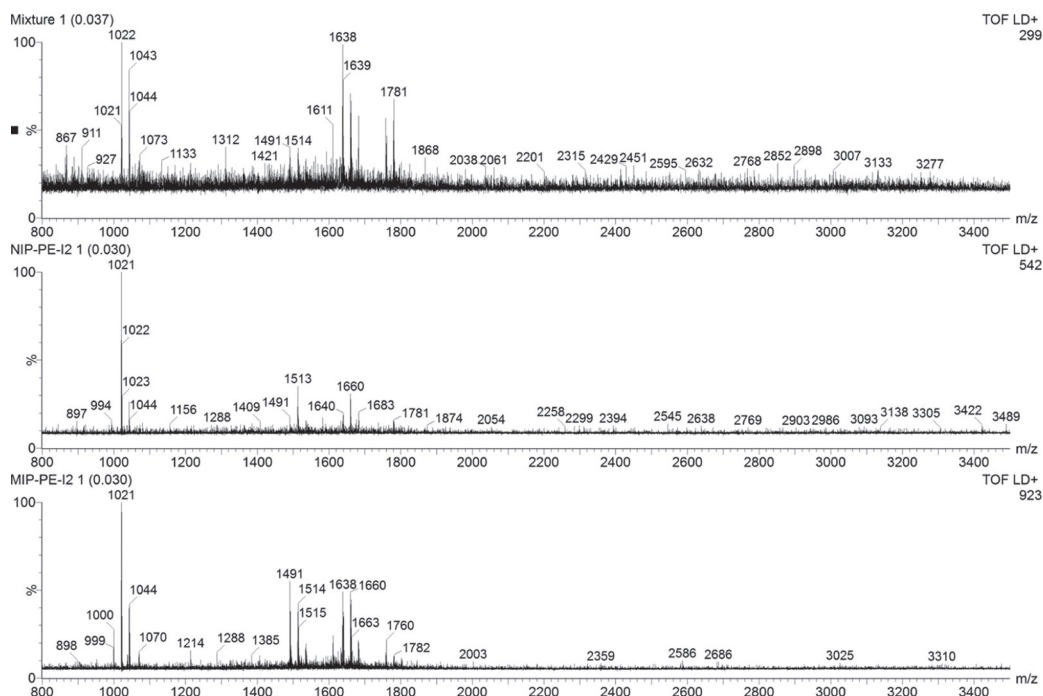


**Figure 6.** MALDI analysis of the cyclic somatostatin (SST, mass 1638) and the byproducts after a 30 min reaction. The oil phase was a mixture of 300  $\mu\text{L}$  of ethyl acetate and 100  $\mu\text{L}$  of toluene. The oxidizing reagent was 100  $\mu\text{L}$  of 2.5  $\text{mmol L}^{-1}$   $\text{I}_2$  in methanol solution.  $m/z$  1639: SST +  $\text{H}^+$ .  $m/z$  1491: SST lost Cys residue.  $m/z$  1660: SST +  $\text{Na}^+$ .  $m/z$  3277: SST dimer +  $\text{H}^+$ .

reaction, the total SST concentration was calculated to be 92  $\mu\text{mol L}^{-1}$  (see SI). The product and the byproduct bound onto the MIP MGs (in the MIP-PE- $\text{I}_2$  system) were measured with high performance liquid chromatography (HPLC) (Figure S18). The SST bound onto the MIP MGs was  $\sim 35\%$ , which is slightly lower than the uptake of SST (40%) on MIP MGs for an initial SST concentration of 92  $\mu\text{mol L}^{-1}$  (150  $\text{mg L}^{-1}$ ) (Figure 3a). This decrease might be caused by the coexisting reagents. Moreover, it is seen in Figure S18 that almost no L-SST and byproducts remained on the catalysts, indicating the reaction system was an efficient system for both the catalytic reaction and purification of the products.

The effect of the initial L-SST concentration on the cyclopeptide yield was investigated for the MIP-PE- $\text{I}_2$  system (see Figure S17b). It is clear that a lower product yield was obtained when a higher initial L-SST concentration was used. In Figure S17a, the MIP MGs show a binding capacity of  $\sim 15 \text{ mg g}^{-1}$  (saturation) toward L-SST when the initial L-SST concentration was higher than 183  $\mu\text{mol L}^{-1}$ . Therefore, we can suggest that the limitation of binding capacity of the MIP MGs toward L-SST decreases the product yield in high L-SST concentration. Interestingly, when the SST analogue (L-rSST) was used as the linear peptide, the MIP-PE- $\text{I}_2$  system also displayed higher product yield than the NIP-PE- $\text{I}_2$  system (Table 1, entries 7 and 8). To further investigate this inhibition selectivity, the cyclization of L-DDAVP was carried out under the same conditions (Table 1, entries 3 and 4). Presumably due

to the weak affinity of L-DDAVP to the MIP MGs (Figure 3b), the MGs show no effect on the cyclization reaction.

To demonstrate the role of the MIP MGs in the MIP-PE- $\text{I}_2$  system, ZnO nanoparticles were used as solid particles for the preparation of the Pickering emulsions. It is seen in Figure S15 that the latter displayed a much higher binding capacity to the SST and L-SST than the MIP MGs. However, the ZnO-PE- $\text{I}_2$  system showed a low cyclopeptide yield (Table 1, entry 11). This finding indicates that the enhanced cyclopeptide yield obtained using the MIP MGs is not only a result of an enhanced rate of mass transfer but also a change in the reaction pathway via the tailor-made “catalytic sites” (Figure 5c).

The recovery and reuse of imprinted catalyst are important in the catalytic system. In this work, the cyclization of the linear peptide (L-SST) was performed in 5 successive batches (see SI). As shown in Figure S20, the yield of cyclopeptide decreased just slightly during the course of 5 successive experiments, indicating that the MIP MGs possess excellent recycling ability.

## CONCLUSIONS

In conclusion, by integrating molecular imprinting and the Pickering emulsion technique, the first successful construction of a MIP microgel stabilized Pickering emulsion capable of catalyzing the intramolecular disulfide bond formation in peptides has been demonstrated. The Pickering emulsion catalytic system provided high cyclopeptide selectivity and a

remarkable inhibition of byproducts during the cyclopeptide formation. We are currently working on the catalytic formation of more than one disulfide bond with or without a sophisticated side-chain protection strategy using this interfacial catalysis system. We believe the interfacial catalysis system presented in this work may offer significant benefits for synthetic peptide chemistry by raising the reaction selectivity.

## ■ ASSOCIATED CONTENT

### Supporting Information

The Supporting Information is available free of charge on the ACS Publications website at DOI: 10.1021/acsami.6b10131.

Materials, microgel synthesis, Pickering emulsion preparation, equilibrium binding results, MIP-assisted disulfide bond formation, kinetic studies, and MALDI MS analysis (PDF)

## ■ AUTHOR INFORMATION

### Corresponding Authors

\*E-mail: [xtshenlab@hust.edu.cn](mailto:xtshenlab@hust.edu.cn).

\*E-mail: [chuixiuh@student.matnat.uio.no](mailto:chuixiuh@student.matnat.uio.no).

\*E-mail: [borje.sellergren@mah.se](mailto:borje.sellergren@mah.se).

### Notes

The authors declare no competing financial interest.

## ■ ACKNOWLEDGMENTS

We thank the Fundamental Research Funds for the Central Universities in China (201SYGYL024 and 2016YXMS217). This work has been performed as part of the "Robust affinity materials for applications in proteomics and diagnostics" (PEPMIP) project, supported by the Seventh Research Framework Program of the European Commission, Grant agreement number 264699.

## ■ REFERENCES

- (1) Talluri, S.; Falcomer, C. M.; Scheraga, H. A. Energetic and Structural Basis for the Preferential Formation of the Native Disulfide Loop Involving Cys-65 and Cys-72 in Synthetic Peptide Fragments Derived from the Sequence of Ribonuclease A. *J. Am. Chem. Soc.* **1993**, *115*, 3041–3047.
- (2) Wommack, A. J.; Ziarek, J. J.; Tomaras, J.; Chileveru, H. R.; Zhang, Y.; Wagner, G.; Nolan, E. M. Discovery and Characterization of a Disulfide-Locked C2-Symmetric Defensin Peptide. *J. Am. Chem. Soc.* **2014**, *136*, 13494–13497.
- (3) Xu, G.; Narayan, M.; Kurinov, R.; Ripoll, D. R.; Welker, E.; Khalili, M.; Ealick, S. E.; Scheraga, H. A. A Localized Specific Interaction Alters the Unfolding Pathways of Structural Homologues. *J. Am. Chem. Soc.* **2006**, *128*, 1204–1213.
- (4) Wang, X.-Y.; Wang, Q.; Huang, X.-Y.; Wang, T.; Yu, X.-Q. Synthesis of Small Cyclic Peptides Containing Disulfide Bonds. *ARKIVOC* **2006**, No. 11, 148–154.
- (5) Berezkhovskiy, L.; Pham, S.; Reich, E.-P.; Deshpande, S. Synthesis and Kinetics of Cyclization of MHC Class II Derived Cyclic Peptide Vaccine for Diabetes. *J. Pept. Res.* **1999**, *54*, 112–119.
- (6) Wong, C. T.; Rowlands, D. K.; Wong, C. H.; Lo, T. W.; Nguyen, G. K.; Li, H. Y.; Tam, J. P. Orally Active Peptidic Bradykinin B1 Receptor Antagonists Engineered from a Cyclotide Scaffold for Inflammatory Pain Treatment. *Angew. Chem.* **2012**, *124*, 5718–5722.
- (7) White, C. J.; Yudin, A. K. Contemporary Strategies for Peptide Macrocyclization. *Nat. Chem.* **2011**, *3*, 509–524.
- (8) Bulaj, G. Formation of Disulfide Bonds in Proteins and Peptides. *Biotechnol. Adv.* **2005**, *23*, 87–92.
- (9) Čemažar, M.; Craik, D. J. Microwave-Assisted Boc-solid Phase Peptide Synthesis of Cyclic Cysteine-Rich Peptides. *J. Pept. Sci.* **2008**, *14*, 683–689.
- (10) Tulla-Puche, J.; Bayó-Puxan, N.; Moreno, J. A.; Francesch, A. M.; Cuevas, C.; Álvarez, M.; Albericio, F. Solid-Phase Synthesis of Oxathioracalinaline by a Key Intermolecular Disulfide Dimer. *J. Am. Chem. Soc.* **2007**, *129*, 5322–5323.
- (11) Albericio, F.; Hammer, R. P.; García-Echeverría, C.; Molins, M. A.; Chang, J. L.; Munson, M. C.; Pons, M.; Giralte, E.; Barany, G. Cyclization of Disulfide-Containing Peptides in Solid-Phase Synthesis. *Int. J. Pept. Protein Res.* **1991**, *37*, 402–413.
- (12) Pickering, S. U. CXCVI.—Emulsions. *J. Chem. Soc., Trans.* **1907**, *91*, 2001–2021.
- (13) Chen, R.; Pearce, D. J. G.; Fortuna, S.; Cheung, D. L.; Bon, S. A. F. Polymer Vesicles with a Colloidal Armor of Nanoparticles. *J. Am. Chem. Soc.* **2011**, *133*, 2151–2153.
- (14) Crossley, S.; Faria, J.; Shen, M.; Resasco, D. E. Solid Nanoparticles that Catalyze Biofuel Upgrade Reactions at the Water/Oil Interface. *Science* **2010**, *327*, 68–72.
- (15) Chen, H.; Zhu, H.; Hu, J.; Zhao, Y.; Wang, Q.; Wan, J.; Yang, Y.; Xu, H.; Yang, X. Highly Compressed Assembly of Deformable Nanogels into Nanoscale Suprastructures and Their Application in Nanomedicine. *ACS Nano* **2011**, *5*, 2671–2680.
- (16) Chen, Z.; Ji, H.; Zhao, C.; Ju, E.; Ren, J.; Qu, X. Individual Surface-Engineered Microorganisms as Robust Pickering Interfacial Biocatalysts for Resistance-Minimized Phase-Transfer Bioconversion. *Angew. Chem., Int. Ed.* **2015**, *54*, 4904–4908.
- (17) Zhou, W.-J.; Fang, L.; Fan, Z.; Albela, B.; Bonneviot, L.; De Campo, F.; Pera-Titus, M.; Clacens, J.-M. Tunable Catalysts for Solvent-Free Biphasic Systems: Pickering Interfacial Catalysts over Amphiphilic Silica Nanoparticles. *J. Am. Chem. Soc.* **2014**, *136*, 4869–4872.
- (18) Chen, Z.; Zhou, L.; Bing, W.; Zhang, Z.; Li, Z.; Ren, J.; Qu, X. Light Controlled Reversible Inversion of Nanophosphor-Stabilized Pickering Emulsions for Biphasic Enantioselective Biocatalysis. *J. Am. Chem. Soc.* **2014**, *136*, 7498–7504.
- (19) Yang, H.; Fu, L.; Wei, L.; Liang, J.; Binks, B. P. Compartmentalization of Incompatible Reagents within Pickering Emulsion Droplets for One-Pot Cascade Reactions. *J. Am. Chem. Soc.* **2015**, *137*, 1362–1371.
- (20) Shen, X.; Ye, L. Interfacial Molecular Imprinting in Nanoparticle-Stabilized Emulsions. *Macromolecules* **2011**, *44*, 5631–5637.
- (21) Shen, X.; Ye, L. Molecular Imprinting in Pickering Emulsions: A New Insight into Molecular Recognition in Water. *Chem. Commun.* **2011**, *47*, 10359–10361.
- (22) Shen, X.; Zhou, T.; Ye, L. Molecular Imprinting of Protein in Pickering Emulsion. *Chem. Commun.* **2012**, *48*, 8198–8200.
- (23) Shen, X.; Bonde, J. S.; Kamra, T.; Bülow, L.; Leo, J. C.; Linke, D.; Ye, L. Bacterial Imprinting at Pickering Emulsion Interfaces. *Angew. Chem., Int. Ed.* **2014**, *53*, 10687–10690.
- (24) Huang, C.; Shen, X. Janus Molecularly Imprinted Polymer Particles. *Chem. Commun.* **2014**, *50*, 2646–2649.
- (25) Liu, J. Q.; Wulff, G. Functional Mimicry of Carboxypeptidase A by a Combination of Transition State Stabilization and a Defined Orientation of Catalytic Moieties in Molecularly Imprinted Polymers. *J. Am. Chem. Soc.* **2008**, *130*, 8044–8054.
- (26) Pan, G.; Zhang, Y.; Ma, Y.; Li, C.; Zhang, H. Efficient One-Pot Synthesis of Water-Compatible Molecularly Imprinted Polymer Microspheres by Facile RAFT Precipitation Polymerization. *Angew. Chem., Int. Ed.* **2011**, *50*, 11731–11734.
- (27) Takeda, K.; Kuwahara, A.; Ohmori, K.; Takeuchi, T. Molecularly Imprinted Tunable Binding Sites Based on Conjugated Prosthetic Groups and Ion-Paired Cofactors. *J. Am. Chem. Soc.* **2009**, *131*, 8833–8838.
- (28) Hoshino, Y.; Koide, H.; Urakami, T.; Kanazawa, H.; Kodama, T.; Oku, N.; Shea, K. J. Recognition, Neutralization, and Clearance of Target Peptides in the Bloodstream of Living Mice by Molecularly Imprinted Polymer Nanoparticles: A Plastic Antibody. *J. Am. Chem. Soc.* **2010**, *132*, 6644–6645.

- (29) Bie, Z.; Chen, Y.; Ye, J.; Wang, S.; Liu, Z. Boronate-Affinity Glycan-Oriented Surface Imprinting: A New Strategy to Mimic Lectins for the Recognition of an Intact Glycoprotein and Its Characteristic Fragments. *Angew. Chem., Int. Ed.* **2015**, *54*, 10211–10215.
- (30) Wulff, G. Enzyme-like Catalysis by Molecularly Imprinted Polymers. *Chem. Rev.* **2002**, *102*, 1–27.
- (31) Damen, J.; Neckers, D. C. Stereoselective Syntheses via a Photochemical Template Effect. *J. Am. Chem. Soc.* **1980**, *102*, 3265–3267.
- (32) Cutivet, A.; Schembri, C.; Kovensky, J.; Haupt, K. Molecularly Imprinted Microgels as Enzyme Inhibitors. *J. Am. Chem. Soc.* **2009**, *131*, 14699–14702.
- (33) Kim, H.; Spivak, D. A. New Insight into Modeling Non-Covalently Imprinted Polymers. *J. Am. Chem. Soc.* **2003**, *125*, 11269–11275.
- (34) Shen, X.; Zhu, L.; Liu, G.; Yu, H.; Tang, H. Enhanced Photocatalytic Degradation and Selective Removal of Nitrophenols by Using Surface Molecular Imprinted Titania. *Environ. Sci. Technol.* **2008**, *42*, 1687–1692.
- (35) Muratsugu, S.; Tada, M. Molecularly Imprinted Ru Complex Catalysts Integrated on Oxide Surfaces. *Acc. Chem. Res.* **2013**, *46*, 300–311.
- (36) Meng, Z.; Smith, M. H.; Lyon, L. A. Temperature-Programmed Synthesis of Micron-Sized Multi-responsive Microgels. *Colloid Polym. Sci.* **2009**, *287*, 277–285.
- (37) Shirangi, M.; Torano, J. S.; Sellergren, B.; Hennink, W. E.; Somsen, G. W.; van Nostrum, C. F. Methylation of Peptides by *N,N,N,N*-Tetramethylethylenediamine (TEMED) under Conditions Used for Free Radical Polymerization: A Mechanistic Study. *Bioconjugate Chem.* **2015**, *26*, 90–100.
- (38) Sellergren, B.; Karmalkar, R. N.; Shea, K. J. Enantioselective Ester Hydrolysis Catalyzed by Imprinted Polymers 2. *J. Org. Chem.* **2000**, *65*, 4009–4027.
- (39) Sellergren, B.; Shea, K. J. Enantioselective Ester Hydrolysis Catalyzed by Imprinted Polymers. *Tetrahedron: Asymmetry* **1994**, *5*, 1403–1406.
- (40) Pan, G.; Guo, Q.; Ma, Y.; Yang, H.; Li, B. Thermo-Responsive Hydrogel Layers Imprinted with RGDS Peptide: A System for Harvesting Cell Sheets. *Angew. Chem., Int. Ed.* **2013**, *52*, 6907–6911.
- (41) Chen, Q.; Xu, K.; Zhang, W.; Song, C.; Wang, P. Preparation and Characterization of Poly(*N*-isopropylacrylamide)/polyvinylamine Core-shell Microgels. *Colloid Polym. Sci.* **2009**, *287*, 1339–1346.
- (42) Pan, G.; Guo, Q.; Cao, C.; Yang, H.; Li, B. Thermo-Responsive Molecularly Imprinted Nanogels for Specific Recognition and Controlled Release of Proteins. *Soft Matter* **2013**, *9*, 3840–3850.
- (43) Tam, J. P.; Wu, C. R.; Liu, W.; Zhang, J. W. Disulfide Bond Formation in Peptides by Dimethyl Sulfoxide. Scope and Applications. *J. Am. Chem. Soc.* **1991**, *113*, 6657–6662.
- (44) Kubik, S.; Goddard, R. A New Cyclic Pseudopeptide Composed of (1)-Proline and 3-Aminobenzoic Acid Subunits as a Ditopic Receptor for the Simultaneous Complexation of Cations and Anions. *J. Org. Chem.* **1999**, *64*, 9475–9486.
- (45) Elmes, R. B. P.; Jolliffe, K. A. Anion Recognition by Cyclic Peptides. *Chem. Commun.* **2015**, *51*, 4951–4968.

